Universidade do Minho
Escola de Engenharia

Catarina Silva Simão de Oliveira

Respirometric techniques applied to aerobic microbial processes

January 2012

Respirometric techniques applied to aerobic microbial processes
Catarina Silva Simão de Oliveira
UMinho | 2012

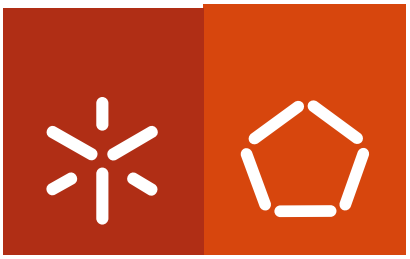

Universidade do Minho
Escola de Engenharia

Catarina Silva Simão de Oliveira

Respirometric techniques applied to aerobic microbial processes

Thesis for the degree of Doctor (Ph.D.)
in Chemical and Biological Engineering

Supervisors:
Madalena Alves
Frédéric Thalasso

January 2012

Autora

Catarina Silva Simão de Oliveira

e-mail

catarinaoliveira@deb.uminho.pt · *cat_ss_oli@msn.com*

Título da Tese

Respirometric techniques applied to aerobic microbial processes

Aplicação de técnicas respirométricas a processos microbianos aeróbios

Orientadores

Maria Madalena dos Santos Alves

Frédéric Thalasso

Ano de Conclusão

2012

Doutoramento em Engenharia Química e Biológica (Tecnologia Ambiental)

_____

Universidade do Minho, 12 January 2012

À minha Família,

Mãe São, Pai Zé, Ricardo

e Diogo.

AGRADECIMENTOS · ACKNOWLEDGEMENTS

Os meus primeiros agradecimentos vão para os meus orientadores: Obrigada Madalena! Merci Fred! Thank you both for the collaboration and guidance, and, especially, for the freedom you gave me to develop my ideas and for always being supportive and always encouraging me.

Quero também agradecer ao Professor Eugénio, por ter estado sempre disponível para me tirar dúvidas referentes a modelos e programas (por muito disparatadas que fossem).

Quiero agradecer a todos los que tornaran mi tiempo en México inolvidable. Muchísimas gracias Familia Feliz (Ceci, Javi y Dieguito), Ita, Azu, Jessy, Joel, Jorge y Armando, roomies (Olga y Rocío, Ily y Ale), Bere y Chío. Obrigada Eugénia e Fred. Gracias Alberto, mi compañero de respirometria.

Agradeço a todos os colegas e muitos amigos do DEB (Departamento de Engenharia Biológica). Obrigada Sr. Santos, por todo o apoio técnico ao trabalho experimental. Obrigada "LBAers" pelo companheirismo, incentivo e troca produtiva de ideia. Obrigada Ladies DEB pelas futeboladas e diversão. Obrigada especial: à Raquel, por muitas muitas vezes se lembrar de mim à hora de jantar e por me acompanhar nos piqueniques@DEB; à Dani pela calma e positivismo que me transmite.

Por fim um Obrigada gigante aos meus Amigos, aos meus Pais, ao "Puto" Ricardo e ao Diogo. Obrigada por todo o apoio, por me aturarem nos momentos mais difíceis (por muito rabugenta que esteja), por estarem sempre comigo, bem…por TUDO!

The work presented in this thesis was financially supported by *Fundação para a Ciência e a Tecnologia* (FCT) through the research grant SFRH/BD/32289/2006.

ABSTRACT

RESPIROMETRIC TECHNIQUES APPLIED TO AEROBIC MICROBIAL PROCESSES

Aerobic microbial processes are extremely important in environmental biotechnology, namely in biological wastewater treatment where activated sludge process represents nowadays the most widespread technology for wastewater purification. The availability of reliable, cheap and versatile real-time monitoring tools providing information on the biological activity is of crucial importance for monitoring and control of bioprocesses, avoiding possible operational troubles through early detection of problems.

This thesis aimed to develop and apply respirometric techniques for the estimation of kinetic and stoichiometric parameters in different systems with increasing complexity.

The first process – nitrification, was chosen for its simplicity. In this process, substrate consumption is related only with growth and energy, no storage phenomena occur. The ASM1 model was used to fit the respirometric data, and an *in situ* pulse respirometric method was validated for the determination of kinetic and stoichiometric parameters of the system at steady state: the maximum exogenous oxygen uptake rate was determined respirometrically [61.15 (4.09) mg O_2 L^{-1} h^{-1}] through the injection of increasing substrate concentration pulses; the biomass growth yield was estimated from respirometric data and by the traditional COD (Chemical Oxygen Demand) mass balance method, and both methods gave similar values [0.10 (0.07) and 0.09 (0.04) g X-COD g NOD^{-1}, respectively]; the affinity constant was indirectly estimated after fitting the ascending part of the respirogram to a theoretical model, and an average value of 0.48 (0.08) mg NH4-N L^{-1} was obtained. Model adjustment was successfully applied to a portion of the respirogram, but not to the complete respirogram. It was concluded that a more complex model, taking into account biological and electrode response time, should give better correlation. Additionally, two methods for the determination of the oxygen volumetric mass transfer coefficient were tested and it was concluded that the dynamic method was the most adequate. The results obtained allowed to establish the basic pulse respirometric methodology, and also the best method for estimating the oxygen mass transfer coefficient. Then a *Pseudomonas putida* pure culture system was chosen to test the applicability of pulse respirometry on biomass with storage ability. ASM3 was used for fitting the obtained data. The model included terms which took into account the biological and electrode response time, thus the entire respirogram could be successfully used for model fitting. The pulse respirometric method was validated for estimation of kinetic and stoichiometric parameters in pure cultures by comparison with the traditional chemostat method. No significance difference was observed between parameters estimated by chemostat and respirometric methods: biomass growth yield was 0.41(0.05) and 0.51 (0.04) g COD-X g $COD\text{-}S^{-1}$; affinity constant was 4.86 (0.70) and 5.13 (1.99) mg COD-S L^{-1}; maximum specific growth rate was 0.20 (0.05) and 0.16 (0.01) h^{-1}, with chemostat and respirometry respectively. Pulse respirometry was then applied to a continuous suspended activated sludge process, fed with a complex synthetic medium. In this stage, a multiple pulses respirometric method was tested and validated by

comparison with chemostat method and with ASM1 model fitting: biomass growth yield was in the range of 0.37 – 0.76, and 0.37 – 0.65 g COD-X g COD-S^{-1}; maintenance coefficient was 0.012 (0.012) and 0.010 (0.006) h^{-1}, by COD mass balance and by respirometry, respectively; affinity constant and maximum specific oxygen consumption rate were estimated with the multiple concentration pulses respirometric method to be 15.5 (2.4) mg COD-S L^{-1} and 0.12 (0.01) h^{-1}, respectively. Considering the assessment and comparison of the experimental and calculation methods, it was concluded that the estimation of kinetic and stoichiometric parameters in mixed aerobic cultures should preferentially be performed by using respirometric techniques, being the most adequate method the multiple concentration pulses injection method, with several advantages such as a simpler experimental data interpretation, and results with better confidence. The developed multiple pulses respirometric method was finally applied to an aerobic granular system. The method proved to be adequate for parameter estimation on this system, and allowed the successful monitoring of aerobic granulation. In a short time and using low cost equipment, the method allowed an exhaustive characterisation of the process in real-time through the determination of six central parameters: (i) biomass growth yield, (ii) specific endogenous respiration rate, (iii) substrate affinity constant, (iv) maximum specific oxygen consumption rate, (v) maximum specific substrate consumption rate, and (vi) maximum specific growth rate. The pulse respirometric method presented the advantage of the determined parameters being those actually prevailing in the system under actual operating conditions, *i.e.* apparent parameters, which is of major interest for control and process operation. At steady state the biomass growth yield was estimated to be 0.6 g COD-X g COD-S^{-1}, the specific endogenous respiration rate was 0.1 g O_2 g COD-X^{-1} d^{-1}, the affinity constant was approximately 20 mg COD-S L^{-1}, maximum specific oxygen consumption rate and maximum specific substrate consumption rate were 0.06 g O_2 g COD-X^{-1} h^{-1} and 0.17 g COD-S g COD-X^{-1} h^{-1}, respectively, and the maximum specific growth rate was roughly 2.5 d^{-1}. The potential of the proposed multiple concentration pulses respirometric method was investigated for monitoring aerobic granular sludge systems, and controlling aeration in an efficient mode. Additionally the multiple concentration pulses respirometric method was applied in two aerobic granular sludge systems operated under different aeration rates (5.0 and 6.6 L min^{-1}), and allowed to assess the influence of shear stress on the biomass kinetic and stoichiometric parameters: the biomass growth yield was higher for the sludge cultivated under higher shear stress [0.6 (0.02) versus 0.5 (0.02) g COD-X g COD-S^{-1} at lower shear stress]; biomass subjected to the higher shear stress presented a higher substrate affinity constant [16.4 (2.6) and 9.1 (0.2) mg COD-S L^{-1}, at higher and lower shear stress, respectively]; and also a higher maximum specific substrate consumption rate [5.4 (0.9) and 2.5 (0.5) g COD-S g COD-X d^{-1}, at higher and lower shear stress, respectively] at the end of the aerobic granulation process.

The global conclusion withdrawn from this thesis is that respirometry, especially pulse respirometry, is a valid and promising technique for kinetic and stoichiometric characterisation of aerobic microbial processes, whether these are pure or mixed cultures, and suspended or aggregated cultures. A respirometric method was developed, the multiple concentration pulses method, which allows an exhaustive characterisation of aerobic microbial processes in a short time period, using low cost material and requiring low computational power.

RESUMO

APLICAÇÃO DE TÉCNICAS RESPIROMÉTRICAS A PROCESSOS MICROBIANOS AERÓBIOS

Os processos microbianos aeróbios são extremamente importantes em biotecnologia ambiental, nomeadamente nos sistemas biológicos de tratamento de águas residuais onde o processo de lamas activadas representa actualmente a tecnologia mais generalizada de purificação de água. A disponibilidade de ferramentas de monitorização em tempo real confiáveis, baratas e versáteis, que forneçam informações sobre a actividade biológica, é de importância crucial para a monitorização e controlo de processos biológicos, evitando problemas operacionais através da detecção precoce de problemas.

Esta tese teve como objectivo desenvolver e aplicar técnicas respirométricas para a determinação de parâmetros cinéticos e estequiométricos em diferentes sistemas com complexidade crescente.

O primeiro processo – nitrificação, foi escolhido pela sua simplicidade. Neste processo, o consumo de substrato está relacionado apenas com o crescimento e produção de energia, nenhum fenómeno de armazenamento de substrato ocorre e um método respirométrico *in situ* foi validado para a determinação de parâmetros cinéticos e estequiométricos em sistemas em estado estacionário: a taxa máxima específica de consumo de oxigénio foi determinada respirometricamente [61.15 (4.09) mg O_2 L^{-1} h^{-1}] através da injecção de pulsos de concentração de substrato crescente; o rendimento de crescimento da biomassa foi estimado a partir de dados respirométricos e a partir do método tradicional de balanço de massa à CQO (Carência Química de Oxigénio) e ambos os métodos deram resultados similares [0.10 (0.07) e 0.09 (0.04) g X-COD g NOD^{-1}, respectivamente]; a constante de afinidade do substrato foi determinada indirectamente após ajuste de um modelo teórico à porção ascendente do respirograma e um valor médio de 0.48 (0.08) mg NH4-N L^{-1} foi determinado. O ajuste de um modelo foi bem sucedido com uma porção do respirograma, mas não com o respirograma inteiro. Foi concluído que um modelo mais complexo, que tome em consideração os tempos de resposta do eléctrodo e da biomassa, deverá ajustar melhor ao respirograma. Adicionalmente, dois métodos para a determinação do coeficiente volumétrico de transferência de massa do oxigénio foram testados e concluiu-se que o método mais adequado é o método dinâmico. Os resultados obtidos permitiram estabelecer os princípios básicos da metodologia da respirometria de pulsos e o melhor método para determinação do coeficiente volumétrico de transferência de massa do oxigénio. Seguidamente um sistema de cultura pura de *Pseudomonas putida* foi seleccionado para testar a aplicabilidade da respirometria de pulso numa biomassa com capacidade de armazenar substrato. O modelo ASM3 foi usado para ajuste aos dados experimentais. O modelo incluiu termos que consideravam os tempos de resposta do eléctrodo e da biomassa, assim o respirograma inteiro pôde ser usado para ajuste do modelo. O método respirométrico de pulsos foi validado para a determinação de parâmetros cinéticos e estequiométricos em culturas puras por comparação com o método tradicional de quimiostato, visto que as diferenças dos parâmetros determinados pelos dois métodos não foram significativas: o rendimento em biomass 0.41 (0.05) e 0.51 (0.04) g COD-X g $COD\text{-}S^{-1}$; a constante de afinidade do substrato 4.86 (0.70) e 5.13 (1.99) mg COD-S L^{-1}; a taxa máxima específica de crescimento 0.20 (0.05) e 0.16 (0.01) h^{-1}, com o método do quimiostato e respirométrico, respectivamente. A respirometria de pulso foi depois aplicada a um processo de lamas activadas suspensas alimentado com meio sintético complexo.

Nesta etapa, um método respirométrico de pulsos múltiplos foi testado e validado por comparação com o método do quimiostato e com ajuste do modelo ASM1: o rendimento em biomassa estava na gama 0.37 – 0.76 e 0.37 – 0.65 g COD-X g COD-S^{-1}; o coeficiente de manutenção 0.012 (0.012) e 0.010 (0.006) h^{-1}, por balanço mássico de CQO e por respirometria, respectivamente; a constante de afinidade do substrato e a taxa máxima específica de consumo de oxigénio foram determinadas com o método respirométrico de pulsos múltiplos obtendo-se os valores 15.5 (2.4) mg COD-S L^{-1} e 0.12 (0.01) h^{-1}, respectivamente. Considerando a acessibilidade e comparação dos métodos experimentais e de cálculo, foi concluído que a determinação de parâmetros cinéticos e estequiométricos em culturas mistas aeróbias deve ser preferencialmente feita usando técnicas respirométricas, sendo o método respirométrico de pulsos múltiplos o mais adequado com várias vantagens tais como uma mais simples interpretação dos dados experimentais e obtenção de resultados mais exactos. O método respirométrico de pulsos múltiplos desenvolvido foi finalmente aplicado a um sistema de grânulos aeróbios. O método mostrou ser adequado para determinação de parâmetros neste tipo de sistema e permitiu a monitorização do processo de granulação aeróbia. Num curto tempo e usando equipamento de baixo custo o método permitiu a caracterização exaustiva do processo em tempo real através da determinação de seis parâmetros centrais: (i) rendimento em biomassa; (ii) taxa específica de respiração endógena; (iii) constante de afinidade do substrato; (iv) taxa máxima específica de consumo de oxigénio; (v) taxa máxima específica de consumo de substrato e (vi) taxa máxima específica de crescimento. O método respirométrico de pulsos múltiplos apresentou ainda a vantagem de fornecer parâmetros relacionados com os que realmente estão a ocorrer no sistema sobre as reais condições operacionais, *i.e.* os parâmetros aparentes, o que é de maior interesse para controlo e operação. Em estado estacionário o rendimento em biomassa foi estimado como sendo de 0.6 g COD-X g COD-S^{-1}, a taxa específica de respiração endógena 0.1 g O_2 g COD-X^{-1} d^{-1}, a constante de afinidade do substrato aproximadamente 20 mg COD-S L^{-1}, a taxa máxima específica de consumo de oxigénio e a taxa máxima específica de consume de substrato 0.06 g O_2 g COD-X^{-1} h^{-1} e 0.17 g COD-S g COD-X^{-1} h^{-1}, respectivamente, e a taxa máxima específica de crescimento 2.5 d^{-1}. O potencial do método respirométrico de pulsos múltiplos proposto foi investigado para monitorização de sistemas de grânulos aeróbios e para o controlo eficiente da taxa de arejamento. Adicionalmente, o método respirométrico de pulsos múltiplos foi aplicado a dois sistemas de grânulos aeróbios operados a diferentes taxas de arejamento (5.0 e 6.6 L min^{-1}), permitindo verificar a influência da tensão de corte nos parâmetros cinéticos e estequiométricos: o rendimento em biomassa foi maior na biomassa cultivada na tensão de corte mais alta [0.6 (0.02) *versus* 0.5 (0.02) g COD-X g COD-S^{-1} a tensão de corte mais baixa]; a biomassa sujeita a uma tensão de corte mais elevada apresentou uma constante de afinidade do substrato mais alta [16.4 (2.6) e 9.1 (0.2) mg COD-S L^{-1}, a tensão de corte mais alta e mais baixa, respectivamente] e também uma taxa máxima específica de consumo de substrato mais alta [5.4 (0.9) e 2.5 (0.5) g COD-S g COD-X d^{-1}, a tensão de corte mais alta e mais baixa, respectivamente] no fim do processo de granulação aeróbia.

A conclusão global retirada desta tese é que a respirometria, especialmente a respirometria de pulsos, é uma técnica válida e promissora para a caracterização cinética e estequiométrica de processos aeróbios, quer sejam culturas puras ou mistas, culturas suspensas ou agregadas. Um método respirométrico foi desenvolvido, o método respirométrico de pulsos múltiplos, que permite a caracterização exaustiva de processos microbianos aeróbios num curto tempo, usando equipamento de baixo custo e requerendo baixo poder computacional.

TABLE OF CONTENTS

4. Respirometry applied to a Pure Culture

5. Respirometry applied to a Suspended Activated Sludge System

6. Respirometry applied to Aerobic Granular Sludge Systems

6A. Method Validation and Aerobic Granulation Assessment

LIST OF FIGURES

List of Tables

NOMENCLATURE

A	(μm^2)	aggregate's area
ADP		adenosine diphosphate
AGS		aerobic granular sludge
AS		activated sludge
ASMi		activated sludge model i (i = 1, 3)
ATP		adenosine triphosphate
ATU		allylthiourea
b_H	($g\ O_2\ g\ COD\text{-}X^{-1}\ h^{-1}$) ($g\ O_2\ g\ COD\text{-}X^{-1}\ d^{-1}$)	specific endogenous respiration rate
b_{Sto}	(h^{-1})	aerobic specific respiration rate for X_{Sto} (ASM3)
C	(–)	maintenance constant of Neijssel and Tempest (1976)
C	($mg\ O_2\ L^{-1}$)	dissolved oxygen concentration
C_b	($mg\ O_2\ L^{-1}$)	baseline dissolved oxygen concentration
C_0	($mg\ O_2\ L^{-1}$)	dissolved oxygen concentration at the beginning of a pulse
C_f	($mg\ O_2\ L^{-1}$)	dissolved oxygen concentration at the end of a pulse
C_{LSto}	($mg\ O_2\ L^{-1}$)	hypothetical dissolved oxygen line separating storage from growth (ASM3)
C_{min}	($mg\ O_2\ L^{-1}$)	set-minimum dissolved oxygen concentration
C^*	($mg\ O_2\ L^{-1}$)	dissolved oxygen concentration at saturation
COD	($mg\ O_2\ L^{-1}$)	chemical oxygen demand
COD-S	($mg\ O_2\ L^{-1}$)	soluble COD fraction
COD-X	($mg\ O_2\ L^{-1}$)	insoluble COD fraction
CSTR		continuous stirred tank reactor
C^*	($mg\ O_2\ L^{-1}$)	dissolved oxygen concentration at saturation
D	(h^{-1})	dilution rate
D_{eq}	(mm)	aggregates equivalent diameter
$D_{eq\ ss}$	(mm)	aggregates equivalent diameter at equilibrium
D_{lag}	(mm)	aggregates equivalent diameter at $t = t_{lag}$
$D_{(K–S)}$	(–)	Kolmogorov–Smirnov goodness of fit statistic
DNS		dinitrosalicylic acid
DO		dissolved oxygen
EDSS		environmental decision support systems

EPS		extracellular polymeric substances
F_{cal}	(μm pixel^{-1}) (mm pixel^{-1})	metric calibration factor
f_E	(mg O_2 mg NOD^{-1})	autotrophs substrate oxidation yield
F_g	(L min^{-1})	air flow rate
f_S	(mg COD-X mg NOD^{-1})	autotrophs biomass yield
f_I	(g COD-I mg COD-S^{-1})	fraction of soluble inert organics (ASM3)
F(i,j)	(–)	One-way ANOVA F value and degrees of freedom
HRT	(d) (h)	hydraulic retention time
IAWQ		International Association of Water Quality
IWA		International Water Association
k	(–)	maintenance constant of Pirt (1982)
k_La	(h^{-1})	oxygen volumetric mass transfer coefficient
k_La_{min}	(h^{-1})	minimum oxygen volumetric mass transfer coefficient
K_{O2}	(mg O_2 L^{-1})	oxygen affinity constant
K_S	(mg COD-S L^{-1})	heterotrophs substrate affinity constant
K_{SA}	(mg N L^{-1})	autotrophs substrate affinity constant
k_{Sto}	(g COD-S g COD-X^{-1} h^{-1})	storage kinetic constant (ASM3)
K_{Sto}	(mg COD-X_{Sto} L^{-1})	storage affinity (ASM3)
L	(μm)	aggregate's length
L_{fil}	(μm)	filament's length
LPE		linear phenomenological equation
m	(g COD-S g COD-X–1 h^{-1})	maintenance coefficient of Pirt (1965)
M	(g mol^{-1})	molecular weight
m'	(g COD-S g COD-X–1 h^{-1})	maintenance coefficient of Neijssel and Tempest (1976)
m''	(g COD-S g COD-X–1 h^{-1})	maintenance coefficient of Pirt (1982)
n	(–)	number of repetitions
N_{agg}	(–)	aggregates number
N_{fil}	(–)	filaments number
NOD	(mg O_2 L^{-1})	nitrogenous oxygen demand
OC	(mg O_2 L^{-1})	amount of oxygen consumed
OUR		oxygen uptake rate
OLR	(g COD-S L^{-1} d^{-1})	organic loading rate
OUR_{end}	(mg O_2 h^{-1} L^{-1})	endogenous OUR
OUR_{exo}	(mg O_2 h^{-1} L^{-1})	exogenous OUR

$OUR_{exo\ max}$	(mg O_2 h^{-1} L^{-1})	maximum exogenous OUR
$OUR_{tot\ max}$	(mg O_2 h^{-1} L^{-1})	maximum total OUR
p		probability (p-value)
P_{conv}	(µm)	aggregate's convex perimeter
PLC		programmable logic controller
q	(g COD-S g COD-X^{-1} d^{-1})	specific substrate consumption rate
q_{max}	(g COD-S g COD-X^{-1} h^{-1})	maximum specific substrate consumption rate
$q_{O2\ max}$	(g O_2 g COD-X^{-1} h^{-1})	maximum specific oxygen consumption rate
RMSE	(–)	root mean squared error
Round	(–)	aggregate's roundness
r^2	(–)	square of the Pearson product-moment correlation coefficient
R1,2		reactor 1, and 2
S	(mg COD-S L^{-1})	substrate concentration
SBAR		sequencing batch airlift reactor
SBR		sequencing batch reactor
S_E		standard error
$SOUR_{exo}$	(g O2 g COD-X^{-1} h^{-1})	specific OUR_{exo}
$SOUR_{exo\ max}$	(g O2 g COD-X^{-1} h^{-1})	specific $OUR_{exo\ max}$
S_N	(mg N L^{-1})	autotrophs substrate concentration
S_{NP}	(mg N L^{-1})	ammonia pulse concentration
S_P	(mg COD-S L^{-1})	substrate concentration obtained after the injection of a pulse
SRT	(d)	sludge retention time
SVI_i	(mL g^{-1})	sludge volume index after i minutes of settling time
t	(d) (h)	time
TA	(mm^2)	aggregates total area
TA_{spec}	(mm^2 ml^{-1})	aggregates specific total area
t_{lag}	(d)	aggregates size-dependent growth lag phase
TL_{fil}	(mm)	total filaments length
TL_{spec}	(mm mL^{-1})	specific total filament length
t_{mix}	(s)	mixing time of the reactor
t_r	(h)	response time of the process
TS	(mg TS L^{-1})	total solids concentration
TSS	(mg TSS L^{-1})	total suspended solids concentration
t_0	(h)	time at which a pulse is injected

t_P	(h)	time at which a pulse ends
VSS	(mg VSS L^{-1})	volatile suspended solids concentration
W	(μm)	aggregate's width
WWTP		wastewater treatment plant
X	(mg COD-X L^{-1}) (mg VSS L^{-1})	biomass concentration
X^{Gran}	(mg COD-X_{Sto} L^{-1}) (mg VSS L^{-1})	granular biomass concentration
X_{Sto}	(mg COD-X_{Sto} L^{-1})	internal cell storage compound concentration (ASM3)
X^{Tot}	(mg COD-X_{Sto} L^{-1}) (mg VSS L^{-1})	total biomass concentration
$Y_{A\ X/S}$	(mg COD-X mg N^{-1})	autotrophs biomass growth yield
$Y_{O2/S}$	(mg O_2 mg COD-S^{-1})	heterotrophs substrate oxidation yield
$Y_{Sto/S}$	(mg COD-X_{Sto} mg COD-S^{-1})	storage yield (ASM3)
$Y_{X/S}$	(mg COD-X mg COD-S^{-1})	heterotrophs biomass growth yield
$Y'_{X/S}$	(mg COD-X mg COD-S^{-1})	true $Y_{X/S}$
$Y_{X/S}$ COD	(mg COD-X mg COD-S^{-1})	biomass growth yield estimated by COD mass balance
$Y_{X/S}$ resp	(mg COD-X mg COD-S^{-1})	biomass growth yield estimated by respirometry
$Y_{X/Sto}$	(mg COD-X mg COD-X_{Sto}^{-1})	storage growth yield (ASM3)
αβγδεζη	(–)	stoichiometric parameters
α	(–)	Variance
μ	(h^{-1})	specific growth rate
μ_{max}	(h^{-1})	maximum specific growth rate
μ_{size}	(d^{-1})	specific aggregates size-dependent growth rate
σ_i		standard deviation associated with parameter value i
Δ_i		absolute error of i

1. Motivation, Aim, and Thesis Outline

Abstract

The motivation behind the research done in this thesis is examined.

The aim of the research is stated.

The thesis outline is presented and explained.

1.1. Motivation

Microorganisms are essential for life. Without microorganisms and their degradative capabilities, life on earth would cease to exist, as life depends absolutely on microbial activities for environment renewal and maintenance of the global elemental compounds cycle (Ratledge, 1991).

Biotechnology is the use of microorganisms, such as bacteria or yeasts, to perform specific industrial processes intended to improve the quality of human life. Specifically, environmental biotechnology aims (i) the manufacture of products in environmentally harmonious ways, which allows for the minimisation of harmful residual outputs (solids, liquids or gaseous), or (ii) the remediation of contaminated environments (water, air, and soil), usually resulting from human activity (Evans and Furlong, 2003). Regarding the later, particularly in wastewater treatment, there is an increasing requirement to improve effluent quality due to the enhance awareness towards receiving waters protection. Additionally, it is required to minimise energy consumption and reduce the use of chemical treatment. Hence, new processes are continuously being developed and optimised.

For the development and optimisation of bioprocesses it is essential to be able to accurately characterise the biological culture in terms of kinetics and stoichiometry (Sipkema *et al*., 1998). Thus, the availability of reliable, cheap and versatile real-time monitoring tools providing information on the biological activity, is of crucial importance for monitoring and control of bioprocesses. Adequate monitoring techniques allow maximising the efficiency of bioprocesses, avoiding possible operational troubles through early detection of problems.

Aerobic microbial processes are extremely important in environmental biotechnology, namely in biological wastewater treatment where activated sludge process represents nowadays the most widespread technology for wastewater purification (Guisasola, 2005). A common feature of aerobic biotechnical processes is the difficulty of obtaining reliable information on the exact state of the biological system. This may be particularly critical in wastewater treatment plants (WWTPs) that receive influent waste streams from diverse sources, with sudden variations of flow and composition (Marsili-Libelli and Vaggi, 1997).

Respirometry has proven to be a powerful tool for monitoring numerous aerobic bioprocesses. The direct link between oxygen consumption and bioprocess behaviour in terms of biomass growth and substrate consumption sets respirometry as an invaluable

tool for real time aerobic bioprocesses characterisation and control (Spanjers *et al*., 1996). Despite the recognition of respirometry's potential for systems control, its implementation in real systems is not yet generalised. This might be due to a lack of understanding of the information which may be withdrawn from respirometric data.

In fact, many works on respirometry have been done in the last years (Figure 1.1), enlightening the relevance of respirometric techniques in biotechnology.

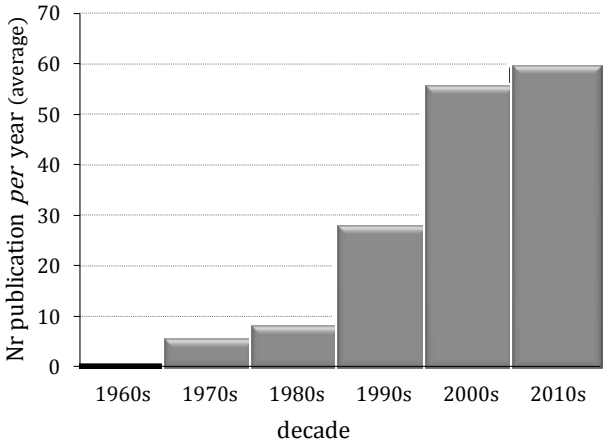

Figure 1.1. Average annual number of publication on respirometry *per* decade
[data from ISI Web of Science, search options: Topic = "respirometry"; Year Published = (***0-***9); Subject Areas = ("Environmental Sciences Ecology" OR "Biotechnology Applied Microbiology")].

During the 1980s and 1990s, great attention was given to respirometry applied to aerobic microbial processes as a tool to obtain practical information for monitoring and controlling purposes, whether for kinetic estimation (Ellis *et al*., 1996b; Grady *et al*., 1989; Cech *et al*., 1985), as for influent characterisation (Orhon *et al*., 1995; Kappeler and Gujer, 1992; Ekama *et al*., 1986) or inhibition, or prediction of toxic effects (Geenes and Thoeye, 1998; Kong *et al*., 1993; Volskay and Grady, 1990). This was associated with simple unstructured mathematical models. However, in the last decades, the wide availability of ever-increasing computational power increased the ability to deal with mathematic calculations (Rehm *et al*., 1991). Consequently the trend has drifted to a more detailed description of biological metabolism through complex mathematical models (Gujer *et al*., 1999; Vázquez-Padín *et al*., 2010). However as the complexity of models increases so does the number of undetermined parameters, *i.e.* complex models often include parameters that are not easily linked with practical observations, difficulting their direct use to assess the real state of the microbial cultures. Moreover, despite the large progress of mathematical modelling in environmental engineering, which allows the successful design

and operation of WWTPs able to achieve efficient and regular treatment levels, the WWTPs response to sudden and harsh influent perturbations is still often unpredictable.

Microbial response is the peremptory factor affecting the response behaviour of a WWTP to changes in the influent wastewater. Therefore, the development of assays able to rapidly and accurately estimate the biological performance and predict the impact on effluent quality during these transient periods is extremely important (Smets *et al*., 1996). In order to achieve the maximum concordance between the assays and reality, experimental conditions during the measurement ought to mimic as much as possible the conditions in the real system. This is due to the strong dependency of mixed bacterial culture response to its physiological state, which in turn is determined by the history of the culture (Grady *et al*., 1996). In other words, to predict the biological response to a certain change, the characteristics of interest are the culture's extant capabilities, rather than its intrinsic capabilities (Grady *et al*. 1995).

Summarising:

- Aerobic microbial processes are extremely important in Biotechnology, particularly, in the scope of this work, in Environmental Biotechnology.
- For the development of new bioprocesses and for the optimum operation of the existing bioprocesses it is crucial to have cheap, fast, and reliable monitoring tools.
- Respirometry has proven to be powerful tool for monitoring aerobic microbial processes due to the direct link between oxygen consumption and biological activity. However there is still a lack of understanding of the information obtained through respirometry, which restrain its wider application for monitoring and control of WWTPs.

So, there is still a niche in Environmental Biotechnology for a cheap and reliable tool for promptly assess kinetic and stoichiometric parameters of aerobic microbial cultures. Respirometry appears as a promising technique to occupy this niche, due to its versatility, rapidity, and economic convenience. Respirometric assays should mimic as close as possible the real system, or even be applied *in situ*, in order to obtain extant parameters which reflect the real state of the microbial culture. Additionally, treatment of respirometric data for the estimation of parameters should be coupled to models that incorporate and produce kinetic and stoichiometric parameters directly linked with

practical observation of the microbial cultures' state.

1.2. Aim

This thesis aims to develop respirometric methods for the reliable characterisation of aerobic bioprocesses used in environmental biotechnology. The developed methods are aimed to be simple, fast and economic, with high potential of being widely applied for monitoring aerobic microbial processes.

1.3. Thesis Outline

This thesis is organised according to the following structure (Figure 1.2).

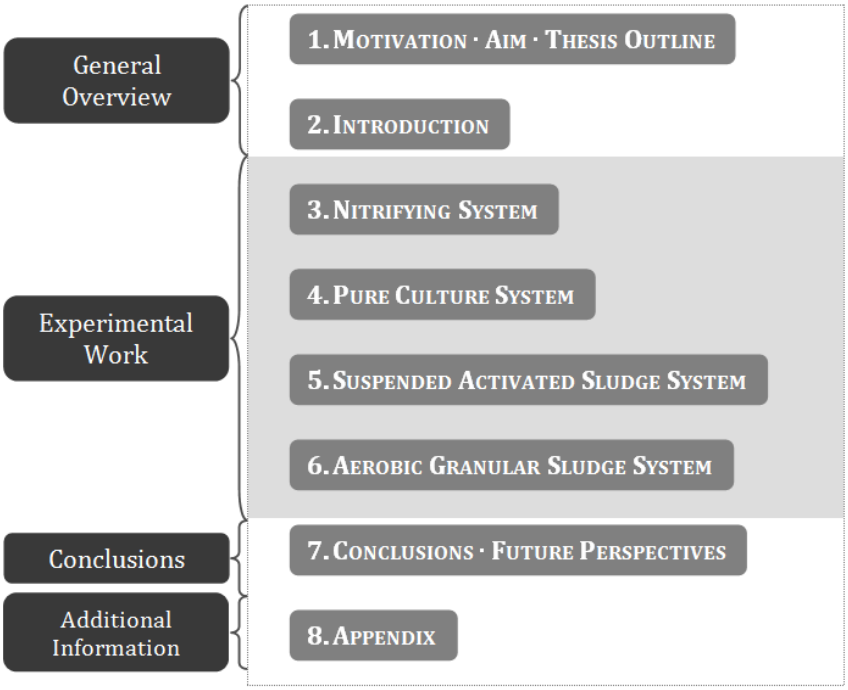

Figure 1.2. Thesis structure.

In this chapter (**Chapter 1**), the motivation and the aim of this thesis are presented.

The basic concepts of biological wastewater treatment, respirometry, and mathematical

modelling of aerobic microbial processes are presented in **Chapter 2**.

Chapters 3 to **6** are devoted to the presentation of the experimental work made in this thesis. In each chapter a concise introduction on the addressed concepts is given and the aim is presented (*Introduction*), the material and methods used are described (*Material and Methods*), the obtained results are presented and discussed (*Results and Discussion*), and finally the main conclusions are stated (*Conclusions*).

The presentation of the experimental work is organised according to the strategy adopted for the concretisation of the thesis. The adopted strategy for developing the respirometric method for the estimation of kinetic and stoichiometric parameters was to sequentially apply respirometry in different systems with increasing complexity. This allowed improving the respirometric method continuously.

In a preliminary phase of the project, pulse respirometry was tested in a suspended nitrifying biomass. **Chapter 3** is devoted to this research stage. Nitrification process was chosen for its simplicity. Substrate consumption is related only with growth and energy, no storage phenomena occur. The ASM1 model was used to fit the respirometric data. The results obtained allowed to establish the basic pulse respirometric methodology, and also the best method for estimating the oxygen mass transfer coefficient (k_La). This work was developed in Cinvestav – Mexico, in collaboration with Alberto Ordaz, whose Ph.D. thesis was entitled *Kinetic parameter determination in bioreactors by in situ pulse respirometry* (Ordaz *et al*., 2009).

After establishing the basic methodology, the pulse respirometric method was tested in a more complex system. A *Pseudomonas putida* pure culture system was chosen to test the applicability of pulse respirometry on biomass with storage ability. ASM3 was used for fitting the obtained data. The work related to this stage is presented in **Chapter 4**.

Pulse respirometry was then applied to a continuous suspended activated sludge process, fed with a complex synthetic medium. In this stage, a multiple pulses respirometric method was tested and it showed good correlation with the data. **Chapter 5** presents the results of this research stage.

The developed multiple pulses respirometric method was then applied to an aerobic granular system. The model proved to be adequate for parameter estimation on this system, and allowed the successful monitoring of aerobic granulation. **Chapter 6** regards

the results obtained on this stage.

Finally, the summary and concluding remarks of this research are presented in **Charter 7** along with some suggestions for further future work.

The research group in which this thesis is framed, the BRIDGE – Bioresources, Bioremediation and Biorefinery Group (former LBA – Laboratório de Biotecnologia Ambiental group) of University of Minho, has vast knowledge in quantitative image analysis (Costa *et al*., 2009a, 2009b, 2007; Abreu *et al*., 2007; Araya-Kroff *et al*., 2004; Amaral *et al*., 2004; Pereira *et al*., 2003; Alves *et al*., 2000). Taking advantage of this knowledge, quantitative image analysis was applied to the aerobic granular sludge system. The principal results obtained are included in the Appendix of this thesis (**Chapter 8**).

1.4. References

Abreu AA, Costa JC, Araya-Kroff P, Ferreira EC, Alves MM (**2007**). *Quantitative image analysis as a diagnostic tool for identifying structural changes during a revival process of anaerobic granular sludge*. Water Res. 41(7):1473–1480.

Alves MM, Cavaleiro AJ, Ferreira EC, Amaral AL, Mota M, Motta M, Vivier H, Pons MN (**2000**). *Characterisation by image analysis of anaerobic sludge under shock conditions*. Water Sci. Technol. 41(12):207–214.

Amaral AL, Pereira MA, Motta M, Pons MN, Mota M, Ferreira EC, Alves MM (**2004**). *Development of image analysis techniques as a tool to detect and quantify morphological changes in anaerobic sludge: II. Application to a granule deterioration process triggered by contact with oleic acid*. Biotechnol. Bioeng. 87(2):194–199.

Araya-Kroff P, Amaral AL, Neves L, Ferreira EC, Pons MN, Mota M, Alves MM (**2004**). *Development of image analysis techniques as a tool to detect and quantify morphological changes in anaerobic sludge: I. Application to a granulation process*. Biotechnol. Bioeng. 87(2):184–193.

Cech JS, Chudoba J, Grau P (**1985**). *Determination of kinetic constants of activated-sludge microorganisms*. Water Sci. Technol. 17(2–3): 259–272.

Costa JC, Alves MM, Ferreira EC (**2009a**). *Principal Component Analysis and quantitative image analysis to predict effects of toxics in anaerobic granular sludge*. Bioresource Technol. 100(3):1180–1185.

Costa JC, Moita I, Ferreira EC, Alves MM (**2009b**). *Morphology and physiology of anaerobic granular sludge exposed to organic solvents*. J. Hazard. Mater. 167(1–3):393–398.

Evans GM, Furlong JC (**2003**). *Environmental Biotechnology: Theory and Application*. England: John Wiley & Sons, Ltd. pp:2–3.

Grady CPL, Smets BF, Barbeau DS (**1996**). *Variability in kinetic parameter estimates: A review of possible causes and a proposed terminology*. Water Res. 30(3): 742–748.

Guisasola A (**2005**). *Modelling biological organic matter and nutrient removal processes from wastewater using respirometric and titrimetric.* Ph.D. Thesis. Universitat Autònoma de

Barcelona, Spain.

Gujer W, Henze M, Mino T, van Loosdrecht M (**1999**). *Activated Sludge Model No. 3*. Water Sci. Technol. 39(1):183–193.

Henze M, Grady CPL Jr, Gujer W, Marais GvR, Matsuo T (**1987**). *Activated Sludge Model No. 1. IAWPRC Scientific and Technical Report No. 1.* UK: IAWPRC.

Marsili-Libelli S, Vaggi A (**1997**). *Estimation of respirometric activities in bioprocesses*. J. Biotechnol. 52(3):181–192.

Ordaz A (**2009**). *Kinetic parameter determination in bioreactors by* in situ *pulse respirometry*. Pd.D. Thesis. Biotechnology and Bioengineering Department, Centro de Investigación y de Estudios Avanzados del Instituto Politecnico Nacional, Mexico DF, Mexico.

Pereira MA, Roest K, Stams AJM, Akkermans ADL, Amaral AL, Pons, MN, Ferreira EC, Mota M, Alves MM (**2003**). *Image analysis, methanogenic activity measurements, and molecular biological techniques to monitor granular sludge from an EGSB reactor fed with oleic acid*. Water Sci. Technol. 47(5):181–188.

Ratledge C (**1991**). Editorial in: *Physiology of Biodegradative Microorganisms*. The Netherlands: Kluwer Academic Publisher. pp:vii–viii.

Rehm HJ, Reed G, Pühler A, Stadler S (**1991**). *Biotechnology: A multivolume comprehensive treatise*. *Vol. 4 – Measuring, Modelling, and Control*. New York: VCH.

Sipkema EM, de Koning W, Ganzeveld KJ, Janssen DB, Beenackers AACM (**1998**). *Experimental pulse technique for the study of microbial kinetics in continuous culture*. J. Biotechnol. 64(2–3):159-176.

Smets BF, Fehniger SM, Grady CPL (**1996**). *Development of a respirometric assay to measure the transient load response of activated sludge to individual organic chemicals*. Water Sci. Technol. 33(6):49–55.

Spanjers H, Vanrolleghem P, Olsson G, Dold P (**1996**). *Respirometry in control of the activated sludge process*. Water Sci. Technol. 34(3–4): 117–126.

Vázquez-Padín JR, Mosquera-Corral A, Campos JL, Mendez R, Carrera J, Pérez J (**2010**). *Modelling aerobic granular SBR at variable COD/N ratios including accurate description of total solids concentration*. Biochem. Eng. J. 49(2): 173–184.

2. INTRODUCTION

Abstract

A small literature review on the main topics of this thesis is presented.

The basic principles of respirometry are presented, and the main applications are reviewed. The fundamentals of biological wastewater treatment are presented, and the processes studied in this thesis are briefly described, namely activated sludge process, aerobic biological oxidation, biological nitrification, and aerobic granular sludge process. Mathematical modelling concept is introduced, with focus on its applications, level of complexity, and model representation. Finally, the basic objectives and grounds of monitoring and process control are succinctly given.

2.1. Respirometry

Respirometry consists on the direct measurement and interpretation of the respiration rate of microorganisms (amount of oxygen consumed per unit of volume and time) under well defined experimental conditions (Spanjers *et al*., 1998). Respirometry data is often displayed by means of a respirogram, *i.e.* a graphical representation of the respiration rate as a function of time.

The basis of respirometry is the direct link between substrate consumption rate and oxygen-consumption rate in aerobic processes. Microorganisms obtain the required energy for cell living, growth, and reproduction through the generation of adenosine triphosphate (ATP). Cells convert the energy of intracellular bonds of the organic substrates (energy source) to the high-energy phosphate bonds of ATP. There are two routes for ATP production. One is cytoplasmic synthesis of ATP which is the direct transfer of a phosphate group to adenosine diphosphate (ADP), storing the energy of that reaction in chemical bonds. The second, and most significant cellular ATP production process, is oxidative phosphorylation, by which ATP is generated as electrons removed from the substrate by oxidation are transferred along an electron transport chain towards the terminal electron acceptor – oxygen in aerobic processes. Metabolic pathways operating in the overall direction of synthesis are termed anabolic while those operating in the direction of breakdown or degradation are described as catabolic: the terms catabolism and anabolism being applied to describe the degradative or synthetic processes respectively. Hence, a portion of the consumed substrate – the substrate portion which is oxidised consuming oxygen – is used in catabolic reaction, providing the energy requirements of the cells through oxidation to produce ATP, and the remainder portion is used in anabolic reactions, in which the substrate molecules are incorporated into new cells, promoting growth. Consequently catabolism is directly correlated with oxygen consumption as final electron acceptor, and the measurement of the respiration rate is an indirect measurement of substrate consumption rate and biomass growth (Figure 2.1).

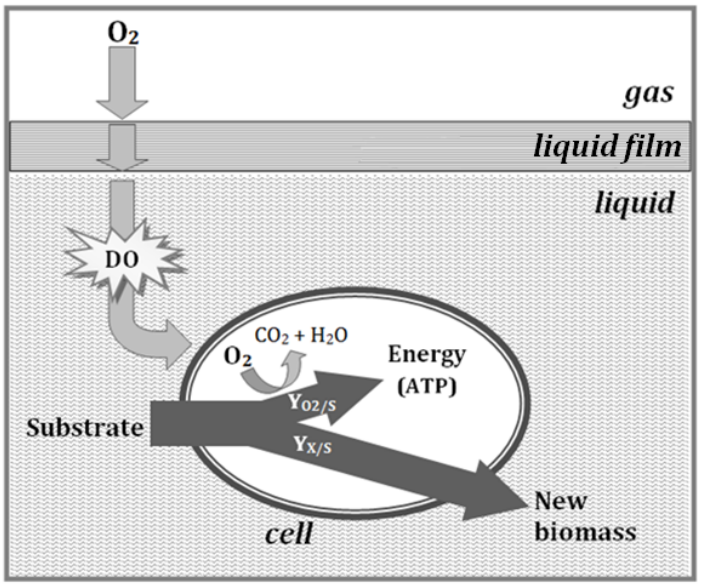

Figure 2.1. Schematic representation of the relationship between oxygen transfer, respiration, substrate consumption and biomass growth (adapted from Vanrolleghem, 2002a).

2.1.1. Measuring Principles

Dissolved oxygen (DO) concentration can be measured easily and continuously with relative small input of experimental effort and producing high-quality data. DO concentration changes in the order of ten parts-per-billion can be monitored online and at high frequency (Vanrolleghem and Verstraete, 1993). The absolute value of DO concentration (C) does not give sufficient information on the growth and substrate utilisation *per se*, it is necessary to determine the respiration rate, or in other words oxygen uptake rate (OUR).

Respirometry is typically applied in respirometers, although *in situ* application has been reported in lab-scale (Riefler *et al*., 1998). Respirometers range from a simple manually operated bottle equipped with a DO sensor, to complex instruments that operate fully automatically (Vanrolleghem, 2002a). A respirometer is not a traditional sensor, but rather it is a reactor in itself, where different components are brought together under controlled conditions to perform what may be called an "In-Sensor-Experiment", and in which the experimental conditions generally have a very large influence on the measurement results (Spanjers *et al*., 1996).

Many types of respirometers have been developed in the past, using different respiration rate measuring techniques. However the International Water Association – IWA (former

IAWQ) Task Group found that all these measuring techniques can be classified into merely eight basic principles according to two criteria: (1) the phase where oxygen concentration is measured (gas or liquid); and (2) whether or not there is input and output of liquid and/or gas (flowing or static) (Spanjers *et al.*, 1996). According to these principles, respirometric techniques can be classified as indicated in Figure 2.2.

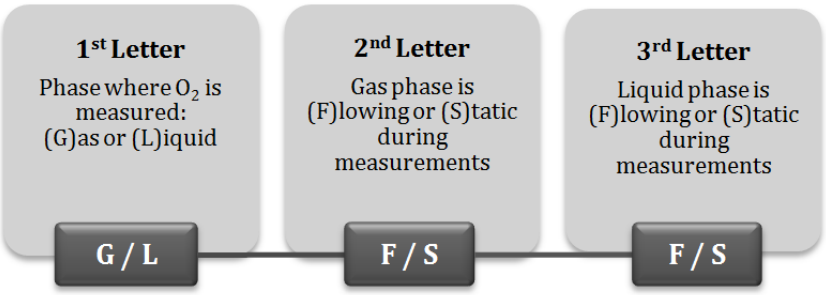

Figure 2.2. Classification of respirometers (adapted from Guisasola, 2005).

For most practical applications oxygen measurements are performed in the liquid phase. For a long time OUR was measured using LSS (static gas-static liquid) respirometers, *i.e.* oxygen was measured in the liquid phase when the aeration was stopped and the OUR value was determined as the slope of the DO drop. However, LSS respirometry had a great drawback: it's low measuring frequency, does not allow to measure fast occurring processes. Additionally, it had some technical problems, since the non-aerated periods required the reactor to be hermetic for an accurate OUR calculation, and the aerated periods needed an open-air reactor (Guisasola, 2005). In the mid 90s the LFS (flowing gas-static liquid) respirometric technique was developed at Ghent University (Vanrolleghem *et al.*, 1994). In a flowing gas-static liquid respirometer, the oxygen mass transfer must be pondered in the DO mass balance. According to the Lewis-Whitman theory (Lewis and Whitman, 1924), oxygen transfer is considered to be limited by diffusion through the liquid film at the gas/liquid interface. Consequently, a DO gradient is determined by DO concentration found at each side of the liquid film; namely saturation at gas/liquid interface and bulk concentration at liquid film/bulk liquid interface (Figure 2.1). Thus, the mass transfer term in the DO mass balance is $k_La(C^* - C)$ (Equation 2.1).

$$\frac{dC}{dt} = k_La(C^* - C) - OUR \qquad (2.1)$$

where, C is the DO concentration in the liquid phase; t is time; k_La is the oxygen mass transfer volumetric coefficient; C^* is the DO saturation concentration in the liquid phase;

and OUR is the biomass oxygen uptake rate, or in other words the respiration rate.

To obtain the respiration rate, both the differential term and the mass transfer term must be determined. The differential term is obtained from DO measurements along time. To calculate the mass transfer term, the k_La and the C^* must be known.

The main advantages of the LFS respirometer are: (i) a continuous OUR profile can be obtained, with a frequency that equals the DO frequency; (ii) the LFS technique implementation is very simple, since it only requires an accurate mass flow meter and a fast DO probe; and (iii) since flowing gas-static liquid respirometers are continuously aerated, the continuous input of oxygen avoids oxygen limitation and allows high sludge concentrations to be used (Blok, 1974; Farkas, 1981; Ros *et al*., 1988), which in turn allow shorter experiment times. The main inconvenience of this setup is that it requires knowledge of the k_La and C^* to measure OUR (Equation 2.1). Moreover, these coefficients have to be determined regularly because they depend on environmental conditions such as temperature, barometric pressure and the properties of the liquid (Vanrolleghem, 2002a). The most common methodology of k_La estimation is based on a perturbation on the aeration of the system, *i.e.* turning the aeration off for a period and then re-aerating the system. C^* is generally considered the oxygen saturation concentration in water at the temperature, altitude, and salinity conditions existing in the respirometer, albeit the probable inaccuracy of this consideration, since oxygen solubility is also dependent on the characteristics of the liquid. It should be noted that the oxygen dynamics might not be visible if the oxygen transfer coefficient k_La is too high. Moreover, too high aeration intensity may increase the risk of measurement noise. It is thus important to optimise the aeration in the respirometer in such a way that a reliable respiration rate value can be obtained (Gernaey *et al*., 2001).

LFS respirometers are based on measuring the rate at which microorganisms takes up DO from the liquid (Equation 2.1). After the introduction of the polarographic oxygen sensor, often referred as “Clark cell”, in 1959, this type of sensor became more and more commonly used in respirometers. Currently about 50 % of the commercial respirometer brands are based on a polarographic DO-sensor (Vanrolleghem, 2002a).

A polarographic oxygen electrode is composed of two half cells separated by a salt bridge: the cathode (typically gold or platinum) is separated from the anode (typically silver) by insulating material, and both are immersed in an aqueous electrolyte solution of potassium chloride. The electrodes are separated from the sample by a semi-permeable membrane (Teflon or silicone) that allows for DO to diffuse to the internal chamber where

it is reduced at the cathode, generating an electrical current (Equation 2.2–2.4).

$$\textit{Cathode:} \quad 2e^- + {}^1/_2\, O_2 + H_2O \leftrightarrow 2OH^- \tag{2.2}$$

$$\textit{Anode:} \quad 2Ag^+ + 2Cl^- \leftrightarrow 2AgCl + 2e^- \tag{2.3}$$

$$\textit{Overall:} \quad 2Ag^+ + 2Cl^- + H_2O + {}^1/_2\, O_2 + 2e^- \leftrightarrow 2AgCl + 2OH^- + 2e^- \tag{2.4}$$

The generated current is proportional to the diffusion rate of oxygen molecules through the membrane, which in turn is proportional to the DO concentration in the sample, guaranteed the sample is stirred to ensure homogeneity and to ensure that oxygen can freely diffuse into the electrode. The relationship between electrical current and DO concentration is established through the DO sensor calibration. A reliable respiration rate measurement is only possible if the DO sensor is correctly calibrated and if a number of environmental variables, such as temperature, salinity of the sample and altitude where measurement is done are defined, as all these parameters affect the DO concentration. Nowadays, most DO-meters offer DO automatic compensation adjustments for temperature, salinity, and altitude. Additionally, DO sensors have a response time, which must be accounted for in respirometric measurements.

2.1.2. Respirometry Applications

The respiration rate of a microbial community is affected by (i) the rates of metabolic processes, which in turn depend on the kinetics, stoichiometry, and components concentrations (substrate, inhibitors, *etc*.), and by (ii) the transport rates, which are in turn dependent on the substrate and biomass concentrations. Because all these characteristics of a biological system affect respiration rate, the other way around, respiration rate measurements, *i.e.* respirometry, can be used to assess these characteristics. Hence, all parameters and components involved in the microbial process that are, directly or indirectly, connected to the respiration rate can be assessed from respirometry, namely: (i) kinetic parameters; (ii) stoichiometric parameters; and (iii) component concentrations (Vanrolleghem *et al*., 1999). All these parameters are of undoubted importance in an activated sludge process, and thus respirometry is a valuable tool for the design, monitoring, and control of the process.

Within many respirometric techniques, pulse respirometry, developed in the mid 80s and 90s is probably one of the most used (Cech *et al*., 1985; Spanjers and Vanrolleghem, 1995;

Riefler *et al*., 1998). It consists in following the respiration rate response of an endogenous microbial community to the injection of a defined substrate concentration pulse. After the injection of substrate pulses, the kinetic parameters are usually estimated by direct model fitting to a respirometric curve.

There are two approaches for the estimation of stoichiometric and kinetic parameters, and components: (i) direct methods, which focus on specific parameters and components directly evaluated from the measured respiration rates (Spanjers *et al*., 1999); and (ii) fitting methods, in which a model is used to fit the measured data, obtaining the parameter values that lead to the smallest deviation between model predicted respiration rates and the measured respiration rates (Vanrolleghem *et al*., 1999). These later are the most common methods, whether using simpler or more complex models (Spangers and Vanrolleghem, 1995; Goudar and Ellis, 2001).

Pulse Respirometry

The DO concentration in a continuous aerated respirometer is determined by two processes, (i) the oxygen supply by continuous aeration, and (ii) the microbial oxygen uptake rate (OUR). During aerobic biological oxidation, oxygen is consumed by aerobic organisms for endogenous respiration, *i.e.* oxygen consumption for maintenance (Dawes and Ribbons, 1964), and for exogenous respiration, *i.e.* oxygen consumption for carbon-substrate oxidation (Equation 2.5).

$$\frac{dC}{dt} = k_L a\left(C^* - C\right) - OUR_{tot} = k_L a\left(C^* - C\right) - OUR_{end} - OUR_{exo} \qquad (2.5)$$

where, C (mg O_2 L^{-1}) is the DO concentration; t (h) is time; C^* (mg O_2 L^{-1}) is the DO saturation concentration; and OUR_{end} and OUR_{exo} (mg O_2 L^{-1} h^{-1}) are the endogenous and exogenous oxygen uptake rates, respectively.

An example of the DO profile resulting from the addition of a substrate pulse to a continuously aerated system (respirometer) under endogenous state is shown in Figure 2.3.

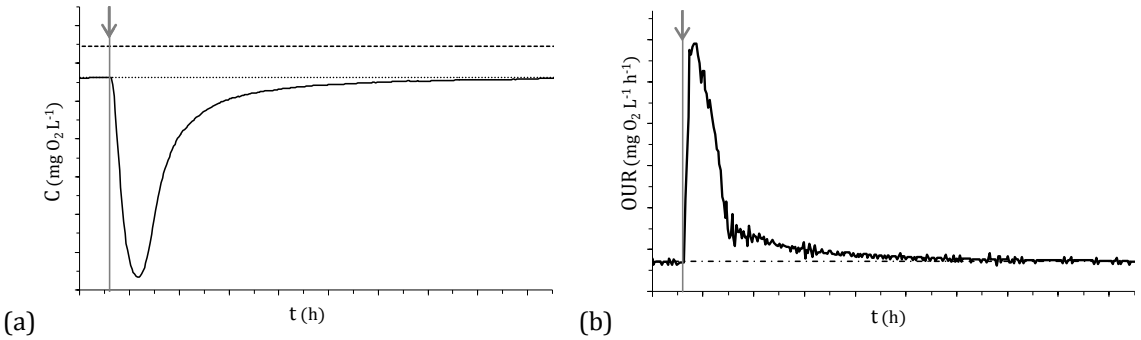

Figure 2.3. DO concentration profile obtained with the injection of a substrate pulse (*injection time marked by grey arrow and line*) in to an endogenous state system (a), and corresponding respirogram (b). DO saturation concentration (*dashed line*); DO baseline level (*dotted line*); Endogenous oxygen uptake rate (*dash-dotted line*).

Before pulse injection, *i.e.* in the absence of substrate, only endogenous respiration occurs. Endogenous oxygen consumption is constant with time and is dependent only on the biomass and the rate coefficient for endogenous metabolism (Button, 1985). Biomass growth due to substrate pulse addition is usually negligible within the time of the experiment, so endogenous respiration is constant. Thus, the DO concentration before pulse addition is in a steady state, the so called baseline level (C_b) (Vanrolleghem and Verstraete, 1993). Accordingly to Equation 2.5, endogenous OUR can be determined by the area between the saturation DO concentration and the baseline level (Equation 2.6).

$$\frac{dC}{dt} = k_L a\left(C^* - C_b\right) - OUR_{end} = 0 \Rightarrow OUR_{end} = k_L a\left(C^* - C_b\right) \quad (2.6)$$

When a substrate pulse is injected, there is an immediate increase in respiration due to exogenous respiration, and so DO concentration rapidly decreases (Figure 2.3). Since the available substrate is limited, the exogenous respiration decreases due to substrate limitations. As a result the DO level increases and returns to the baseline level once substrate is depleted and microorganisms re-enter endogenous metabolism (Vanrolleghem and Verstraete, 1993). The system is then ready for the injection of another substrate pulse. Accordingly to Equation 2.5, and since endogenous respiration is constant, the exogenous OUR can be determined by the area between the DO baseline level and the DO concentration during the pulse (Equation 2.7).

$$\frac{dC}{dt} = k_L a(C_b - C) - OUR_{exo} \quad (2.7)$$

Due to the strong stoichiometric link (Equation 2.8) between oxygen consumption and substrate consumption, OUR_{exo} reflects the kinetics of substrate aerobic biodegradation by heterotrophic microorganisms. A portion of the consumed substrate is oxidised to provide

the energy required for the cells, and the remainder portion is used for the growth of new cells (Figure 2.1).

$$Y_{X/S} + Y_{O2/S} = 1 \quad (2.8)$$

where, $Y_{X/S}$ (g COD-X g COD-S^{-1}) is the biomass growth yield, and $Y_{O2/S}$ (g O_2 g COD-S^{-1}) is the substrate oxidation yield.

$Y_{O2/S}$ is defined as the amount of oxygen consumed (OC) per COD unit of substrate oxidised (Equation 2.9).

$$Y_{O2/S} = \frac{OC}{S_P} = \frac{\int_{t_0}^{t_P} OUR_{exo}}{S_P} = \frac{k_L a \int_{t_0}^{t_P} (C_b - C) dt}{S_P} \quad (2.9)$$

Accordingly to Equation 2.8, $Y_{X/S}$, expressed in COD units, can be estimated from $Y_{O2/S}$ (Equation 2.10).

$$Y_{X/S} = 1 - Y_{O2/S} = 1 - \frac{k_L a \int_{t_0}^{t_P} (C_b - C) dt}{S_P} \quad (2.10)$$

where, S_P (mg COD-S L^{-1}) is the substrate concentration obtained after the injection of the pulse, and t_0 and t_P (h) are the time at which a pulse is injected and the time the same pulse ends, respectively.

Because substrate and oxygen are directly linked stoichiometrically, exogenous OUR profiles yield the same information as substrate consumption profiles (Equation 2.11), allowing the estimation of substrate degradation kinetics.

$$\frac{dC}{dt} = -Y_{O2/S} \frac{dS}{dt} \quad (2.11)$$

where, S (mg COD-S L^{-1}) is the substrate concentration.

2.2. Biological Wastewater Treatment

Wastewater is any water that has been adversely affected in quality by anthropogenic influence, *i.e.* caused or produced by humans. Wastewater is typically categorised into one of the following groups: (i) *domestic wastewater*, produced only in households; (ii) *municipal wastewater*, composed of domestic wastewater mixed with effluent from commercial and industrial works, pre-treated or not pre-treated; and (iii) *industrial wastewater*, produced by industrial or commercial activities, pre-treated or not pre-treated.

Biological processes for wastewater treatment consist of mixed communities with a wide variety of microorganisms, including bacteria, protozoa, fungi, rotifers, and possibly algae (Metcalf and Eddy, 2003), which are able to consume pollutants present in wastewater. The large majority of wastewater containing biodegradable components is feasible to be biologically treated, provided the proper conditions. Therefore, it is essential to understand the characteristics of each biological process in order to ensure that the proper environment is produced, and effectively controlled, to assure efficient treatment.

Biological degradation of organic chemicals during wastewater treatment proceeds either in the presence of molecular oxygen – *aerobic treatment*, by respiration under anoxic conditions – e.g. *denitrification*, or under anaerobic conditions – *anaerobic treatment*. Focus will be given to aerobic processes.

Until the early 1900s the main purpose of biological wastewater treatment was to remove organic constituents (***aerobic biological oxidation***) and suspended solids, and to reduce the concentration of pathogenic organisms, preventing the development of nuisance conditions in receiving waters, namely excessive dissolved oxygen (DO) depletion and accumulation of solids. Later it was recognised that the discharge of nutrients via domestic wastewater was the main cause for eutrophication, which is the excessive growth of algae in surface and coastal waters, and several new wastewater treatment concepts have been developed which allow the biological removal of nutrients, particularly nitrogen (***nitrification***) and phosphorus.

2.2.1. Activated Sludge Process

Activated sludge process is the most common process in the world for treating municipal and industrial wastewater. Activated sludge consists of a community of microorganisms capable of stabilising a waste under aerobic conditions. Activated sludge is obtained by the continuous repetition of four basic steps: (1) aeration of sewage for several hours, (2) sludge sedimentation, (3) removal of the clarified water, and (4) addition of new sewage. This process was discovered by Edward Arden and William T. Lockett, and first presented in Manchester in 1914. The first technical-scale activated sludge plant was constructed in Sheffield, UK, in 1920 (Wiesmann *et al*., 2007).

A conventional activated sludge process is represented in Figure 2.4. The wastewater flows into an aeration tank where it is mixed with the activated sludge, constituting the mixed liquor. In the aeration tank, contact time is provided for mixing and aerating. Oxygen can either be supplied by aeration or by injection of pure oxygen. The two process variants for oxygen supply differ mainly in their capacity for oxygen transfer and the stripping efficiency for carbon dioxide from respiration. Stripping of carbon dioxide is required to prevent a drop in pH and to remove heat energy (Jördening and Winter, 2005). The mixed liquor then flows to a clarifier, where the microbial suspension is settled and thickened, producing the actual activated sludge. In fact, a central feature of the activated sludge process is the formation of flocculent biomass, which can be easily removed by gravity in clarifiers. The clarified liquid, *i.e.* the treated effluent, is finally withdrawn. Part of the activated sludge is removed from the system, while the rest is returned to the aeration tank to continue biodegradation of the influent wastewater. The performance of the activated sludge process is affected by a number of factors, among which the aeration efficiency, the microbial community profile, the settling ability of the sludge, temperature, pH, wastewater toxicity, *etc*.

Depending on process loading and environmental conditions, a number of undesirable organisms can also develop in the activated sludge process. One of the principal problems caused by nuisance organisms is the bulking sludge, in which the biological flocs have poor settling characteristics due to an excessive growth of filamentous bacteria. In the extreme, bulking sludge can result in high effluent suspended solids concentration and poor treatment performance. Another nuisance condition, foaming, has been related to the development of bacteria which have hydrophobic cell surfaces and attach to air bubble surfaces, where they stabilise the bubbles to cause foam.

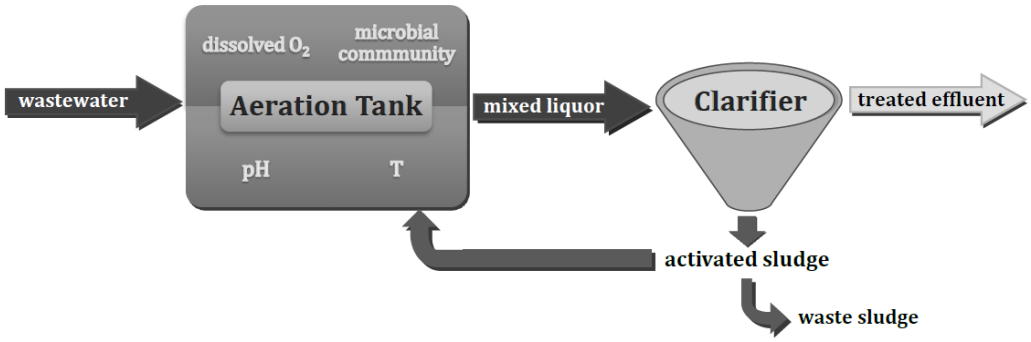

Figure 2.4. Scheme of the activated sludge process.

In most cases, the activated sludge process is employed in conjunction with physical and chemical processes which are used for preliminary and primary wastewater treatment, and post treatment. Numerous process configurations of the activated sludge process have been proposed, mainly aiming at the integration of carbon, nitrogen and phosphorus removal.

2.2.2. Aerobic Biological Oxidation

Most wastewater treatment applications involve the removal of a wide range of carbonaceous constituents, which should be quantified by aggregated general parameters. Usually the organic content of a wastewater is quantified in terms of soluble chemical oxygen demand (COD) or biological oxygen demand (BOD). Though BOD has been the common parameter to characterise carbonaceous material in wastewaters, COD is recently becoming more common, being the primary parameter for carbonaceous organic matter in most WWTP models. Because biomass is mostly organic material, it can be measured by volatile suspended solids (VSS) or particulate/insoluble COD (total COD minus soluble COD). Typically, the biomass concentration (X) is measured as VSS. Considering its general formula $C_5H_7NO_2$, biomass expressed in VSS can easily be converted to COD (1.42 g O_2 g X^{-1}) (Equation 2.12).

$$C_5H_7NO_2 + 5O_2 \rightarrow 5CO_2 + 2\,H_2O + NH_3 \qquad (2.12)$$

(M = 113 g mol^{-1}); (X = 1.42 g COD-X g VSS-X^{-1})

The most common approach used to define the fate of the substrate is to apply a COD mass balance to the wastewater treatment process. COD allows describing both the substrate and the biomass concentration in terms of oxygen equivalence – the general formula

assumed for new cells being $C_5H_7NO_2$ (Metcalf and Eddy, 2003). This way, through the COD balance, the fate of carbonaceous fraction oxidised (catabolism) and the fraction incorporated into the cell (anabolism) can be more easily followed (Metcalf and Eddy, 2003).

The removal of carbonaceous matter can be accomplished in a variety of aerobic suspended growth or attached growth treatment processes. The main requirements for the efficiency of the processes are sufficient contact time between the wastewater and the microorganisms, and sufficient oxygen and nutrients supply. During the biological uptake of the organic material, more than half of it is oxidised and the remainder is assimilated as new biomass. As a consequence, for both suspended and attached growth processes, the excess biomass produced each day is removed and processed to maintain proper operation and performance (Metcalf and Eddy, 2003). In WWTPs, the two costliest processes are aeration and excess sludge treatment. Hence, it is extremely important, in an economical point of view, to efficiently control these two processes.

2.2.3. Biological nitrification

Nitrogen concentration in raw municipal wastewater range from 15 to 50 mg N L^{-1}, of which approximately 60 % is in the form of ammonia, 40 % is organic nitrogen, and a negligible amount is nitrite and nitrate nitrogen. These values highlight the urgency of nitrogen removal during wastewater treatment for environment protection, given that high level of nitrogen in aquatic habitats may severely disturb the ecological balance, affecting the DO concentration and fish toxicity, and contributing for eutrophication (Weismann *et al*., 2007). Accordingly, there are increasing discharge demands for nitrogen. In comparison to physical/chemical approaches, the cheapest alternative to meet the required effluent standards is biological nitrogen removal through nitrification and denitrification processes (Gernaey *et al*., 1997).

Biological nitrification refers to the biological oxidation of ammonia to nitrate. This process involves two distinguish steps (Equations 2.13–2.15): (1) first ammonia is oxidised to nitrite (***nitritation***), and then (2) nitrite is converted to nitrate (***nitratation***). These two steps involve two phylogenetically different groups of aerobic, autotrophic bacteria, being the two most common genera in wastewater treatment *Nitrosomonas* and *Nitrobacter*, performing nitritation and nitratation, respectively (Weismann *et al*., 2007). Since the growth rate of *Nitrobacter* is higher than that of *Nitrosomonas*, the rate limiting

step in nitrification is usually the degradation of ammonia to nitrite (Bitton, 2005).

Nitritation: $NH_4^+ + {}^3/_2\, O_2 \rightarrow NO_2^- + 2H^+ + H_2O$ (2.13)

Nitratation: $NO_2^- + {}^1/_2\, O_2 \rightarrow NO_3^-$ (2.14)

Nitrification (overall)*:* $NH_4^+ + 2O_2 \rightarrow NO_3^- + 2H^+ + H_2O$ (2.15)

(NOD = 4.57 g O_2 g N-NH_4^{-1})

The oxygen demand of nitrogenous compounds is referred to as nitrogenous oxygen demand (NOD). Theoretically, for the complete nitrification of ammonia to nitrate, a total of 4.57 g of oxygen are needed to oxidise 1 g of nitrogen in the form of ammonia (Equation 2.15). However, in practice the oxygen required for nitrification is always lower than the theoretical value presented, because a part of the consumed nitrogen is used for cell synthesis, *i.e.* for biomass growth (Equation 2.16). Nitrifying bacteria oxidise nitrogen compounds to obtain energy for growth and maintenance, and obtain carbon for cell building through the reduction of carbon dioxide.

$$\alpha\, NH_4^+ + \beta\, O_2 + \gamma\, CO_2 \rightarrow \delta\, C_5H_7NO_2 + \varepsilon\, NO_3^- + \zeta\, H^+ + \eta\, H_2O \quad (2.16)$$

Considering the oxygen demand, only ammonia (expressed as NOD, Equation 2.15), oxygen, and biomass (expressed as COD, Equation 2.12) have to be taken into account in Equation 2.16. Applying an oxygen mass balance, Equation 2.17 is obtained, where 64 is the mass of oxygen (g) needed to oxidise 1 mole of ammonia, and 160 is the amount of oxygen (g) needed to oxidise 1 mole of biomass produced.

$$64.0\,\alpha - 32.0\,\beta = 160.0\,\delta \quad (2.17)$$

Rearranging Equation 2.17, Equation 2.18 is obtained, where the first term is the substrate oxidation yield (f_E), *i.e.* the fraction of nitrogen-substrate used for energy production, and the second term is the biomass growth yield (f_S), *i.e.* the fraction of nitrogen-substrate captured for biomass synthesis.

$$\underbrace{\frac{32.0\beta}{64.0\alpha}}_{f_E} + \underbrace{\frac{160.0\delta}{64.0\alpha}}_{f_S} = 1 \quad (2.18)$$

There are two approaches for nitrification by activated sludge: (i) the combined stage, where nitrification is achieved along with organic matter removal in a single-sludge system consisting of an aeration tank, a clarifier, and sludge recycling (Figure 2.4), and where the fraction of nitrifying organisms in the activated sludge is dependent of the

N/COD ratio in the wastewater (Dinçer and Kargi, 2000); and (ii) the separate stage systems, consisting of two units (two aeration tank and two clarifiers) in series, isolating the organic matter removal and the nitrification processes so that each can be separately controlled and optimised. The combined stage systems are more compact than the separate stage systems; on the other hand, the chances for toxic and inhibitory disturbances are greater, while in the separate stage systems toxic substances are removed in the first unit, so that nitrification can proceed unhindered in the second unit (Bitton *et al*., 2005; Metcalf and Eddy, 2003; Cheremisinof, 1996).

2.2.4. Aerobic Granular Sludge

The two major challenges recognised worldwide in the field of wastewater biological treatments are (i) the treatment of high organic loads, and (ii) the treatment of diluted wastewater.

The treatment of wastewaters with high organic loads in conventional activated sludge systems, gives rise to an excess of sludge production and high energy consumption, which originates high treatment costs; in such cases anaerobic processes are an alternative, since besides having a much lower sludge production, also allow the production of biogas which can be used as a renewable energy source. On the other hand, for diluted wastewaters anaerobic treatment is not feasible (Liu and Tay, 2004; Jördening and Winter, 2005); conventional activated sludge systems, although efficient in this kind of wastes with low sludge production, require large areas, especially for biomass-effluent separation. There is, therefore, a niche in wastewater treatment technology for systems with operational flexibility in terms of loading capacity, and ability to remove both organics and nutrients in compact structures. Activated sludge processes with aerobic granular sludge constitute a strong alternative due to its: small footprint (De Bruin *et al.*, 2004), ability to remove organics and nutrients in a single unit (Yang *et al*., 2003; De Kreuk *et al*., 2005a; Kishida *et al*., 2008), high conversion capacity (Carvalho *et al.*, 2006), low sludge production (Di Iaconi *et al.*, 2007), operational flexibility (Di Iaconi *et al.*, 2008), and versatility in treating a variety of wastewater (De Kreuk and van Loosdrecht; 2006; Carucci *et al.*, 2008; Adav *et al.* 2007; Inizan *et al.*, 2005).

Aerobic granules definition was set by a panel of experts during the 1st Aerobic Granular Sludge Workshop in 2004 (De Kreuk *et al*., 2005b):

Granules making up aerobic granular activated sludge are to be understood as aggregates of microbial origin, which do not coagulate under reduced hydrodynamic shear, and which settle significantly faster than activated sludge flocs.

In the 2nd Aerobic Granular Sludge Workshop in 2006, the characteristics of aerobic granules stated in the previous definition were explained, clarifying when to refer to aerobic sludge (De Kreuk *et al*., 2007b):

- *Aggregates of microbial origin* – This implies that aerobic granules need to contain active microorganisms, aggregates composed only of components of microbial origin (as proteins, EPS, *etc*.) are not to be considered aerobic granules. This states also that aerobic granules are formed with no addition of carrier material. Aerobic granulation is a self-immobilisation process.

- *No coagulation under reduced hydrodynamic shear* – This sets the difference between activated sludge flocs and aerobic granular sludge in terms of mode of settling, when mixed liquor is not mixed, *i.e.* no aeration nor stirring: activated sludge flocs tend to coagulate while they settle; whereas aerobic granules do not coagulate and settle as individual units.

- *Which settle significantly faster than activated sludge flocs* – Sludge volume index (SVI) is used for characterisation of settling properties of a sludge. For activated sludge SVI over a settling period of 30 minutes (SVI_{30}) is used, and values of SVI_{30} between 100 and 150 mL g^{-1} indicate good settling of the sludge. However, aerobic granular sludge settles much faster, *i.e.* the terminal SVI_{30} is already reached after 5 minutes of settling (SVI_5) (Schwarzenbeck *et al*., 2004). This means that SVI_5 and SVI_{30} should be used for characterising the settling ability of granular activated sludge. The difference between the SVI_5 and SVI_{30} value gives an indication of granules formation and indicates the extent of thickening after settling.

- *The minimum size of the granules should be such that the biomass still fulfils the previous point* – Based on the previous knowledge on aerobic granules this minimum size was set to 0.2 mm. Nevertheless, this could be adjusted per case or granule type, provided that all the other conditions of the definition stand.

- *Sieving is considered a proper method to harvest granules from activated sludge tanks or from aerobic granule reactors* – This, besides providing a tool to handle aerobic granules, also determines certain required strength of the aerobic granules.

Aerobic Granulation Process

Aerobic granulation is a gradual self-immobilisation process in which loose sludge flocs convert to compact aggregates, and further to mature granules (Tay *et al*., 2001a). The most favourable form for microorganisms to grow is in suspension, since it is the form in which less substrate and nutrient diffusion resistance exist. The next favourable form of growth is in flocs, where diffusion resistance is slender, and finally in granules or biofilms, where diffusion resistance is considerable (Beun *et al*., 2002). Hence, for aerobic granulation process to occur, an inducing force or a set of inducing forces must act on microorganisms, bringing them together and making them aggregate (Liu and Tay, 2004).

Even though aerobic granulation was first reported in a continuous aerobic up flow sludge blanket reactor (Mishima and Nakamura, 1991), it has ever since been reported chiefly in sequencing batch reactors (SBR). The operation of a SBR comprises essentially four steps (Figure 2.5): (1) influent feeding; (2) aeration phase; (3) settling; and (4) effluent withdrawal.

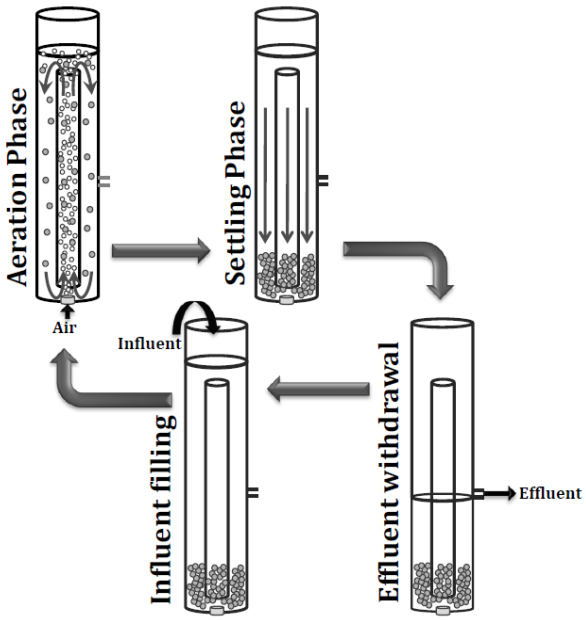

Figure 2.5. Sequencing Batch Airlift Reactor (SBAR) scheme of operation (○–*air bubbles*; and ●–*aerobic granules*).

This mode of operation allows manipulating key operational parameters, associated with inducing forces which trigger microorganisms to aggregate, among which the most significant are listed below.

- ***Critical settling velocity*** – Critical settling velocity is the minimum settling

velocity that particles must have to be effectively retained in the reactor (Beun *et al*., 2000). In a SBR, this restriction is controlled through the manipulation of three operational parameters (Liu *et al*., 2005a,b): the settling time (McSwain *et al*., 2004; Qin *et al*., 2004a,b; Wang *et al*., 2005; Ni *et al*., 2009); the effluent withdrawal time (Arrojo *et al*., 2004); and the volume exchange ratio (Ni *et al*., 2009), which is defined as volume of the effluent withdrawn to total working volume of the reactor, and is determined by the depth of the effluent withdrawal port. The critical settling velocity is recognised as the main selection pressure for inducing aerobic granulation in SBR (Wang *et al*., 2006; Liu *et al*., 2005a,b; Beun *et al*., 1999,2000; Kim *et al*., 2004). Selection is based on screening of fast settling particles: particles settling slower than the critical settling velocity will be washed-out, while those settling faster will be retained in the reactor. The typical settling velocity of activated sludge is less than 3 to 5 m h^{-1} (Giokas *et al*., 2003), thus by selecting a higher critical settling velocity, the suspended sludge and flocs are washed out and aerobic granulation is fomented. On the other hand, if the selected critical settling velocity is lower than that of suspended sludge and flocs, these will not be efficiently washed out, this will lead to aerobic granulation failure due to the production of mixtures of aerobic granules and suspended sludge, or by the inexistence of aerobic granules (Qin *et al*., 2004a,b). Therefore the critical settling velocity must be set to a value higher than the settling velocity of activated sludge; otherwise successful aerobic granulation will not be achieved and maintained.

- ***Shear stress*** – Shear stress is a key factor influencing aerobic granulation (Liu and Tay, 2002; De Kreuk and van Loosdrecht, 2006). In a bioreactor, shear force is caused by hydraulics, *i.e.* gas or liquid flow, and by particles collisions. Hydrodynamic shear force in bubble columns and airlift SBRs is essentially caused by the aeration rate. Shear stress is thought to be involved in the initial cell-to-cell attachment phenomena (Liu and Tay, 2002). Relatively high shear force as superficial up flow air velocity (above 1.2 cm s^{-1}), has been shown to be required for enhancing aerobic granulation, whereas at low shear force as superficial air velocity, stable aerobic granules did not form (Tay *et al*., 2001b; Beun *et al*., 1999; Tay *et al*., 2004a). Aeration rate, besides contributing for the hydrodynamic shear force in a reactor, is also involved in reducing substrate mass transfer resistance and supplying oxygen to the system. This role of aeration rate has been shown to be of great importance in aerobic granulation process (McSwain and Irvine, 2008; Adav *et al*., 2008). Shear stress constitutes the main source of detachment force during

granulation. When granules are already formed, the collisions between granules also contribute as detachment force. For successful aerobic granules formation, a compromise between detachment and growth forces must exist (Chen *et al*., 2008; Beun *et al*., 1999; Liu *et al*., 2004). Growth is fomented by the organic loading rate supplied to the reactor. Granules may be considered a special case of biofilm growth, in which self-immobilisation occurs with no need for a carrier (Beun *et al*., 2000; Wilderer and McSwain, 2004; McSwain *et al*., 2005). Nevertheless, the growth mechanism may be considered the same. A general accepted growth mechanism suggests biofilms to outgrow preferentially in protuberances extending from the biofilm surface (Van Loosdrecht *et al*., 1995). These protuberances, subjected to detachment by shear force, are continuously removed. Consequently, stability is achieved by a balance between growth and detachment forces. Thus, an adequate shear stress as aeration rate is needed for the formation of stable aerobic granules.

- ***Feast-famine regime*** – In the SBR, microorganisms are subjected to cyclic fluctuations in the environmental conditions. During the aeration phase of the SBR cycle microorganisms experience feast and famine/starvation periods: after the feeding phase, substrate is available and is depleted to a minimum, after which microorganisms go through a starvation period. Starvation plays an important role in the aerobic granulation process (Liu and Tay, 2004; Liu and Tay, 2007b), comprising an effective trigger for microbial aggregation and further strengthening cell-to-cell interactions, supporting granules stabilisation (Tay *et al*., 2001; Di Iaconi *et al*., 2006; Li *et al*., 2006; Schwarzenbeck *et al*., 2005). Starvation is controlled in a SBR through the organic loading rate fed to the system and the duration of the aeration phase.

These inducing forces act on microorganisms which respond by modifying some characteristics in such a way that self-immobilisation occurs and aerobic granules are formed.

Mechanisms of aerobic granulation

Beun *et al*. (1999) suggested the first mechanism of aerobic granulation (Figure 2.6). The suggested mechanism stated that filaments play a preponderant role in the start-up of granulation, building up pellets which settle well and are therefore retained in the reactor, while suspended bacteria and free filaments tend to be washed out from the reactor (2–4 in Figure 2.6). These filamentous pellets function as an immobilisation support where

bacteria can grow out to form micro-colonies (5 in Figure 2.6). Latter, the filamentous pellets break out due to lysis of the inner part, probably due to oxygen transport limitation, and the bacterial micro-colonies and filaments are released; while filaments are discharged from the reactor due to their low settling ability (6–7 in Figure 2.6), the micro-colonies are retained in the reactor (8 in Figure 2.6) and further grow out, transforming into granules (9 in Figure 2.6).

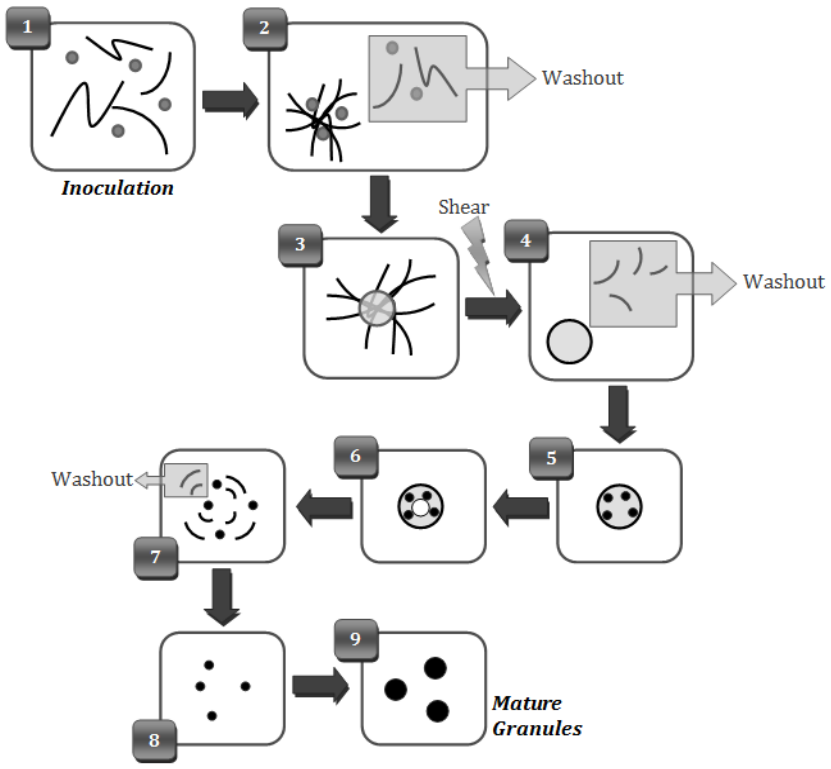

Figure 2.6. Aerobic granulation mechanism: 1. *Inoculation;* 2. *Washout of free bacteria and filaments;* 3. *Formation of filamentous pellets;* 4. *Removal of protruding filaments from pellets surface due to shear forces;* 5. *Bacterial micro-colonies form in the filamentous pellets;* 6. *Core of the pellet weakens;* 7. *Lysis of the pellet and washout of free filaments;* 8. *Retention of bacterial micro-colonies;* 9. *Development of mature aerobic granules* (adapted from Beun *et al.*, 1999).

More recently, with larger insights into the granulation process, a more structured mechanism was proposed (Liu and Tay, 2002). This mechanism of aerobic granulation is composed essential of four steps:

Step 1. Initial cell-to-cell contact by physical movement through: hydrodynamics, diffusion mass transfer, gravity, thermodynamic effects, and cell mobility.

Step 2. Primary aggregates formation through the action of initial attractive forces,

namely: physical forces (Van der Waals forces, opposite charge attraction, thermodynamically driven reduction of the surface free energy, surface tension, hydrophobicity, filamentous bacteria can bridge individual cells); chemical forces (hydrogen liaison, formation of ionic pairs and triplet, inter-particulate bridge, *etc*.); biochemical forces (cellular surface dehydration, cellular membrane fusion and collective action in bacterial community) .

Step 3. Maturation of the aggregates through microbial forces, such as production of EPS, growth of cellular clusters, metabolic changes, and environment-induced genetic effects, that strengthen cell–cell interactions, resulting in organised microbial structures, *i.e.* granules.

Step 4. Stabilisation of the three dimensional structure of the granules by hydrodynamic shear forces. The characteristics of the stable granules are determined by the interactive between detachment and growth forces, *i.e.* between hydrodynamic shear force and microbial species and substrate loading rate.

Aerobic Granular Sludge Stability

The application of aerobic granular sludge is viewed as a very promising wastewater treatment technology. However, long-term stability of aerobic granules is the current bottleneck obstructing the practical settlement of aerobic granular sludge technology as a viable alternative to conventional wastewater treatment.

Aerobic granules stability is associated with characteristics such as settling ability, morphology, granules density and strength, bioactivity, microbial structure and diversity, and EPS content and composition. Some mechanisms have been shown to be responsible for the loss of granule stability at long-term operation, including: (i) outgrowth of filamentous organisms which produces light and bulky granules easily washed out (Morgenroth *et al*., 1997; Liu and Liu, 2006, Li *et al*., 2010); (ii) hydrolysis of the anaerobic core (Tay *et al*., 2002a; Zheng *et al*., 2006, Adav *et al*., 2009); (iii) function loss of strains (Adav *et al*., 2010); (iv) role of EPS; and (v) other mechanisms (Lemaire *et al*., 2008; Moy *et al*., 2002).

Some strategies were proposed to enhance granule stability during long-term operation: (i) applying appropriate operational conditions (Liu and Tay, 2007; Li *et al*., 2007; Wang *et al*., 2007a; Liu *et al*., 2010); (ii) selecting slow-growing organism; (De Kruek and van Loosdrecht, 2004; Liu *et al*., 2004); (iii) suppressing activity of anaerobes; (Tay *et al*.,

2002b); (iv) strengthening granule (Wang *et al*., 2007). Nevertheless, stability loss of aerobic granular sludge at long-term operation is still an unsolved problem.

2.3. Mathematical Modelling

A mathematical model is a description of reality, which facilitates understanding of natural processes and allows predicting and controlling certain aspects of reality on the basis of past observations. There is a direct relationship between the capability of a model to faithfully describe real systems and its mathematical complexity (Rehm *et al*., 1991). Gleick (1987) perfectly described this dichotomy:

You can make your model more complex and more faithful to reality or you can make it simpler and easier to handle. Only the most naive scientist believes that the perfect model is one that perfectly represents reality. Such a model would have the same drawbacks as a map as large and detailed as the city it represents, a map depicting every park, every street, every building, every tree, every pothole, every inhabitant and every map. Were such a map possible its specificity would defeat its purpose: to generalise and abstract.

2.3.1. Applications and Level of complexity

Most processes in nature are far too complex to be understood in detail, activated sludge is an example. In order to perceive complex processes, simplifications must be postulated. The perspective and the extent of the considered simplifications will determine the application of a model. Mathematical models may have several applications with regard to WWTPs (Olson and Nessel, 1999):

- ***Research and design*** – Mathematical models allow predicting the system behaviour under different circumstances, optimising the process design and the process control. The consequences of new knowledge may be explored, testing new control strategies on the process, surveying the influence of different input disturbances and parameter changes in the systems efficiency. For such application, deterministic models are often required. Deterministic models aim to give a realistic description of the main processes of the plant.

- ***Operation and control*** – Mathematical models allow operating and controlling the process to the desired performance with the use of on-line and laboratory measurements to develop new control actions. Control of treatment plants is an important field, for which it is often possible to use simplified models.

- ***Diagnosis*** – Mathematical models allow interpreting patterns in the plant data, detecting abnormalities and suggesting causes. Either complex or simplified models may be required, depending on the insight needed for the diagnosis.

The depth of detail needed depends on the intended use of the model and on the amount of information available on the wastewater and the treatment plant. Thus, the intended use of a model determines its structure (Jördening and Winter, 2005).

In the automated design of WWTPs and in the context of environmental decision support systems (EDSS), where it is necessary to characterise WWTPs as a dynamic system, there is a growing demand for sophisticated models (Iacopozzi *et al*., 2007, Poch *et al*., 2004, Gabaldón *et al*., 1999).

On the other hand, in control applications, simplified models are often adequate. A common approach is to consider the macroscopic system description, in which the system is treated in terms of macroscopic variables, such as mass and energy. A well known example is the black-box model. In black-box models the actual system is not known, instead it is described in terms of balances, *i.e.* exchanges (influents and effluents) of compounds with the environment A black-box model only describes the system behaviour under specific conditions. The details happening in the actual process remain unknown (Meijer, 2004).

2.3.2. Model Representation

Models in the biological wastewater treatment area are commonly presented in the matrix notation for chemical reactions, as used by Petersen (1965). This practice was started in 1986, when the first Activated Sludge Model (ASM1) for biological carbon and nitrogen removal was introduced. The matrix notation allows presenting the complex interrelationships between the various components and processes in a simple and comprehensive way. Additionally, the common representation and nomenclature facilitates the communication and allows the focusing of discussions on essential aspects of bio-kinetic modelling (Henze *et al.*, 2000).

For terms of illustration, the matrix of a very simple model of organic matter removal in a continuous aerated system is presented in Table 2.1.

Table 2.1. Simple model matrix for activated sludge organic removal under constant aeration

Process	***Component***			***Process Rate***
	C	**S**	**X**	
aeration	1			$k_L a(C^* - C)$
aerobic growth	$-\frac{Y_{O2/S}}{Y_{X/S}}$	$-\frac{1}{Y_{X/S}}$	1	$\mu_{max}\, X\, \frac{S}{K_S + S}$
decay			-1	$b_H X$

The matrix notation presents (i) the processes considered in the model in the left column; (ii) the rate equations of the processes in the right column; (iii) stoichiometric coefficients of each component associated with each process in the middle columns. Through the matrix notation is easy to have a handle on:

- ***Component Participation*** – The middle columns give an overview of which processes the various components participate in (according to the model). As an example, in the forth column in Table 2.1, associated with the biomass component (X), it is shown that biomass is produced by the *aerobic growth* process (positive stoichiometric coefficient) and consumed by the *decay* process (negative stoichiometric coefficient).

- ***Rates*** – The rate equations of each process allow to obtain the rate at each component is consumed or produced by each process. In Table 2.1, for example, to obtain the rate at which biomass is consumed by *decay*, the rate equation of decay is multiplied by the stoichiometric coefficient (Equation 2.19).

$$\left(\frac{dX}{dt}\right)_{decay} = (-1)\cdot b_H X \qquad (2.19)$$

- ***Mass balances*** – Mass balances are obtained by following the column of the component to balance and summing the product of each stoichiometric coefficient with the corresponding rate equation of each process in which the component is involved. For example, from Table 2.1 the mass balance regarding dissolved oxygen concentration (C) is given by Equation 2.20.

$$\frac{dC}{dt} = (1) \cdot k_L a\left(C^* - C\right) \left(-\frac{Y_{O2/S}}{Y_{X/S}}\right) \cdot \mu_{max} X \frac{S}{K_S + S} \quad (2.20)$$

2.4. Monitoring and Process Control

The basic objectives in the operation of WWTPs are to keep the plant running, while meeting the effluent standard and minimising costs. To achieve these basic objectives, a number of operational objectives must be defined, and control objectives must be met through the use of either manual or automatic controllers (Figure 2.7; Vanrolleghem, 2002b).

The WWTP treatment efficiency is ensured through the proper choice of operating variable, which in turn is done based on the feedback given by monitoring results.

Monitoring is the systematic collection of information which allows assessing the state of the process. It is applied to the different variables involved in the process:

- ***Inputs*** are variables that influence the process. Inputs can be manipulatable – manipulated variables; or non-manipulatable – disturbances
- ***Outputs*** are variables which are influenced by the inputs (Figure 2.8).

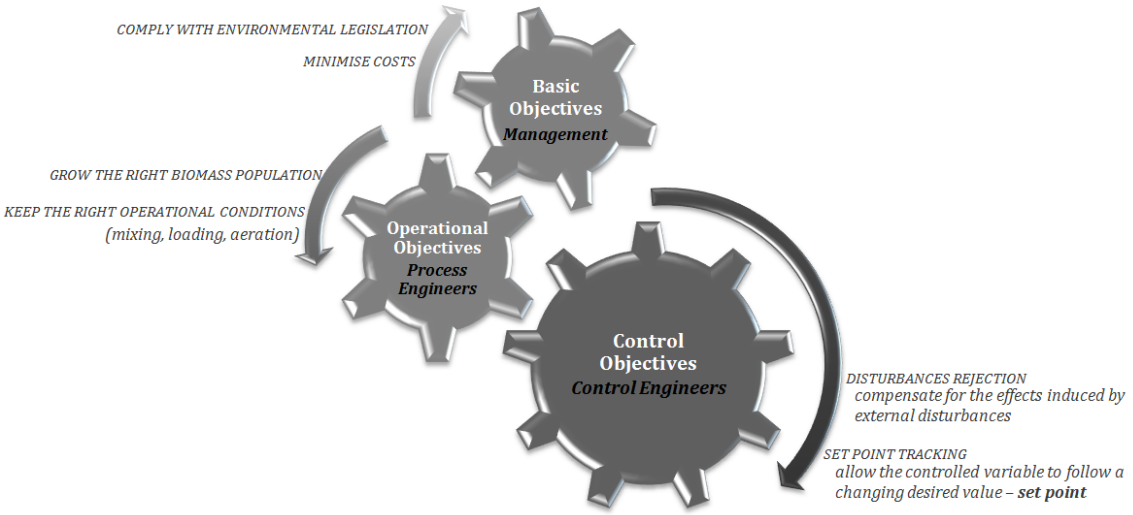

Figure 2.7. Levels of objectives in the operation of WWTPs and relation to professionals involved (*inside the gears*), and the pressures acting to accomplish these objectives (adapted from Vanrolleghem, 2002b).

An adequate regime of sampling and monitoring, supported by means to ensure corrective action when the monitoring results show it necessary, is essential to ensure proper operation of WWTP.

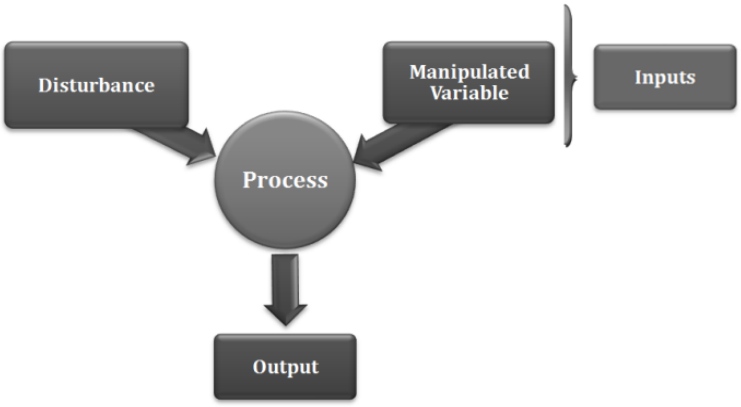

Figure 2.8. Diagram with *inputs* (*disturbance* and *manipulated variable*), *process*, and *output* relations (adapted from Vanrolleghem, 2002b).

There are two basic types of control, the feedback and the feedforward (Figure 2.9). In the classical feedback (Figure 2.9a) the measured variables are compared to the set point values, *i.e.* the reference values, and the manipulated variables are adjusted in such a way the measured variables are kept as close as possible to the set point values, despite the disturbances (disturbance rejection). Alternatively, when disturbance can be measured, feedforward may be used (Figure 2.9b). In feedforward control, the manipulated variable is adjusted to compensate for the anticipated effect of the disturbance on the process. Ideally, the effects of the measured disturbance are entirely anticipated and the adjustments made on the manipulated variable allow completely cancelling out these effects, and there is no deviation from the set point.

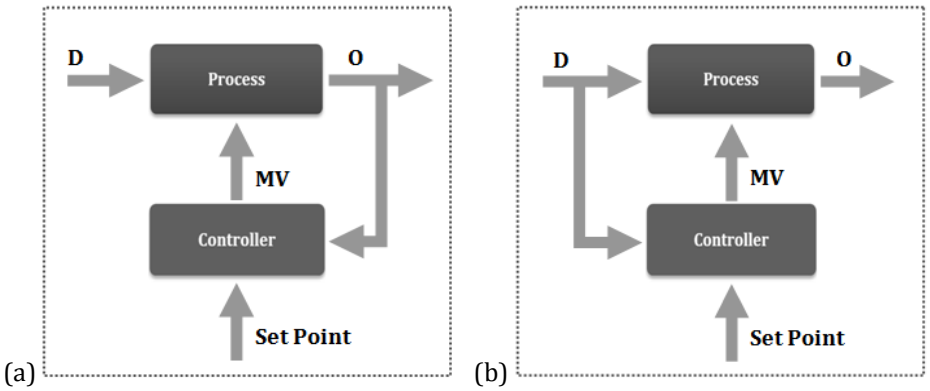

Figure 2.9. Types of control: feedback (a), and feedforward (b)
(*D – disturbance; MV – manipulated variable; O – output*).

A feedforward controller requires a ***model,*** to calculate how much adjustment of the manipulated variable is required in order to cancel out the effect of the disturbances. Thus, the performance of feedforward control depends greatly on the quality of the model used, and its accuracy in predicting the effect of the disturbance.

In a biological wastewater treatment process, the key determinant in the response behaviour of the system is the microbiological response. Parameters traditionally used to assess the operation of the WWTP, such as COD or solids content, are often insufficient for controlling purposes in the biological process operation. There is also a need to predict how activated sludge would respond to different influents as well as to changes in their composition and concentration (Orupold *et al*., 1999). To do so, the kinetic and stoichiometric parameters of the microbial community need to be regularly assessed to evaluate the state and activity of the culture. . Nevertheless, the accuracy of the estimated parameters is profoundly dependent on the nature of the experiments by which parameters are estimated. To estimate parameters which accurately characterise the microbiological system response (*extant parameters*), the measurement experiment must closely mimic the conditions in the continuous system (Grady *et al*., 1996).

2.5. References

Adav SS, Lee DJ, Lai JY (**2010**). *Potential cause of aerobic granular sludge breakdown at high organic loading rates*. Appl. Microbiol. Biot. 85(5):1601–1610.

Adav SS, Lee DJ, Lai JY (**2009**). *Proteolytic activity in stored aerobic granular sludge and structural integrity*. Bioresource Technol. 100(1):68–73.

Adav SS, Lee DJ, Show KY, Tay JH (**2008**). *Aerobic granular sludge: Recent advances*. Biotechnol. Adv. 26(5):411-423.

Adav SS, Chen MY, Lee DJ, Ren NQ (**2007**). *Degradation of phenol by aerobic granules and isolated yeast* Candida tropicalis. Biotechnol. Bioeng. 96(5):844–852.

Arrojo B, Mosquera-Corral A, Garrido JM, Mendez R (**2004**). *Aerobic granulation with industrial wastewater in sequencing batch reactors*. Water Res. 38(14–15):3389–3399.

Beun JJ, van Loosdrecht MCM, Heijnen JJ (**2002**). *Aerobic granulation in a sequencing batch airlift reactor*. Water Res. 36(3):702-712.

Beun JJ, van Loosdrecht MCM, Heijnen JJ (**2000**). *Aerobic granulation*. Water Sci. Technol. 41(4–5):41–48.

Beun JJ, Hendriks A, van Loosdrecht MCM, Morgenroth E, Wilderer PA, Heijnen JJ (**1999**). *Aerobic granulation in a sequencing batch reactor*. Water Res. 33(10):2283–2290.

Bitton G (**2005**). *Wastewater microbiology*. NJ, USA: Wiley-Liss.

Blok J (**1974**). *Respirometric measurements on activated sludge*. Water Res. 8(1):11–18.

Carucci A, Milia S, de Gioannis G, Piredda M (**2008**). *Acetate-fed aerobic granular sludge for the degradation of chlorinated phenols*. Water Sci. Technol. 58(2): 309–315.

Carvalho G, Meyer RL, Yuan Z, Keller J (**2006**). *Differential distribution of ammonia- and nitrite-oxidising bacteria in flocs and granules from a nitrifying/denitrifying sequencing batch reactor*. Enzyme Microb. Tech. 39(7): 1392–1398.

Cech JS, Chudoba J, Grau P (**1985**). *Determination of kinetic constants of activated-sludge microorganisms*. Water Sci. Technol. 17(2–3): 259–272.

Chen Y, Jiang W, Liang DT, Tay JH (**2008**). *Aerobic granulation under the combined hydraulic and loading selection pressures*. Bioresource Technol. 99(16):7444–7449.

Cheremisinoff NP (**1996**). *Biotechnology for Waste and Wastewater Treatment*. NJ, USA: Noyes Publications.

Dawes EA, Ribbons DW (**1964**). *Some aspects of endogenous metabolism of bacteria*. Bacteriol. Rev. 28(2): 126–149.

De Bruin LMM, de Kreuk MK, van der Roest HFR, Uijterlinde C, van Loosdrecht MCM (**2004**). *Aerobic granular sludge technology: an alternative to activated sludge?* Water Sci. Technol. 49(11–12):1–7.

De Kreuk MK, van Loosdrecht MCM (**2006**). *Formation of aerobic granules with domestic sewage*. J. Environ. Eng.–ASCE 132(6):694–697.

De Kreuk M, Heijnen JJ, van Loosdrecht MCM (**2005a**). *Simultaneous COD, nitrogen, and phosphate removal by aerobic granular sludge*. Biotechnol. Bioeng. 90(6): 761-769.

De Kreuk MK, McSwain BS, Bathe S, Tay STL, Schwarzenbeck N, Wilderer PA (**2005b**). *Discussion outcomes*. In Aerobic Granular Sludge, Bathe, S., De Kreuk, M.K., Mc Swain, B.S. and Schwarzenbeck, N. London, UK: IWA, pp.153–169.

De Kreuk MK, van Loosdrecht MCM (**2004**). *Selection of slow growing organisms as a means for improving aerobic granular sludge stability*. Water Sci. Technol. 49(11–12):9–17.

Di Iaconi C, de Sanctis M, Rossetti S, Ramadori R (**2008**). *Technological transfer to demonstrative scale of sequencing batch biofilter granular reactor (SBBGR) technology for municipal and industrial wastewater treatment*. Water Sci. Technol. 58(2):367–372.

Di Iaconi C, Ramadori R, Lopez A, Passino R (**2007**). *Aerobic granular sludge systems: The new generation of wastewater treatment technologies*. Ind. Eng Chem. Res. 46(21):6661–6665.

Di Iaconi C, Ramadori R, Lopez A, Passino R (**2006**). *Influence of hydrodynamic shear forces on properties of granular biomass in a sequencing batch biofilter reactor*. Biochem. Eng. J. 30(2):152–157.

Dinçer AR, Kargi F (**2000**). *Kinetics of sequential nitrification and denitrification processes*. Enzyme Microb. Tech. 27(1–2):37–42.

Farkas PA (**1981**). *The use of respirography in biological treatment plant control*. Water Sci. Technol. 13(9):125–131.

Gabaldón C, Ferrer J, Seco A, Marzal P (**1999**). *A software for the integrated design of wastewater treatment plants*. Environ. Modell. Softw. 13:31–44.

Gernaey AK, Petersen B, Ottoy JP, Vanrolleghem P (**2001**). *Activated sludge monitoring with combined respirometric-titrimetric measurements*. Water Res. 35(5): 1280–1294.

Gernaey K, Bogaert H, Massone A, Vanrolleghem P, Verstraete W (**1997**). *On-line nitrification monitoring in activated sludge with a titrimetric sensor*. Environ. Sci. Technol. 31(8):2350–2355.

Giokas DL, Daigger GT, von Sperling M, Kim Y, Paraskevas PA (**2003**). *Comparison and evaluation of empirical zone settling velocity parameters based on sludge volume index using a unified settling characteristics database*. Water Res. 37(16):3821–3836.

Gleick J (**1987**). *Chaos*. England: Penguin Books, p:278.

Goudar CT, Ellis TG (**2001**). *Explicit oxygen concentration expression for estimating biodegradation kinetics from respirometric experiments*. Biotechnol. Bioeng. 75(1):74–81.

Grady CPL, Smets BF, Barbeau DS (**1996**). *Variability in kinetic parameter estimates: A review of possible causes and a proposed terminology*. Water Res. 30(3): 742–748.

Guisasola A (**2005**). *Modelling biological organic matter and nutrient removal processes from wastewater using respirometric and titrimetric.* Ph.D. Thesis. Universitat Autònoma de Barcelona, Spain.

Henze M, Gujer W, Mino T, van Loosdrecht MCM (**2000**). *Activated Sludge Models ASM1, ASM2, ASM2d, and ASM3*. *IWA Scientific and Technical Report*. London, UK: IWA Publishing.

Iacopozzi I, Valentina Innocenti, Stefano Marsili-Libelli , Elisabetta Giustin (**2007**). *A modified Activated Sludge Model No. 3 (ASM3) with two-step nitrification–denitrification*. Environ. Modell. Softw. 22(6): 847-861.

Inizan M, Freval A, Cigana J, Meinhold J (**2005**). *Aerobic granulation in a sequencing batch reactor (SBR) for industrial wastewater treatment*. Water Sci. Technol. 52(10–11): 335–343.

Jördening HJ, Winter J (**2005**). *Environmental Biotechnology – Concepts and Applications*. Germany: Wiley–VCH, Weinheim.

Kim SM, Kim SH, Choi HC, Kim IS (**2004**). *Enhanced aerobic floc-like granulation and nitrogen removal in a sequencing batch reactor by selection of settling velocity*. Water Sci. Technol. 50(6):157–162.

Kishida N, Tsuneda S, Sakakibara Y, Kim JH, Sudo R (**2008**). *Real-time control strategy for simultaneous nitrogen and phosphorus removal using aerobic granular sludge*. Water Sci. Technol. 58(2): 445–450.

Lemaire R, Webb RI, Yuan ZG (**2008**). *Micro-scale observations of the structure of aerobic microbial granules used for the treatment of nutrient-rich industrial wastewater*. ISME J. 2(5):528–541.

Li AJ, Zhang T, Li XY (**2010**). *Fate of aerobic bacterial granules with fungal contamination under*

different organic loading conditions. Chemosphere 78(5):500–509.

Li J, Garny K, Neu T, He M, Lindenblatt C, Horn H (**2007**). *Comparison of some characteristics of aerobic granules and sludge flocs from sequencing batch reactors*. Water Sci. Technol. 55(8–9):403–411.

Li ZH, Kuba T, Kusuda T (**2006**). *The influence of starvation phase on the properties and the development of aerobic granules*. Enzyme Microb. Tech. 38(5):670–674.

Liu Y, Liu QS (**2006**). *Causes and control of filamentous growth in aerobic granular sludge sequencing batch reactors*. Biotechnol. Adv. 24(1):115–127.

Liu YQ, Tay JH (**2007**). *Characteristics and stability of aerobic granules cultivated with different starvation time*. Appl. Microbiol. Biot. 75(1):205-210.

Liu Y, Tay JH (**2004**). *State of the art of biogranulation technology for wastewater treatment*. Biotechnol. Adv. 22(7): 533–563.

Liu Y, Tay JH (**2002**). *The essential role of hydrodynamic shear force in the formation of biofilm and granular sludge*. Water Res. 36(7):1653–1665.

Liu YQ, Moy B, Kong YH, Tay JH (**2010**). *Formation, physical characteristics and microbial community structure of aerobic granules in a pilot-scale sequencing batch reactor for real wastewater treatment*. Enzyme Microb. Tech. 46(6):520–525.

Liu Y, Wang ZW, Tay JH (**2005a**). *A unified theory for upscaling aerobic granular sludge sequencing batch reactors*. Biotechnol. Adv. 23(5):335–344.

Liu Y, Wang ZW, Qin L, Liu YQ, Tay JH (**2005b**). *Selection pressure-driven aerobic granulation in a sequencing batch reactor*. Appl. Microbiol. Biot. 67(1):26–32.

Liu Y, Yang SF, Tay JH (**2004**). *Improved stability of aerobic granules by selecting slow-growing nitrifying bacteria*. J. Biotechnol. 108(2):161–169.

McSwain BS, Irvine RL (**2008**). *Dissolved oxygen as a key parameter to aerobic granule formation*. Water Sci. Technol. 58(4):781–787.

McSwain BS, Irvine RL, Hausner M, Wilderer PA (**2005**). *Composition and distribution of extracellular polymeric substances in aerobic flocs and granular sludge*. Appl. Environ. Microb. 71(2):1051–1057.

McSwain BS, Irvine RL, Wilderer PA (**2004**). *The influence of-settling time on the formation of aerobic granules*. Water Sci. Technol. 50(10): 195–202.

Meijer SCF (**2004**). *Theoretical and practical aspects of modeling activated sludge processes*. Ph.D. Thesis. Delft University of Technology, The Netherlands.

Metcalf & Eddy Inc (**2003**). *Wastewater Engineering: Treatment and Reuse*, Fourth Edition. Civil and Environmental Engineering Series, McGraw–Hill International Editions.

Mishima K, Nakamura M (**1991**). *Self-immobilization of aerobic activated sludge a pilot study of the aerobic upflow sludge blanket process in municipal sewage treatment*. Water Sci. Technol. 23(4–6):981–991.

Morgenroth E, Sherden T, van Loosdrecht MCM, Heijnen JJ, Wilderer PA (**1997**). *Aerobic granular sludge in a sequencing batch reactor*. Water Res. 31(12):3191–3194.

Moy BYP, Tay JH, Toh SK, Tay TL (**2002**). *High organic loading influences the physical characteristics of aerobic sludge granules*. Lett. Appl. Microbiol. 34(6):407–412.

Ni BJ, Xie WM, Liu SG, Yu HQ, Wang YZ, Wang G, Dai XL (**2009**). *Granulation of activated sludge in a pilot-scale sequencing batch reactor for the treatment of low-strength municipal wastewater*.

Water Res. 43(3):751–761.

Olsson G, Newell B (**1999**). *Wastewater treatment systems*. London, UK: IWA Publishing.

Orupold K, Hellat K, Tenno T (**1999**). *Estimation of treatability of different industrial wastewaters by activated sludge oxygen uptake measurements*. Water Sci. Technol. 40(1): 31–36.

Petersen EE (**1965**). *Chemical reaction analysis*. NJ, USA*:* Prentice Hall.

Poch M, Comas J, Rodríguez-Roda J, Sànchez-Marrè M, Cortés U (**2004**). *Designing and building real environmental decision support systems*. Environ. Modell. Softw. 19:857–873.

Qin L, Liu Y, Tay JH (**2004a**). *Effect of settling time on aerobic granulation in sequencing batch reactor*. Biochem. Eng. J. 21(1): 47–52.

Qin L, Tay JH, Liu Y (**2004b**). *Selection pressure is a driving force of aerobic granulation in sequencing batch reactors*. Process Biochem. 39(5): 579–584.

Rehm HJ, Reed G, Pühler A, Stadler S (**1991**). *Biotechnology: a multivolume comprehensive treatise*. *Vol. 4 – Measuring, Modelling, and Control*. NY, USA: Wiley-VCH.

Riefler RG, Ahlfeld DP, Smets BF (**1998**). *Respirometric assay for biofilm kinetics estimation: Parameter identifiability and retrievability*. Biotechn. Bioeng. 57(1):35–45

Ros M, Dular M, Farkas PA (**1988**). *Measurement of respiration of activated sludge*. Water Res. 22(11):1405–1411.

Schwarzenbeck N, Erley R, Wilderer PA (**2004**). *Aerobic granular sludge in an SBR-system treating wastewater rich in particulate matter*. Water Sci. Technol. 49(11–12):41–46.

Spanjers H, Takacs I, Brouwer H (**1999**). *Direct parameter extraction from respirograms for wastewater and biomass characterization*. Water Sci. Technol. 39(4): 137–145.

Spanjers H, Vanrolleghem P, Nguyen K, Vanhooren H, Patry GG (**1998**). *Towards a simulation-benchmark for evaluating respirometry-based control strategies*. Water Sci. Technol. 37(12): 219–226.

Spanjers H, Vanrolleghem P, Olsson G, Dold P (**1996**). *Respirometry in control of the activated sludge process*. Water Sci. Technol. 34(3–4): 117–126.

Spanjers H, Vanrolleghem P (**1995**). *Respirometry as a tool for rapid characterization of waste-water and activated-sludge*. Water Sci. Technol. 31(2): 105–114.

Tay JH, Liu QS, Liu Y (**2004**). *The effect of upflow air velocity on the structure of aerobic granules cultivated in a sequencing batch reactor*. Water Sci. Technol. 49(11–12):35–40.

Tay STL, Ivanov V, Yi S, Zhuang WQ, Tay JH (**2002a**). *Presence of anaerobic* Bacteroides *in aerobically grown microbial granules*. Microb. Ecol. 44(3):278–285.

Tay JH, Ivanov V, Pan S, Tay STL (**2002b**). *Specific layers in aerobically grown microbial granules*. Lett. Appl, Microbiol. 34(4):254–257.

Tay JH, Liu QS, Liu Y (**2001a**). *Microscopic observation of aerobic granulation in sequential aerobic sludge blanket reactor*. J. Appl. Microbiol. 91(1):168–175.

Tay JH, Liu QS, Liu Y (**2001b**). *The effects of shear force on the formation, structure and metabolism of aerobic granules*. Appl. Microbiol. Biot. 57(1–2):227–233.

Van Loosdrecht MCM, Eikelboom D, Gjaltema A, Mulder A, Tijhuis L, Heijnen JJ (**1995**). *Biofilm structures*. Water Sci. Technol. 32(8):35–43.

Vanrolleghem PA (**2002a**). *Principles of Respirometry in Activated Sludge Wastewater Treatment*. Biomath (15/10/02). Department of Applied Mathematics, Biometrics and Process Control,

Universiteit Gent, Belgium.

Vanrolleghem PA (**2002b**). *Control of Activated Sludge Wastewater Treatment by using Respirometry*. Biomath (16/10/02). Department of Applied Mathematics, Biometrics and Process Control, Universiteit Gent, Belgium.

Vanrolleghem PA, Spanjers H, Petersen B, Ginestet P, Takacs I (**1999**). *Estimating (combinations of) Activated Sludge Model No. 1 parameters and components by respirometry*. Water Sci. Technol. 39(1): 195–214.

Vanrolleghem PA, Kong Z, Rombouts G, Verstraete W (**1994**). *An on-line respirographic biosensor for the characterisation of load and toxicity of wastewaters*. J. Chem. Technol. Biotechnol. 59:321–333.

Vanrolleghem PA, Verstraete W (**1993**). *Simultaneous Biokinetic Characterization of Heterotrophic and Nitrifying Populations of Activated-Sludge with an Online Respirographic Biosensor*. Water Sci. Technol. 28(11–12): 377–387.

Wang XH, Zhang HM, Yang FL, Xia LP, Gao MM (**2007a**). *Improved stability and performance of aerobic granules under stepwise increased selection pressure*. Enzyme Microb. Tech. 41(3):205–211.

Wang ZW, Liu Y, Tay JH (**2007b**). *Biodegradability of extracellular polymeric substances produced by aerobic granules*. Appl. Microbiol. Biot. 74(2):462–466.

Wang ZW, Liu Y, Tay JH (**2006**). *The role of SBR mixed liquor volume exchange ratio in aerobic granulation*. Chemosphere 62(5):767–771.

Wang F, Yang FL, Zhang XW, Liu YH, Zhang HM, Zhou J (**2005**). *Effects of cycle time on properties of aerobic granules in sequencing batch airlift reactors*. World J. Microb. Biot. 21(8–9):1379–1383.

Wiesmann U, Choi IS, Dombrowski EM (**2007**). *Fundamentals of Biological Wastewater Treatment*. Germany: Wiley-VHC, pp.11–18.

Wilderer PA, McSwain BS (**2004**). *The SBR and its biofilm application potentials*. Water Sci. Technol. 50(10):1–10.

Yang SF, Tay JH, Liu Y (**2003**). *A novel granular sludge sequencing batch reactor for removal of organic and nitrogen from wastewater*. J. Biotechnol. 106(1):77–86.

Zheng YM, Yu HQ, Liu SJ, Liu XZ (**2006**). *Formation and instability of aerobic granules under high organic loading conditions*. Chemosphere 63(10):1791–1800.

3. RESPIROMETRY APPLIED TO A NITRIFYING SYSTEM

Abstract

A simple in situ *pulse respirometric method for the estimation of kinetic and stoichiometric parameters is proposed. The method is validated in a suspended biomass nitrifying reactor for the determination of: (i) maximum exogenous oxygen uptake rate; (ii) autotrophic substrate oxidation yield; (iii) autotrophic biomass growth yield; and (iv) substrate affinity constant.*

The maximum exogenous oxygen uptake rate ($OUR_{exo\ max}$) was determined respirometrically through the injection of increasing substrate concentration pulses in the system under endogenous state. In the presented case study, a minimum substrate pulse of 10 mg NH_4-N L^{-1} was necessary to determine $OUR_{exo\ max}$ which was 61.15 ± 4.09 mg O_2 L^{-1} h^{-1} (5 repetitions). The substrate oxidation yield was determined directly from respirograms. The biomass growth yield was indirectly estimated from the substrate oxidation yield and, simultaneously, by the traditional COD mass balance method under steady state conditions. Both methods gave similar values when the system was at steady state (0.10 ± 0.07 and 0.09 ± 0.04 g X-COD g NOD^{-1}, respectively). The affinity constant was indirectly estimated after fitting the ascending part of the respirogram to a theoretical model. An average value of 0.48 ± 0.08 mg NH_4-N L^{-1} was obtained, which is in the range of affinity constants reported in the literature for the nitrification process (0.16 – 2 mg NH_4-N L^{-1}).

This chapter is published as:

Ordaz A, **Oliveira CS**, Aguilar R, Carrion M, Ferreira EC, Alves M, Thalasso F (**2008**). *Kinetic and stoichiometric parameters estimation in a nitrifying bubble column through "in-situ" pulse* respirometry. Biotechnol. Bioeng. 100(1):94–102 (doi:10.1002/bit.21723)

3.1. Introduction

Respirometry consists in the measurement of the biological oxygen consumption rate under well-defined conditions (Spanjers *et al*., 1999). Respirometry has been largely used for the characterisation of numerous biological systems at least since the beginning of the last century (Meiklejohn, 1937; Thompson, 1932). More recently, respirometry combined with the injection of a substrate pulse has been applied in biological systems for the determination of kinetic parameters (Ciudad *et al*., 2006; Checchi and Marsili-Libelli, 2005; Jubany *et al*., 2005). This technique consists in measuring the dissolved oxygen (DO) concentration profile after the injection of a defined concentration of substrate into the system. This can be done maintaining aeration (Guisasola *et al*., 2003; Ficara *et al*., 2000; Kong *et al*., 1994) or without aeration (Guisasola *et al*., 2005; Jubany *et al*., 2005; Chandran and Smets, 2000).

Pulse respirometry has been mainly used to estimate the substrate affinity constant, the substrate oxidation yield, the maximum substrate degradation rate, and the maximum growth rate (μ_{max}) (Chandran and Smets, 2005; Vanrolleghem *et al*., 2004). Other authors also refer the pulse respirometry technique to estimate the oxygen affinity constant (Guisasola *et al*., 2005), the biomass growth yield (Chandran and Smets, 2001, 2000; Dircks *et al*., 1999) and the aerobic endogenous decay constant (Avcioglu *et al*., 1998). The literature also reports the use of respirometry for the evaluation of inhibitory effects of several compounds (Carrera *et al*., 2004; Villaverde *et al*., 2000; Kong *et al*., 1996).

The number of publications in the field of pulse respirometry underlines the large interest of this method for the kinetic and stoichiometric parameters characterisation. So far, pulse respirometry has been applied in closed or open respirometers. The use of respirometers allows a better control of the test conditions and improves the results precision. However, this practice implies sampling that could be not fully representative of the reactor conditions, especially in heterogeneous sequential or fixed biomass reactors. To avoid the potential drawbacks of sampling, Riefler *et al*. (1998) suggested a theoretical *in situ* model, and Yoong *et al*. (2000) presented results obtained with *in situ* respirometry but without pulse addition and in a reactor without aeration. *In situ* pulse respirometry, defined as pulses of substrate directly applied in biological reactors, has not been reported yet.

This articles aims to apply an *in situ* pulse respirometric technique in order to estimate (i) the parameters that can be retrieved from *in situ* respirograms; (ii) the error of the technique through an error propagation method; and (iii) the effect of the pulse

respirometry on the bioreactor process. A nitrifying reactor with suspended biomass was used as a model system. A special emphasis was also given to the accuracy of the growth yield estimated by respirometry in comparison with a more traditional method based on chemical oxygen demand (COD) measurements.

3.2. Material and Methods

3.2.1. Nitrifying Reactor

A glass bubble column was used (0.12 m diameter, 0.64 m height, 5.3 L useful volume). A porous plate was placed at the bottom of the reactor for air supply.

The reactor was continuously fed with a mineral solution containing (g L^{-1}); $(NH_4)_2SO_4$, 5.60; $NaHCO_3$, 10.00; KH_2PO_4, 0.19; $MgSO_4.7H_2O$, 0.114; $CaCl_2$, 76; $FeCl_3.6H_2O$, 0.012.

The medium was fed with a peristaltic pump (Masterflex L/S precision, Cole- Parmer) with a flow rate of 0.040 L h^{-1} (hydraulic retention time (HRT) of 5.3 days). Air was supplied continuously at an air flow rate of 0.56 L min^{-1}, controlled by a mass flow controller (GFC171S, Aalborg, Monterrey, Mexico). pH was maintained at 8.0 ± 0.3 with the addition of NaOH 1 M using a pH controller (Black Stone BL 7916, Cole-Parmer). DO concentration (C) was measured with a polarographic DO bench meter (HI2400, Hanna Instruments, Mexico DF, Mexico). This bench meter was connected to a PC for data acquisition. The oxygen probe was placed at the top of the reactor. The reactor was inoculated with 1 L of mixed liquor obtained from a lab-scale fixed-bed nitrifying reactor continuously operated, and the initial ammonia concentration was 100 mg NH_4-N L^{-1}. The reactor was maintained at ambient room temperature (21 – 25 ^oC).

3.2.2. Methods

Analytical Methods

Ammonia, nitrate, and nitrite were measured in triplicate according to colorimetric standards methods (APHA, 1999) and confirmed with an SAN plus analyser (Sampler SA 1000, Skalar, Boom, Belgium). Nitrogen mass balance was confirmed through total

nitrogen measurement (Shimadzu Vcsn equipped with a TNM-1 module, Shimadzu, Mexico). Biomass concentration (X) was estimated in triplicate as the insoluble COD fraction, determined by the closed reflux colorimetric method according to standard method (APHA, 1999). Mass transfer coefficient (k_La) was measured by the dynamic method as described by Badino *et al*. (2000). The oxygen probe was calibrated before each respirometric experiment. The concentration of the ammonia solution used to make the pulses was confirmed by analysis made in triplicate.

Pulse Respirometric Method

In situ respirometric pulse experiments were done according to the following procedure: (i) the data acquisition system was switched on and the system was maintained until stable DO concentration (C) readings were obtained; (ii) the reactor feeding was then stopped; (iii) the oxygen concentration slowly increased until reaching a new stationary state (C_b), corresponding to the endogenous respiration state (Moussa *et al*., 2003); (iv) the k_La of the reactor was measured; (v) a pulse of a determined ammonia concentration (S_{NP} = 2.5, 5.0, or 10 mg NH_4-N L^{-1}) was injected and the DO concentration was acquired until the system returned to the previous stationary state (C_b); (vi) the pulse was eventually repeated; and (vii) the k_La was measured again before the feeding of the reactor was switched back on.

3.2.3. Data Interpretation

In this study, nitrification was considered as a single step process (Equation 4.1). The single step assumption allows simpler data interpretation and parameter retrieval from single ammonia pulse injection instead of ammonia plus nitrite pulse injection. The single step assumption is based on the fact that the ammonia oxidation is considered as the limiting step of the process (Sperandio *et al*., 2005; Langergraber *et al*., 2003; Khin *et al*., 2002), which is also considered valid by the Activated Sludge Model 1 (ASM1) under non-limiting oxygen concentration (Jubany *et al*., 2005). However, the literature reports that the validity of the single step assumption depends on the temperature. As the optimal temperature of the ammonia oxidation process is higher than the optimal temperature of nitrite oxidation, there is a boundary temperature above what the single step assumption is no more valid. Hellinga *et al*. (1998) suggests that this temperature is 20 ^oC and Nowak *et al*. (1995) suggest 25 ^oC. Kong *et al*. (1996) operated a respirometer at 25 ^oC and assumed a single step process. In this work, the reactor was maintained at ambient

temperature (21 – 25 °C). As it will be presented in the result section, except during the first few days of the experiment, no nitrite accumulation was observed in the reactor and the single step assumption was considered valid. The absence of nitrite during pulse experiments was also confirmed experimentally, from samples taken when the minimum oxygen concentration was reached.

$$NH_4^+ + 2O_2 \rightarrow NO_3^- + 2H^+ + H_2O \quad (3.1)$$

According to Equation 3.1, the total amount of oxygen needed to oxidise the ammonia injected is 4.57 g O_2 g^{-1} N, which is often called the nitrogen oxygen demand (NOD). This amount of oxygen is theoretical since Equation 3.1 does not consider biomass growth. When biomass growth is considered Equation 3.1 becomes:

$$\alpha\, NH_4^+ + \beta\, O_2 + \gamma\, CO_2 \rightarrow \delta\, C_5H_7NO_2 + \varepsilon\, NO_3^- + \zeta\, H^+ + \eta\, H_2O \quad (3.2)$$

However, if reagents and products are expressed in oxygen demand, that is, the amount of oxygen needed for their complete oxidation, only ammonia, oxygen, and biomass have to be considered. An oxygen balance can be then written as Equation 3.3.

$$64.0\,\alpha - 32.0\,\beta = 160.0\,\delta \quad (3.3)$$

In Equation 3.3, 64.0 is the mass of oxygen (g) needed to oxidise 1 mole of ammonia (4.57 g O_2 g^{-1} N), and 160.0 is the amount of oxygen (g) needed to oxidise 1 mole of biomass produced ($C_5H_7NO_2$, 1.42 g O_2 g^{-1} COD-X). Equation 3.4 is obtained by rearranging Equation 3.3.

$$\frac{32.0\beta}{64.0\alpha} + \frac{160.0\delta}{64.0\alpha} = 1 \quad (3.4)$$

The first term Equation 3.4 represents the fraction of substrate (expressed as NOD) used for energy production, and is defined as the substrate oxidation yield (f_E). The second term is the fraction of substrate (expressed as NOD) captured for biomass (expressed as COD) synthesis, and is defined as the biomass growth yield (f_S). According to Equation 3.4, f_S and f_E are complementary (Equation 3.5).

$$f_E + f_S = 1 \quad (3.5)$$

Stoichiometric Parameters

When a known amount of substrate is oxidised during the pulse injection, f_E is given by the

amount of oxygen consumed per unit NOD of ammonia oxidised (4.57 S_{PN}). The $Y_{A\,O2/S}$ can therefore be expressed by Equation 3.6.

$$f_E = \frac{\int_0^t OUR_{exo}\,dt}{4.57\,S_{PN}} = \frac{k_La\int_0^t (C_b - C)dt + (C_0 - C_f)}{4.57 S_{PN}} \quad (3.6)$$

During a pulse injection, the initial (C_0) and final (C_f) dissolved oxygen concentrations are usually equal to the baseline concentration (C_b), thus the accumulation term ($C_0 - C_f$) can be omitted.

Taking into account Equation 3.5 and 3.6, f_S can be easily estimated (Equation 3.7).

$$f_S = 1 - \frac{k_La\int_0^t (C_b - C)dt}{4.57 S_{PN}} \quad (3.7)$$

K_{SA} Estimation

The nitrification process can be expressed by the Monod equation (Ficara *et al.*, 2000), expressed in oxygen demand (Equation 3.8).

$$OUR_{exo} = OUR_{exo\,max}\frac{S_N}{S_N + K_{SA}} \quad (3.8)$$

Where, $OUR_{exo\,max}$ (mg O_2 h^{-1} L^{-1}) is the maximum exogenous oxygen uptake rate (OUR), S_N (mg N L^{-1}) is the ammonia concentration, and K_{SA} (mg N L^{-1}) is the affinity constant of nitrifiers.

After a substrate pulse injection, the oxygen mass balance in the reactor can be described by a balance between the exogenous respiratory activity and the oxygen provided by continuous aeration. The oxygen mass balance can be expressed by Equation 3.9 (Kong *et al.*, 1994).

$$\frac{dC}{dt} = k_La(C_b - C) - OUR_{exo} \quad (3.9)$$

Where, OUR_{exo} (mg O_2 L^{-1} h^{-1}) is the exogenous respiration rate of the microorganism, and C_b (mg O_2 L^{-1}) is the oxygen concentration during the pseudo-steady state, defined as the baseline concentration.

Substituting OUR_{exo} (Equation 3.8) in Equation 3.9, Equation 3.10 is obtained.

$$\frac{dC}{dt} = k_La\,(C_b - C) - \frac{S_N}{S_N + K_{SA}} OUR_{exo\,max} \quad (3.10)$$

Equation 3.10 was adjusted to the experimental data obtained from pulse experiments. For that purpose, k_La was measured as described above. $OUR_{exo\ max}$ was experimentally determined from the injection of pulses of increasing concentration (2.5, 5, and 10 mg NH_4-N L^{-1}), as it will be described in the *3.3. Results and Discussion* section.

Equation 3.10 was adjusted with a fitting procedure based on Runge-Kutta method with a Marquardt optimisation with 20 convergence steps (Model Maker, Cherwell Scientific Publishing, Oxford, UK) to determine K_{SA}. The adjustment was made taking into account the response time as previously described by Vanrolleghem *et al*. (2004).

Statistical Analysis

The absolute error (Δ_f) was estimated through error propagation according to Equation 3.11 (Elden and Wittmeyer-Koch, 1990).

$$\Delta f^2 \approx \sum_{k=1}^{n} \left| \frac{\partial f}{\partial x_k} \Delta x_k \right|^2 \quad (3.11)$$

The errors on the dissolved oxygen measurement (1.5 %) and on the volume of ammonia injected (transferpette, 0.6 %) were given by the equipment suppliers. The error made on the k_La (3.33 ± 1.03 %) and the error on the actual ammonia concentration injected (0.93 ± 0.58 %) were estimated after nine repetitions. The standard error (S_E) was estimated from Equation 3.12, using the standard deviation (σ) of n measures (Freund and Wilson, 1996).

$$S_E = \frac{\sigma}{\sqrt{n}} \quad (3.12)$$

The dissolved oxygen data obtained from respirometric experiments were softened by a standard 7-point smooth (UN-SCAN-IT software, Silk Scientific Corporation, Orem, UT, 1996).

3.3. Results and Discussion

The nitrifying reactor was inoculated and operated during 60 days under a constant loading rate of 210 ± 24 mg NH_4-N L^{-1} d^{-1} and constant hydraulic retention time (HRT) of 5.6 d. Since the onset, a clear nitrification was observed (Figure 3.1). The ammonia concentration rapidly decreased from 1000 to less than 0.1 mg NH_4-N L^{-1}. As a

consequence of the nitrification activity, a clear increase of the nitrate concentration was observed as well as an increase in biomass concentration (Figure 3.1). A temporary accumulation of nitrite was also observed from days 0 to 15. From the data presented in Figure 3.1, it can be concluded that the system reached a steady state approximately after 40 days of continuous operation. By the end of this period, it was observed that the nitrate concentration was inferior to the ammonia concentration fed to the reactor. Indeed, the ammonia concentration in the feeding solution was 1140 ± 41 mg NH_4-N L^{-1}, while the effluent nitrate concentration appeared steadily around 983 ± 26 mg NO_3-N L^{-1}. In order to understand such a difference, a nitrogen balance over the reactor was estimated taking into account ammonia oxidation, biomass growth (Equation 3.2), and stripping processes. Ammonia oxidation accounted for 86.2 %, biomass growth for 3.0 %, and stripping for 10.8 % of the total ammonia loading rate. Ammonia stripping from 10 % to 30 % of the ammonia loading rate has been also reported by Jokela *et al*. (2002) in a fixed-bed nitrifying reactor operated under similar working conditions (pH 7.5–8.5, temperature 25 ^{o}C).

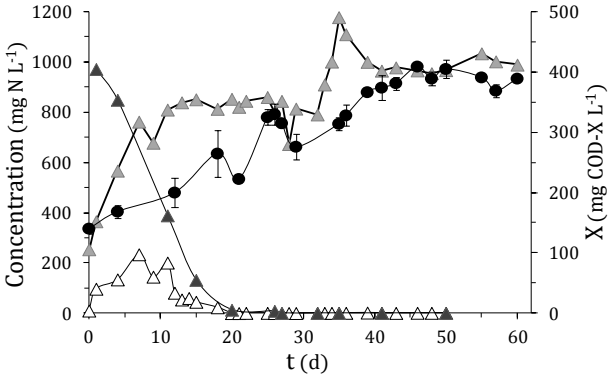

Figure 3.1. Time course of ammonia (▲), nitrite (△), nitrate (▲), and biomass concentrations (●) in the reactor.

To discard stripping during short-term pulse experiments, which could reduce the amount of ammonia which actually oxidised, an abiotic experiment was done. This experiment consisted of injecting a pulse of ammonia in a bubble column operated as the biological reactor but without biomass. The actual ammonia concentration was followed during 2 h. No reduction of ammonia concentration was detected. This concludes that ammonia was not subject to significant stripping during short-term experiments, although about 10 % was probably lost by stripping in the reactor over the HRT of 5.6 days.

At day 5, a first pulse respirometric experiment was done with the injection of two pulses of 10 mg NH_4-N L^{-1}. Figure 3.2a presents both respirograms after being softened to allow comparison. These respirograms show a similar behaviour. The dissolved oxygen concentration descended sharply from 5.9 to 5.6 mg O_2 L^{-1}, followed by a stable period and then by a slow increase up to the initial steady state. In Figure 3.2b, the thin line represents the second pulse, made immediately after the first one. The sole difference between both pulses is a slight delay of the second pulse. This delay generated a small difference in the determination of the oxidation yield (f_E), which was 0.69 and 0.71 (+ 2.9 %) for the first and second pulses, respectively.

In situ respirometry involves feeding suspension, which could have a significant impact on the process itself and/or on the repeatability of the pulses. To evaluate the effect of the feeding suspension, the feeding pump was switched off and four pulses of 10 mg NH_4-N L^{-1} were injected in a row over a total time of 5.5 h. No significant difference was observed between the pulses (Figure 3.2c). A standard deviation of 4.23 % on the substrate oxidation yield (f_E) was observed between the four pulses. At the end of the fourth pulse, the system was returned to normal operation and no change was observed in the dissolved oxygen concentration or the biomass and ammonia concentration. These results show that the application of repeated pulse during 5.5 h did not significantly affect the behaviour of the system.

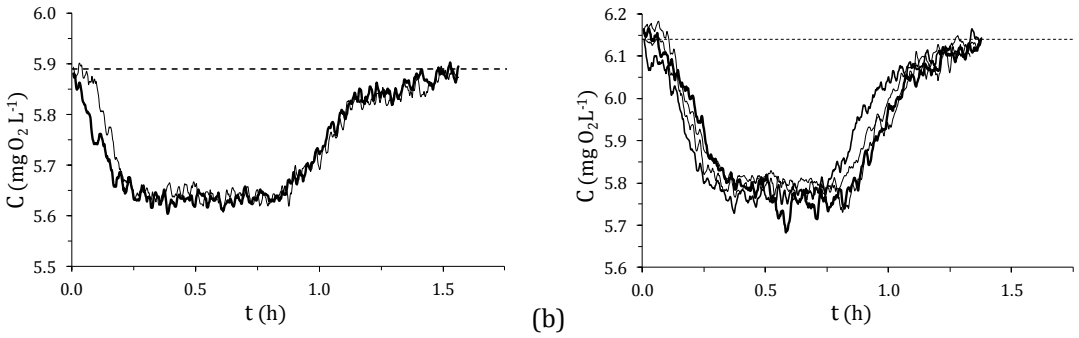

Figure 3.2. Comparison of respirograms obtained after the injection of two 10 mg NH_4-N L^{-1} consecutive pulses (a), and comparison of three pulses injected a row over a total time of 5.5 h (b).

Figure 3.3 shows the 10 mg NH_4-N L^{-1} pulses made at days 5, 17, 46, and 57. This figure shows OUR_{exo} respirograms instead of DO profile, for a clearer representation. The OUR_{exo} observed at four different periods present the same sharp increase followed by a pseudo-steady state. This pseudo-steady state corresponds to a short period of time during which

the process is independent of the substrate concentration. These OUR_{exo} correspond to the $OUR_{exo\ max}$ as it was confirmed by the injection of higher substrate concentration without any change in the maximum OUR_{exo} observed (Table 3.1).

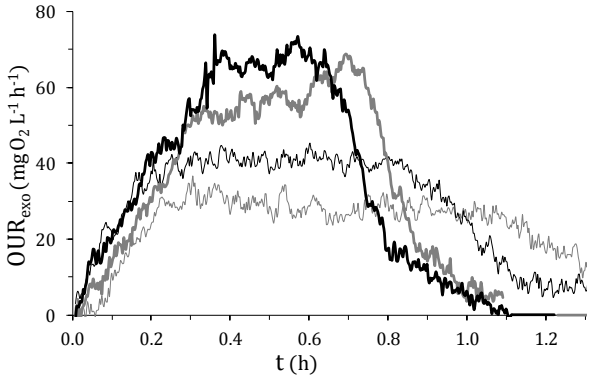

Figure 3.3. Exogenous oxygen uptake rate observed with the injection of 10 mg NH_4-N L^{-1} pulses on day 5 (*thin grey line*), 17 (*thin black line*), 46 (*thick grey line*), and 57 (*thick black line*).

Table 3.1. Maximum OUR_{exo} observed values, and associated standard deviation, obtained along time after the injection of pulses of 2.5 to 15.0 mg NH_4-N L^{-1}

S_{NP} (mg NH_4-N L^{-1})	$OUR_{exo\ max}$ (mg O_2 L^{-1} h^{-1})			
	day 32	**day 43**	**day 46**	**day 56**
2.5	47.8 ± 2.4	40.8 ± 2.9	39.7 ± 2.9	36.9 ± 1.8
5.0	60.1 ± 3.0	61.6 ± 4.3	63.3 ± 4.6	50.9 ± 2.5
10.0	60.2 ± 3.0	64.2 ± 4.5	66.5 ± 4.9	67.5 ± 3.2
15.0	61.2 ± 3.1		61.7 ± 4.5	68.1 ± 3.3

Figure 3.4 presents the f_S estimated by pulse respirometry and the apparent f_S determined through COD and NOD mass balance to the reactor, during the whole reactor's operation. From day 43 onwards the reactor reached a steady state, and the values of growth yield obtained through respirometry and mass balance were similar, 0.10 ± 0.04 and 0.09 ± 0.01 mg COD-X mg NOD^{-1}, respectively. However, before steady state was reached, a significant difference was observed between the f_S determined through mass balance and those estimated through respirometry. The initial respirometry values are probably largely overestimated, as the literature on nitrifying process reports biomass growth yield from 0.03 (Gapes *et al*., 2003) to 0.13 (Gee *et al*., 1990). However, to our knowledge, literature does not mention growth yields in nitrifying reactor during start-up. Thermodynamically,

according to Equation 3.2, the maximum theoretical growth yield that ensures exergonic reaction is 0.20. This confirms that at least the first growth yield determined respirometrically (day 6, f_S = 0.30) was overestimated. One of the reasons could be that on day 6 the reactor showed a small accumulation of nitrite (Figure 3.1). The single step nitrification assumption could no longer be valid under these conditions, and a partial ammonia oxidation to nitrite would suggest a higher oxidation yield (f_E) and a lower growth yield (f_S) than those actually observed. Sampling during the pulses made on day 6 showed a low nitrite concentration when the lowest DO concentration was reached, but no nitrite by the end of the pulse. No nitrite was observed during the pulses made afterwards, which confirm that the single step assumption was valid for the pulses made after day 6. Another reason for the large difference between f_S estimated by mass balance and respirometry could be simply accounted to large experimental errors as it will be discussed latter. The results presented in Figure 3.4 suggest that *in situ* respirometry allows the determination of the biomass growth yield when the process is under steady state. The applicability of respirometry on processes under transient state requires further research to understand why the oxygen consumption after pulse injection is relatively low compared to that observed under steady state.

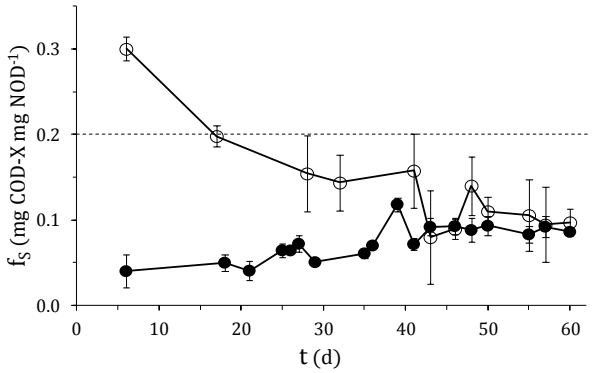

Figure 3.4. Biomass growth yield estimated by respirometry (○), and by mass balance to the reactor (●) during experiment. Dotted line represents the maximum theoretical growth yield that ensures exergonic process.

The global ammonia affinity constant (K_{SA}) was also estimated. In a first step, K_{SA} was estimated from complete respirograms. Figure 3.5a shows an example of how the theoretical model (Equation 3.10) fitted the experimental data. In a second step, K_{SA} was estimated from the second half of the respirograms (Figure 3.5b), in which the ammonia concentration becomes limiting and the oxygen concentration starts to rise. Under these conditions, the respiration rate observed is probably less sensitive to external factors such

as the biological and electrode response time or the external mass transfer limitations. This is probably why the correlations were better than those made from the complete respirograms (r^2 = 0.89 ± 0.04). From days 32 to 57, the K_{SA} of the process was estimated to be 0.48 ± 0.08 mg NH_4-N L^{-1}, from 15 pulses of 2.5 to 10 mg NH_4-N L^{-1}. This is close to the affinity constant values reported by Sperandio *et al*. (2005) (0.24–0.32 mg NH_4-N L^{-1}) in a membrane nitrifying reactor. The global affinity constant estimated here by respirometry is also close to the affinity constant reported for the ammonia oxidation step by Ciudad *et al*. (2006), 0.30 mg NH_4-N L^{-1}, by Carrera *et al*. (2004), 0.16 mg NH_4-N L^{-1}, and by Ficara *et al*. (2000), 0.30–2 mg NH_4-N L^{-1}.

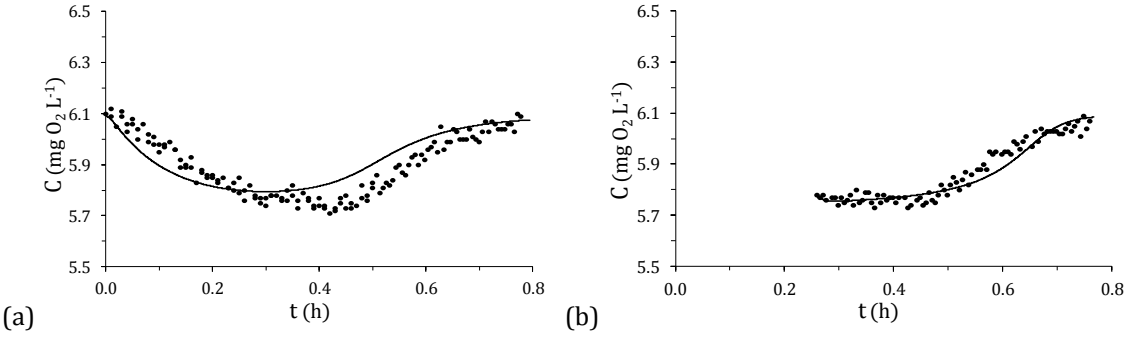

Figure 3.5. Example of best model fitting to the experimental data, considering complete respirogram (a), and the second half of the respirogram (b).

Parameter estimation from the second part of respirograms was previously used by Pratt *et al*. (2004) to estimate the k_La. The method is based on the assumption that, during a pulse injection, when oxygen concentration increases, no more substrate is available and therefore the shape of the oxygen concentration increase is directly linked to mass transfer phenomena, *i.e.* to the transfer of oxygen from the gas to the liquid phase. To confirm this point, k_La values estimated according to the Pratt method were compared to those estimated by the dynamic method (Badino *et al*., 2000) (Table 3.2). The k_La estimated from the Pratt method was systematically about 10 times lower than the k_La estimated from the dynamic method. The k_La estimated from the Pratt method were clearly erroneous, as the biomass growth yield (f_S) estimated from Equation 3.7 with these k_La values would have been systematically around 0.90, which is almost five times higher than the maximum theoretical exergonic growth (0.20).

Table 3.2. Comparison of the k_La measured by the respirometric (Pratt *et al*., 2004), and measured by the dynamic method (Badino *et al*., 2000)

Day	k_La (h^{-1})	
	Respirometric method	**Dynamic method**
32	10 ± 2	99 ± 5
39	9 ± 3	76 ± 7
43	10 ± 2	116 ± 8
46	12 ± 4	123 ± 9
57	12 ± 5	125 ± 6

Ammonia and nitrite concentrations were measured in the reactor when the oxygen concentration started to increase after the pulse injection, and both concentrations were below the detection limit of the technique used (0.04 mg NO_2-N L^{-1} and 0.10 mg NH_4-N L^{-1}, respectively). This was done to corroborate the initial hypothesis of the absence of significant substrate concentration when oxygen is increasing after pulse injection, as suggested by Pratt *et al*. (2004). However the absence of measurable nitrite and ammonia in the bulk phase does not mean these compounds are totally absent from the system. According to Costa *et al*. (2006), ammonia oxidation and nitrite oxidation occur in the cytoplasm of the cells. Both ammonia and nitrite could be undetectable by the method used in this work but still available for biomass. This would explain why, at least under the conditions of this work, the method suggested by Pratt *et al*. (2004) gave erroneous results. A finer analysis based on more precise nitrite and ammonia concentrations measurement associated to a two step (ammonia and nitrite oxidation) model would possibly allow understanding the difference observed.

According to the results obtained along the 60 days experiment, typical error on the substrate oxidation yield (f_E) was 5.6 %. According to Equation 3.5, f_S is linearly proportional to f_E. Therefore, the estimated error on f_E is proportionally propagated to the estimated error on f_S, as it can be observed in Figure 3.6. In our case, we observed through respirometry a growth yield of about 0.09 and therefore the standard error on the growth yield can be estimated to be 56 %. Of course, this error can be substantially reduced by increasing the number of repetitions. From Equation 3.12, the effect of the replicates number on the standard deviation was calculated for one to five repetitions. Standard deviation can be represented by a second order polynomial function in terms of the number of replicates (Equation 3.13). From this, it was observed that the standard error (S_E) on f_S decreases from 54 % to 12 % as n increases from 1 to 5 (

Table 3.3). This behaviour is in accordance with the central limit theorem.

$$\sigma = 0.26n^2 - 8.528n + 62.988 \quad (3.13)$$

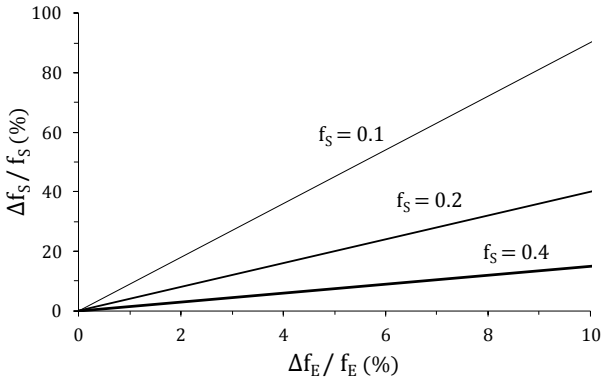

Figure 3.6. Sensitivity of the biomass growth yield to the oxidation yield.

The same error estimation procedure was repeated for all the parameters that can be retrieved from the respirometric experiments (

Table 3.3). As it can be observed, the main error is made on the affinity constant and on the biomass growth yield.

Table 3.3. Standard error inherent to each parameter estimation

Parameter	**S_E (%)**	
	n = 3	**n = 5**
f_E	4.7	3.4
f_S	19.6	12.3
$OUR_{exo\ max}$	7.4	6.7
K_{SA}	30.1	27.1

3.4. Conclusions

The injection of substrate pulses in a nitrifying reactor under endogenous respiration state allowed the retrieval of four important kinetic and stoichiometric parameters, namely: (i) the maximum oxygen uptake rate ($OUR_{exo\ max}$); (ii) the oxidation yield (f_E); (iii) the growth yield (f_S); and (iv) the affinity constant (K_{SA}).

The injection of pulses of increasing concentration was a suitable method to determine at

which substrate concentration the $OUR_{exo\ max}$ is reached. Once this concentration is identified, the $OUR_{exo\ max}$ can be directly measured in subsequent experiments.

The substrate oxidation yield was also measured directly from the respirograms, with a standard error around 5.6 %. As the oxidation yield and the growth yield are complementary, the same respirograms brought both parameters. Due to the low biomass growth yield observed in nitrifiers, this parameter was estimated with a large error (about 56 % for single measurement and 20 % for triplicate measurement). Additionally, it was observed that when the reactor was under transient state, the oxidation yield was probably underestimated and the growth yield overestimated. Complementary research is needed to understand this.

The affinity constant was also determined from *in situ* pulse respirometry but with significant standard error (about 30 % when measurements made in triplicate). The interpretation of the second part of the respirograms brings better correlated results than the interpretation of complete respirograms. This is probably due to the inability of the chosen model to interpret fast changing conditions. A more complex model taking into account biological and electrode response time as well as a two step biological model should give better correlation.

It is concluded that the pulse respirometry method can be usefully applied *in situ*. Further research is needed to understand the response of the method under transient state and to verify the applicability of the method to other processes and other reactor designs especially in larger scale reactor where mixing and hydrodynamics play a key role.

3.5. References

APHA (**1999**). *Standard methods for the examination of water and wastewater*. 20th edn. Washington, DC: American Publishers Health Association.

Avcioglu E, Orhon D, Sözen S (**1998**). *A new method for the assessment of heterotrophic endogenous respiration rate under aerobic and anoxic conditions*. Water Sci. Technol. 38(8–9):95–103.

Badino AC, Facciotti MCR, Schmidel W (**2000**). *Improving k_La determination in fungal fermentation, taking into account electrode response time*. J. Chem. Technol. Biot. 75(6):469–474.

Carrera J, Jubany I, Carvallo L, Chamy R, Lafuente J (**2004**). *Kinetic models for nitrification inhibition by ammonia and nitrite in a suspended and an immobilized biomass systems*. Process Biochem. 39:1159–1165.

Chandran K, Smets B (**2000**). *Single-step nitrification models erroneously describe batch ammonia oxidation profiles when nitrite oxidation becomes rate limiting*. Biotechnol. Bioeng. 68(1):396–

406.

Chandran K, Smets B (**2001**). *Estimating biomass yield coefficients for autotrophic ammonia and nitrite oxidation from batch respirograms*. Water Res. 35(13):3153–3156.

Chandran K, Smets B (**2005**). *Applicability of an extant batch respirometric assay in describing dynamics of ammonia and nitrite oxidation in a nitrifying bioreactor*. Water Sci. Technol. 52(10):503–508.

Checchi N, Marsili-Libelli S (**2005**). *Reliability of parameter estimation in respirometric models*. Water Res. 39:3686–3696.

Ciudad G, Werner A, Bornhardt C, Muñoz C, Antileo C (**2006**). *Differential kinetics of ammonia and nitrite oxidizing bacteria: A simple kinetic study based on oxygen affinity and proton release during nitrification*. Process Biochem. 41(8):1764–1772.

Costa E, Perez J, Kreft JU (**2006**). *Why is metabolic labour divided in nitrification?* Trends Microbiol. 14(5):213–219.

Dircks K, Pind PF, Mosbaek H, Henze M (**1999**). *Yield determination by respirometry - The possible influence of storage under aerobic conditions in activated sludge*. Water SA 25(1):69–74.

Elden L, Wittmeyer-Koch L (**1990**). *Numerical analysis: An introduction*. New York: Academic Press.

Ficara E, Musumeci A, Rozzi A (**2000**). *Comparison and combination of titrimetric and respirometric techniques to estimate nitrification kinetic parameters*. Water SA 26(2):217–224.

Freund R, Wilson W (1996). *Statistical methods*. Boston: Academic Press.

Gapes D, Pratt S, Yuan ZG, Keller J (**2003**). *Online titrimetric and off-gas analysis for examining nitrification processes in wastewater treatment*. Water Res. 37:2678–2690.

Gee CS, Pfeffer JT, Suidan MT (**1990**). *Nitrosomonas and Nitrobacter interactions in biological nitrification*. J. Environ. Eng.-ASCE 116(1):4–17.

Guisasola A, Baeza JA, Carrera J, Casas C, Lafuente J (**2003**). *An off-line respirometric procedure to determine inhibition and toxicity of biodegradable compounds in biomass from an industrial WWTP*. Water Sci. Technol. 48(11–12):267–275.

Guisasola A, Jubany I, Baeza JA, Carrera J, Lafuente J (**2005**). *Respirometric estimation of the oxygen affinity constants for biological ammonia and nitrite oxidation*. J. Chem. Technol. Biotechnol. 80(4):388–396.

Hellinga C, Schellen AAJC, Mulder JW, van Loosdrecht MCM, Heijnen JJ (**1998**). *The SHARON process: An innovative method for nitrogen removal from ammonium-rich wastewater*. Water Sci. Technol. 37(9):135–142.

Jokela JPY, Kettunen RH, Sormunen KM, Rintala JA (**2002**). *Biological nitrogen removal from municipal landfill leachate: Low-cost nitrification in biofilters and laboratory scale in-situ denitrification*. Water Res. 36(16):4079–4087.

Jubany I, Baeza JA, Carrera J, Lafuente J (**2005**). *Respirometric calibration and validation of a biological nitrite oxidation model including biomass growth and substrate inhibition*. Water Res. 39(18):4574–4584.

Khin T, Gheewala SH, Annachhatre AP (**2002**). *Modeling of nitrification inhibition with aniline in suspended-growth processes*. Water Environ. Res. 74(6):531–540.

Kong Z, Vanrolleghem P, Verstraete W (**1994**). *Automated respiration inhibition-kinetics analysis (ARIKA) with a respirographic biosensor*. Water Sci. Technol. 30(4):275–284.

Kong Z, Vanrolleghem P, Willems P, Verstraete W (**1996**). *Simultaneous determination of inhibition*

kinetics of carbon oxidation and nitrification with a respirometer. Water Res. 30(4):825–836.

Langergraber G, Wuchty M, Fleischmann N, Lechner M (**2003**). *Rapid automated detection of nitrification kinetics using respirometry*. Water Sci. Technol. 47(2):149–155.

Meiklejohn J (**1937**). *The oxygen uptake of suspensions and cultures of a freeliving bacterium*. J. Exp. Biol. 14:158–170.

Moussa MS, Lubberding HJ, Hooijmans CM, van Loosdrecht MCM, Gijsen HJ (**2003**). *Improved method for the determination of ammonia and nitrite oxidation activities in mixed bacterial cultures*. Appl. Microbiol. Biot. 63(2):217–221.

Nowak O, Svardal K, Shweighofer P (**1995**). *The dynamic behaviour of nitrifying activated sludge systems influenced by inhibiting wastewater compounds*. Water Sci. Technol. 31(2):115–124.

Pratt S, Yuan Z, Keller J (**2004**). *Modeling aerobic carbon oxidation and storage by integrating respirometric, titrimetric and off-gas CO_2 measurements*. Biotechnol. Bioeng. 88(2):135–147.

Riefler RG, Ahlfeld DP, Smets BF (**1998**). *Respirometric assay for biofilm kinetics estimation: Parameter identifiability and retrievability*. Biotechnol. Bioeng. 57(1):35–45.

Spanjers H, Takacs I, Brouwer H (**1999**). *Direct parameter extraction from respirograms for wastewater and biomass characterisation*. Water Sci. Technol. 39(4):137–145.

Sperandio M, Masse A, Espinoza-Bouchot MC, Cabassud C (**2005**). *Characterisation of sludge structure and activity in submerged membrane bioreactor*. Water Sci. Technol. 52(10–11):137–145.

Thompson W (**1932**). *Studies in respirometry I. A combined gas burette-interferometer respirometer*. J. Gen. Physiol. 16(1):5–22.

Villaverde S, Fdz-Polanco F, Lacalle ML, Garcia PA (**2000**). *Influence of the suspended and attached biomass on the nitrification in a two submerged biofilters in series system*. Water Sci. Technol. 41(4–5):169–176.

Yoong ET, Lant PA, Greenfield PF (**2000**). In situ *respirometry in an SBR treating wastewater with high phenol concentrations*. Water Res. 34(1):239–245.

4. RESPIROMETRY APPLIED TO A PURE CULTURE

Abstract

The applicability of pulse respirometry for the estimation of kinetic and stoichiometric parameters in pure cultures was evaluated by comparison with traditional chemostat method. Pseudomonas putida *F1 was cultured in a continuous stirred tank reactor, using glucose as sole carbon source. The reactor was operated under steady state with six dilution rates, ranging from 0.06 to 0.35* h^{-1}*. Substrate and biomass concentration were measured and used to estimate kinetic and stoichiometric parameters according to the Monod model. An* in situ *respirometry method was also applied to the reactor, with the injection of pulses of glucose from 19 to 97 mg COD-S* L^{-1}*. The respirograms obtained were used to estimate kinetic and stoichiometric parameters according to ASM1 and ASM3 models. No significance difference was observed between parameters estimated by chemostat and respirometric method using ASM3 adjustment: biomass growth yield was 0.41(0.05) and 0.51 (0.04); affinity constant was 4.86 (0.70) and 5.13 (1.99); maximum specific growth rate was 0.20 (0.05) and 0.16 (0.01), with chemostat and respirometry respectively. These results show that* in situ *pulse respirometry is a suitable method for kinetic and stoichiometric parameters.*

This chapter is published as:

Oliveira CS, Ordaz A, Alba J, Alves M, Ferreira EC, Thalasso F (**2009**). *Determination of kinetic and stoichiometric parameters of* Pseudomonas putida *F1 by chemostat and* in situ *pulse respirometry*. Chemical Product and Process Modeling 4(2): 1–14. (doi:10.2202/1934-2659.1304)

4.1. Introduction

The development and optimisation of new bioprocesses requires continuous information about the kinetic and stoichiometric parameters of the microorganisms used in those processes (Sipkema *et al*., 1998). The estimation of these parameters for pure cultures is traditionally performed through batch or chemostat culture. Among these two, the chemostat is considered the most suitable method for determining substrate affinity constant (K_S) (Duarte *et al.*, 1994). It consists in measuring the steady state residual limiting substrate concentration for different dilution rates applied to a chemostat. The chemostat culture, just as the batch method, involves the direct measurement of the growth limiting substrate at concentrations close to the K_S (Kovarova-Kovar and Egli, 1998). Koch (1997) pointed out the precision and accuracy of substrate measurements as the main limitation of the method. Additionally, chemostat method is time consuming, as it requires the operation of the reactor under several steady states, each of them maintained for several hydraulic retention times (HRT).

Drawbacks of traditional methods may be overcome by respirometry, which allows the indirect measurement of substrate consumption rates by monitoring the biological oxygen consumption rate, under well defined conditions (Spanjer *et al*., 1999). Within many respirometry techniques, pulse respirometry, developed in the 1990s (Riefler *et al*., 1998; Vanrolleghem *et al*., 1995; Kong *et al*., 1994) is probably one of the most promising techniques. This technique consists of measuring the dissolved oxygen (DO) concentration during the transient state observed after the injection of a defined concentration of substrate into the system. The exogenous oxygen uptake rate (OUR_{exo}) curves reflect the kinetic of the aerobic biodegradation process. The interest of respirometry for parameter estimation, compared with techniques based on substrate concentration measurement, is that respirometry allows the retrieval of numerous parameters from relatively small experimental effort in real time, and using a low cost probe (Riefler *et al*., 1998). Additionally, since pulse respirometry is based on the observation of induced transient states, it may be applied without drastically changing the normal operation of the system.

Many works on respirometry can be found in literature, with a special emphasis given to parameters retrievability, precision, and sensitivity analysis. Comparatively, little weight has been given to the accuracy of the retrieved parameters. Their comparison to parameters retrieved by more standard methods is often avoided. Pulse respirometry has been frequently used to characterise mixed cultures applied to wastewater treatment, such as nitrificants (Ordaz *et al*., 2008) and activated sludge (Kong *et al*., 1994). There are

few works that used respirometric techniques to characterise pure cultures. Goudar and Strevett (1998) used OUR measurements for the estimation of growth kinetic parameters of *Penicillium chrysogenum*. Latter, Insel *et al*. (2006) used respirometry and glucose consumption profiles to obtain kinetic parameters of *Escherichia coli*. In this last mentioned work, process kinetic was described by a mathematic model similar to Activated Sludge Model 3 (ASM3). However, little attention was given to the accuracy of the retrieved parameters.

In the present work, pulse respirometry was applied for the retrieval of kinetic and stoichiometric parameters of a pure culture of a *Pseudomonas putida* F1 strain fed with glucose as sole carbon source in a continuous stirred reactor. *In situ* pulse respirometry, defined as pulses of substrate directly applied to biological reactors as reported previously by Ordaz *et al*. (2008), was used. The ASM1 (Henze *et al*., 1987) and the ASM3 (Gujer *et al*., 1999) models were use for respirometric data interpretation. To assess the accuracy of the proposed method, the kinetic and stoichiometric parameters retrieved from respirometric experiments were compared to those obtained through traditional chemostat method.

4.2. Material and Methods

4.2.1. Pure Culture Bioreactor

A continuous stirred tank reactor (CSTR) (Bioflo3000, New Brunswick Scientific, Mexico) with a working volume of 3 L was used. Air was continuously supplied at an air flow rate of 5 L min^{-1}. The reactor was continuously fed at defined flow rates. The composition of the growth media used was (g L^{-1}): KH_2PO_4, 1.25; $NH_4(SO_4)_2$, 1.32; $MgSO_4 \cdot 7H_2O$, 0.10; $FeSO_4 \cdot 7H_2O$, 0.75. Additionally, 1 mL L^{-1} of trace elements (Vecht *et al*., 1988) was added, as well as 5 g L^{-1} of glucose as sole carbon source. Temperature and pH in the reactor were maintained constant at 25 ^oC and 7, respectively.

Microorganisms and Culture conditions

The microorganism used was *Pseudomonas putida* F1 (CDBB-B100, National Collection of Microbial Strains, Cinvestav, Mexico). The preparation of the inoculum was made in a 2 L

Erlenmeyer flask containing 600 mL of culture medium, incubated for 24 h at 30 ^{o}C and 200 rpm in an orbital shaker (Innova4300, New Brunswick Scientific, Mexico).

4.2.2. Methods

Analytical Methods

Influent and effluent were characterised by the measurement of glucose, and total and soluble chemical oxygen demand (COD). Glucose concentration was measured by two methods depending on the concentration; an enzymatic kit (Amplex Red, Invitrogen, USA) for the 1 to 100 mg L^{-1} range, and DNS (dinitrosalicylic acid) method for concentrations over 100 mg L^{-1}. COD was measured by the closed reflux colorimetric method, in accordance to standard methods (APHA, 1999). Total COD was determined by measuring the COD of a homogenised sample. Substrate concentration (S) was considered the soluble COD determined by measuring the COD of a filtered sample (0.45 μm). Insoluble COD was estimated as the difference between total and soluble COD. Since the feeding medium contained no suspended solids, the insoluble COD was considered as biomass (X). DO concentration was measured continuously in the reactor with a polarographic probe (InPro6800, Mettler Toledo, Mexico). The DO probe was connected to a computer for data acquisition. The calibration of the DO probe was done using water at 25 ^{o}C, bubbled with nitrogen gas for 0 % and with air for 100 % saturation. The k_La was measured in triplicate using the dynamic method as described by Badino *et al*. (2000).

Chemostat Method

For the estimation of kinetic and stoichiometric parameters through chemostat method, the bioreactor was operated continuously at six dilution rates (D): 0.06, 0.09, 0.10, 0.17, 0.21, and 0.35 h^{-1}. Each D was maintained until steady state was reached and kept for at least 6 HRT (from 30 to 100 h). Steady state was considered to be reached when cellular and residual substrate concentrations were stable, within 10 % variation.

Pulse Respirometric Method

The pulse respirometric methodology used was as follows: (i) the DO data acquisition was started; (ii) the substrate feeding of the reactor was then stopped; (iii) after the DO

concentration reached a pseudo-steady state, called baseline (C_b), a known concentration of substrate (S_P), namely from 19 to 97 mg COD-S L^{-1}, was injected in the reactor; (iv) the DO concentration was monitored until it reached the baseline (C_b) again; and finally (v) the mass transfer coefficient (k_La) was measured in triplicate using the dynamic method (Badino *et al*., 2000). Respirograms were obtained by plotting the DO concentration *versus* time. All the pulse respirometric experiments were made during the operation of the reactor at a single dilution rate (D = 0.17 h^{-1}), since pulse respirometry is based on the observation of induced transient states in the reactor operated temporarily under batch mode and therefore independent of the dilution rate.

4.2.3. Data Analysis

Chemostat Method

The determination of the maximum specific growth rate (μ_{max}) and K_S by the chemostat method was made by adjustment of the Monod equation to the experimental data by least-square fit. Since the bioreactor used was a CSTR, at steady state the specific growth rate (μ) was considered equal to D. The biomass growth yield ($Y_{X/S}$) was determined through COD mass balance.

Pulse Respirometric Method

The oxygen mass balance during pulse experiments can be described by Equation 4.1 (Kong *et al*., 1994).

$$\frac{dC}{dt} = [k_La\,(C_b - C) - OUR_{exo}]\left(1 - e^{t/t_r}\right) \quad (4.1)$$

Where, OUR_{exo} (mg O_2 h^{-1} L^{-1}) is the exogenous OUR and t_r (h) is the response time of the process, according to Vanrolleghem *et al*. (2004).

In Equation 5.1, OUR_{exo} can be described by a simple Monod kinetic (ASM1) or a more complex model, such as ASM3 (Table 4.1). ASM1 is an unstructured model for the simulation of oxygen and substrate consumption associated to biomass growth. ASM3 is a partially structured model for the simulation of oxygen and substrate consumption associated to storage and growth mechanisms. The choice of these two models was based on their wide application in the field of respirometry.

ASM1 parameters estimation

The oxidation yield ($Y_{O2/S}$) was first retrieved from the area of the respirograms according to Equation 4.2 (Ordaz *et al*., 2008). When a known amount of substrate is oxidised during the pulse injection, the $Y_{O2/S}$ is given by the amount of oxygen consumed per unit COD of substrate oxidised (S_P). As both biomass and substrate are expressed in COD units, $Y_{X/S}$ can be easily estimated from $Y_{O2/S}$ (Equation 4.3).

$$Y_{O2/S} = \frac{\int_0^t OUR_{exo} dt}{S_P} = \frac{k_L a \int_0^t (C_b - C) dt + (C_0 - C_f)}{S_P} \quad (4.2)$$

$$Y_{X/S} = 1 - Y_{O2/S} = \frac{\int_0^t OUR_{exo} dt}{S_P} = \frac{k_L a \int_0^t (C_b - C) dt + (C_0 - C_f)}{S_P} \quad (4.3)$$

Where, S_P (mg COD-S L^{-1}) is the substrate pulse concentration, and C_0 and C_f (mg O_2 L^{-1}) are the DO concentrations before and after the pulse, respectively.

The accumulation term ($C_0 - C_f$) can be omitted, as no difference between C_0 and C_f was observed during pulse experiments.

K_S and t_r were estimated by adjustment of ASM1 (Equation 4.4) to the experimental data obtained from the pulse experiments with a fitting procedure based on Runge-Kutta method and a Marquardt optimisation method with 20 convergence steps (Model Maker, Cherwell Scientific Publishing, UK).

$$\frac{dC}{dt} = \left[k_L a\,(C_b - C) - OUR_{exo}\,max\,\frac{S}{S + K_S}\right]\left(1 - e^{t/t_r}\right) \quad (4.4)$$

Where, $OUR_{ex}max$ (mg O_2 h^{-1} L^{-1}) is the maximum OUR_{ex}, and was obtained according to Ordaz *et al*. (2008) method, *i.e.* by the injection of substrate pulse of increasing concentration.

The maximum specific growth rate (μ_{max}) was estimated from Equation 4.5.

$$\mu_{max} = \frac{OUR_{exo}\,max\,Y_{X/S}}{Y_{O2/S}\,X} \quad (4.5)$$

ASM3 parameters estimation

As pointed out above, ASM3 model considers storage (Table 4.1). Storage and growth are considered sequentially in ASM3: first, all the substrate is consumed for storage; and then bacteria consume storage material for growth. Two growth yields are therefore defined:

storage yield ($Y_{Sto/S}$), and storage growth yield ($Y_{X/Sto}$). Both parameters were estimated according to Equations 4.6 and 4.7 (Karahan-Gül *et al.*, 2002; Goel *et al.*, 1999).

$$Y_{Sto/S} = 1 - \frac{k_L a \int_0^t (C_{LSto} - C) dt}{S_P} \quad (4.6)$$

$$Y_{X/Sto} = \frac{Y_{X/S}}{Y_{Sto/S}} \quad (4.7)$$

C_{LSto} is the hypothetical DO line that separates oxygen consumption for storage and for growth. In the present work, C_{LSto} was determined by drawing a line between the origin of the respirogram and the inflection point observed in the DO ascending branch (Figure 4.2a).

Table 4.1. Simplified matrix of ASM1 and ASM3 for organic carbon removal, considering soluble biodegradable COD

Process	Component				Rate
	S	**X_{Sto}**	**X**	**C**	
Growth on S (ASM1)	$-\frac{1}{Y_{X/S}}$		1	$-\frac{(1 - Y_{X/S})}{Y_{X/S}}$	$\mu_{max} X \frac{S}{K_S + S}$
Storage of S (ASM3)	-1	$Y_{X/Sto}$		$-(1 - Y_{Sto/S})$	$k_{Sto} X \frac{S}{K_S + S}$
Growth on X_{Sto} (ASM3)		$-\frac{1}{Y_{X/Sto}}$	1	$-\frac{(1 - Y_{X/Sto})}{Y_{X/Sto}}$	$\mu_{max} X \frac{X_{Sto}/X}{K_{Sto} + X_{Sto}/X}$
Endogenous respiration (ASM3)	-1		-1		$b_H X$
Respiration of X_{Sto} (ASM3)		-1		-1	$b_{Sto} X_{Sto}$

Some of the kinetic and stoichiometric coefficients were set to default values. These default values were those reported by Karahan-Gül *et al.* (2002), and are listed in Table 4.2. The additional kinetic and stoichiometric parameters of the ASM3 model, namely the soluble substrate affinity (K_S), the storage affinity constant (K_{Sto}), the storage kinetic constant (k_{Sto}), and t_r were estimated by adjustment of ASM3 to the experimental data obtained from the pulse experiments with a fitting procedure based on Runge-Kutta method and a Marquardt optimisation method with 20 convergence steps (Model Maker, Cherwell Scientific Publishing, UK). μ_{max} was estimated from Equation 4.5.

Table 4.2. Kinetic and stoichiometric default values used (Karahan-Gül *et al.*, 2002)

Model coefficient	Default value
b_H (h^{-1})	0.0083
b_{Sto} (h^{-1})	0.0083

Statistical Analysis

The parameters obtained by respirometry and chemostat methods were compared using the Tuckey-Kramer tests performed after analysis of variance ($\alpha = 0.05$) using the NCSS 2000 software (NCSS, Jerry Hintze). The impact of the number of measurements on the standard error (S_E) was estimated from Equation 4.7 (Freund and Wilson, 1996), were n was considered the number of independent pulse experiments in respirometry and the number of steady states in the chemostat method.

$$S_E = \frac{\sigma}{\sqrt{n}} \quad (4.7)$$

4.3. Results and Discussion

During a 12 days experiment, the CSTR was operated under steady state with six successive D (0.06, 0.09, 0.10, 0.17, 0.21, and 0.35 h^{-1}). At D = 0.35 h^{-1}, a clear biomass wash-out was observed. Thus, the data obtained with D 0.35 h^{-1} were discarded. Figure 4.1 presents the adjustment of the Monod equation to the experimental data obtained with the chemostat method, which had a correlation factor (r^2) of 0.96.

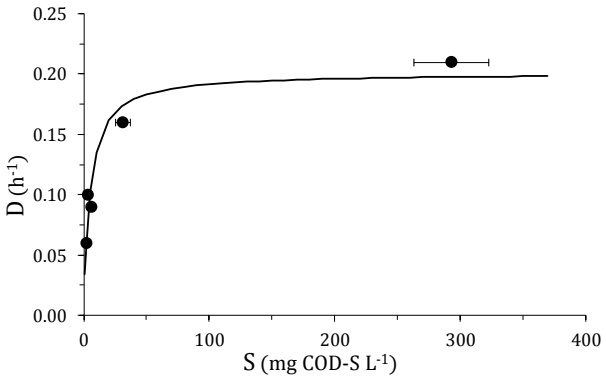

Figure 4.1. Monod model adjustment ($r^2 = 0.96$, *solid line*) to the experimental chemostat data (•).

Average kinetic and stoichiometric parameters are presented in Table 4.3.

Table 4.3. Kinetic and stoiquiometric parameters obtained with the chemostat method and with model ASM1 and ASM3 adjustment to respirometric data

Parameter	Chemostat (Monod Adjustment)	Respirometric Data Adjustment	
		ASM1	ASM3
$Y_{X/Y}$ (g COD-X g COD-S^{-1})	0.41 ± 0.05	0.51 ± 0.04	–
K_S (mg COD-S L^{-1})	4.86 ± 0.70	7.96 ± 2.65	5.13 ± 1.99
μ_{max} (h^{-1})	0.20 ± 0.05	0.14 ± 0.02	0.16 ± 0.01
K_{Sto} (mg COD- X_{Sto} L^{-1})	–	–	0.01 ± 0.00
k_{Sto} (h^{-1})	–	–	0.28 ± 0.07
t_r (s)	–	40.46 ± 4.34	20.85 ± 3.28
r^2	0.96	0.96	0.99

By the end of the chemostat experiment, the reactor was maintained under steady state at D = 0.17 h^{-1}, and pulse respirometry experiments were made. The reactor's feeding was stopped, and after a stable residual glucose concentration was observed, a total of 9 pulses were injected in a row, during a uninterrupted 36 hours experiment. Figure 4.2 shows an example of respirogram observed after the injection of a pulse of 97 mg COD-S L^{-1}. The DO concentration descended sharply from 7.4 to 5.0 mg O_2 L^{-1}, followed by a stable period, and then by a sharp increase up to the initial steady state. Similar curve shapes were observed in all respirometric experiments (data not shown).

ASM1, based on Monod kinetic, did not fit adequately the obtained respirograms (average r^2 = 0.96). On the contrary, ASM3 model fitted well the respirograms (average r^2 = 0.99). This is clearly shown in Figure 4.2a, where ASM1 and ASM3 best fittings are presented. The existence of storage and storage material degradation are therefore suggested. This is also suggested from the shape of respirograms (Figure 4.2b). Indeed, the stable DO concentration observed in the middle of the pulses (*i.e.* from t = 0.05 to 0.15 h in Figure 4.2a) as well as the sudden change in the OUR_{exo} slope followed by tailing (t = 0.2 h in Figure 4.2b), point to the existence of storage mechanisms (Guisasola *et al.*, 2005; van Loosdrecht *et al.*, 1997).

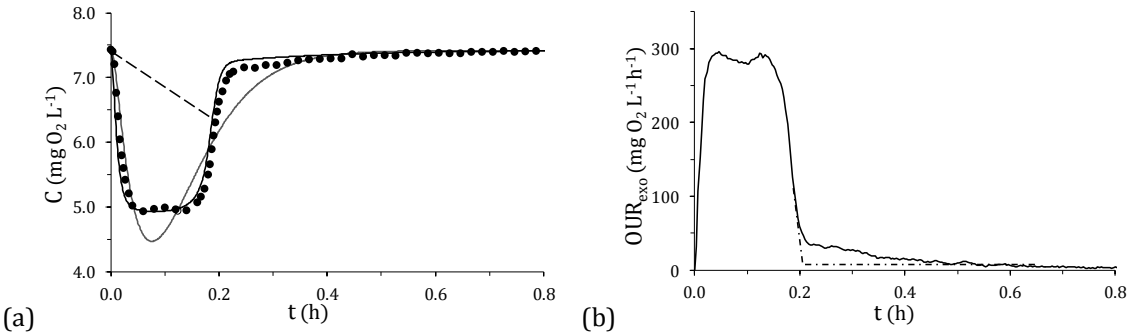

Figure 4.2. (a) Example of a respirogram (•) with the representation of C_{Lb} line (*dashed line*), and model fitting using : ASM1 (r^2 = 0.94, *grey line*), and ASM3 (r^2 = 1.00, *dark line*). (b) Corresponding OUR_{exo} curve (*solid line*), and ASM1-typical fitting (*dash-dotted line*).

The results confirm that ASM3 model better fits the experimental respirometric data and allows the retrieval of a major number of stoichiometric and kinetic parameters. K_S of *Pseudomonas putida* F1 strain was ranging from 4.86 to 9.30 mg COD-S L^{-1}. This range of K_S is significantly inferior to values reported in literature for *Pseudomonas putida* (20 to 1000 mg COD-S L^{-1}) (Wang *et al.*, 1996; Vicente and Cánovas, 1973). The $Y_{X/S}$ of *Pseudomonas putida* F1 obtained by direct measurement in the chemostat was 0.41. This value is lower than the values estimated by respirometry (0.51 and 0.67), which indicates that respirometry probably overestimates the $Y_{X/S}$. The μ_{max} was varying from 0.14 to 0.20 h^{-1}. As observed during chemostat experiment, the reactor was operated successfully at D = 0.21 h^{-1}, without significant wash-out. The μ_{max} was therefore probably underestimated by both chemostat and respirometry methods.

Kinetic and stoichiometric parameters obtained from ASM3 model cannot be compared to those obtained from ASM1 fitting and from the chemostat method, except μ_{max}. On the contrary, ASM1 and Monod are similar and can be compared. No difference between ASM1-respirometry, and chemostat methods were observed for any of the parameters. In the same way, no significant difference between μ_{max} estimated by ASM1 and ASM3 models was observed.

$Y_{X/S}$ and μ_{max} were subject to lower S_E when measured by respirometry than by chemostat. On the other hand, the chemostat method allowed the estimation of the K_S with a lower S_E than the respirometric method for the same number of replicate. The number of replicates of pulse respirometry for a given S_E is about four times the required number of steady states in the chemostat method. However, pulse experiments are much less time demanding than chemostat methods, which requires several steady states. Each steady state has to be maintained for several HRT, which represented in this work from 17 to 100

h of experiment. By comparison, pulse experiments lasted from 0.4 to 0.6 h. It can be therefore concluded that pulse respirometry is a technique that allows similar K_S estimation with a relatively lower experimental effort. The same conclusion can be withdrawn for μ_{max} and $Y_{X/S}$ estimation, since S_E of respirometry estimation was lower than chemostat estimation.

4.4. Conclusions

From the results obtained, it was confirmed that respirometry is a suitable method for parameter estimation of axenic culture, as previously suggested by Goudar and Strevett (1998) and by Insel *et al*. (2006). The ASM3 model fitted adequately the respirometry kinetic of *Pseudomonos putida* F1 with an average correlation factor (r^2) of 0.99. This confirms that *Pseudomonas putida* F1 metabolism includes storage mechanisms. This was previously reported by Huijberts and co-workers (1992), and explains why ASM1 model showed a lower correlation coefficient (average r^2 of 0.96) than ASM3.

A comparison between the parameters estimated by respirometry and chemostat methods showed that no significant difference was observed for any parameter. This is partly due to the relatively large S_E observed in parameter estimation.

The respirometric method showed lower S_E than the chemostat method for $Y_{X/S}$ and μ_{max} estimation, but larger S_E for K_S estimation. However, as respirometry implies relatively lower experimental input, it can be concluded that *in situ* pulse respirometry is an effective method for parameter estimation of axenic cultures of *Pseudomonas putida* F1.

4.5. References

APHA (**1999**). *Standard methods for the examination of water and wastewater*. 20th Edn. Washington, DC: American Publishers Health Association.

Badino AC, Facciotti MCR, Schmidel W (**2000**). *Improving k_La determination in fungal fermentation, taking into account electrode response time*. J. Chem. Technol. Biot. 75(6):469–474.

Duarte LC, Nobre AP, Gírio FM, Amaral-Collaço MT (**1994**). *Determination of the kinetic parameters in continuous cultivation by* Debaryomyces hansenii *grown on D-xylose*. Biotechnol. Tech. 8(12):859–864.

Freund R, Wilson W (**1996**). *Statistical methods*. Academic Press, Boston.

Goel R, Mino T, Satoh H, Matsuo T (**1999**). *Modeling hydrolysis processes considering intracellular*

storage. Water Sci. Technol. 39(1):97–105.

Goudar CT, Strevett KA (**1998**). *Estimating growth kinetics of* Penicillium chrysogenum *through the use of respirometry*. J. Chem. Technol. Biot. 72(3):207–212.

Guisasola A, Sin G, Baeza JA, Carrera J, Vanrolleghem PA (**2005**). *Limitations of ASM1 and ASM3: a comparison based on batch oxygen uptake rate profiles from different full-scale wastewater treatment plants*. Water Sci. Technol. 52(10–11):69–77.

Gujer W, Henze M, Mino T, van Loosdrecht M (**1999**). *Activated Sludge Model No. 3*. Water Sci. Technol. 39(1):183–193.

Henze M, Grady CPL Jr, Gujer W, Marais GvR, Matsuo T (**1987**). *Activated Sludge Model No. 1. IAWPRC Scientific and Technical Report No. 1.* UK: IAWPRC.

Huijberts GNM, Eggink G, de Waard P, Huisman GW, Witholt B (**1992**). Pseudomonas putida *KT2442 cultivated on glucose accumulates poly(3-hydroxyalkanoates) consisting of saturated and unsaturated monomers*. Appl. Environ. Microb. 58(2):536–544.

Insel G, Celikyilmaz G, Ucisik-Akkaya E, Yesiladali K, Cakar ZP (**2006**). *Respirometric evaluation and modeling of glucose utilization by* Escherichia coli *under aerobic and mesophilic cultivation conditions*. Biotechnol. Bioeng. 96(1):94–105.

Karahan-Gül O, Artan N, Orhon D, Henze M, van Loosdrecht MCM (**2002**). *Respirometric assessment of storage yield for different substrates*. Water Sci. Technol. 46(1):345–352.

Koch, AL (**1997**). *Microbial physiology and ecology of slow growth*. Microbiol. Mol. Biol. R. 61(3):305–318.

Kong Z, Vanrolleghem P, Verstraete W (**1994**). *Automated respiration inhibition-kinetics analysis (ARIKA) with a respirographic biosensor*. Water Sci. Technol. 30(4):275–284.

Kovarova-Kovar K, Egli T (**1998**). *Growth kinetics of suspended microbial cells: from single-substrate-controlled growth to mixed-substrate kinetics*. Microbiol. Mol. Biol. R. 62(3):646–666.

Ordaz A, Oliveira CS, Aguilar R, Carrión M, Ferreira EC, Alves M, Thalasso F (**2008**). *Kinetic and stoichiometric parameters estimation in a nitrifying bubble column through "in situ" pulse respirometry*. Biotechnol. Bioeng. 100(1):94–102. (*Chapter 3 of this Thesis*).

Riefler RG, Ahlfeld DP, Smets BF (**1998**). *Respirometric assay for biofilm kinetics estimation: Parameter identifiability and retrievability*. Biotechnol. Bioeng. 57(1):35–45.

Sipkema EM, de Koning W, Ganzeveld KJ, Janssen DB, Beenackers AACM (**1998**). *Experimental pulse technique for the study of microbial kinetics in continuous culture*. J. Biotechnol. 64(2–3):159–176.

Spanjers H, Takacs I, Brouwer H (**1999**). *Direct parameter extraction from respirograms for wastewater and biomass characterization*. Water Sci. Technol. 39(4):137–145.

Van Loosdrecht MCM, Pot MA, Heijnen JJ (**1997**). *Importance of bacterial storage polymers in bioprocesses*. Water Sci. Technol. 35(1):41–47.

Vanrolleghem PA, Sin G, Gernaey KV (**2004**). *Transient response of aerobic and anoxic activated sludge activities to sudden substrate concentration changes*. Biotechnol. Bioeng. 86(3):277–290.

Vanrolleghem P, van Daele M, Dochain D (**1995**). *Practical identifiability of a biokinetic model of activated sludge respiration*. Water Res. 29(11):2561–2570.

Vecht SE, Platt MW, Er-El Z, Goldberg I (**1988**). *The growth of* Pseudomonas putida *on m-toluic acid and on toluene in batch and in chemostat cultures*. Appl. Microbiol. Biot. 27(5–6):587–592.

Vicente M, Cánovas JL (**1973**). *Glucolysis in* Pseudomonas putida*: Physiological Role of Alternative Routes from the Analysis of Defective Mutants*. J. Bacteriol. 116(2):908–914.

Wang KW, Baltzis BC, Lewandowski GA (**1996**). *Kinetics of Phenol Biodegradation in the Presence of Glucose*. Biotechnol. Bioeng. 51(1):87–94.

5. RESPIROMETRY APPLIED TO A SUSPENDED ACTIVATED SLUDGE SYSTEM

Abstract

In situ *pulse respirometry was applied in an activated sludge bubble column treating synthetic wastewater for the estimation of the (i) maximum specific oxygen consumption rate, (ii) substrate affinity constant, (iii) biomass growth yield, (iv) maintenance coefficient, and (v) specific endogenous respiration rate. Parameters obtained from respirometry were compared to those obtained by the chemostat method, based on substrate and biomass measurements, under several dilution rates. Biomass growth yield values varied between 0.37 and 0.76 g COD-X g COD-S^{-1} with the chemostat method, and between 0.37 and 0.65 g COD-X g COD-S^{-1} with the respirometric method. Maintenance coefficient was estimated to be 0.012 ± 0.012 and 0.010 ± 0.006 h^{-1} by COD mass balance and by respirometry, respectively. The low sensitivity of substrate measurement methods and the difficulties of sampling heterogeneous biomass suspension are critical issues limiting the applicability of the chemostat method. Additionally, the extensive time consuming nature of this method allows concluding that chemostat method presents several disadvantages in comparison with* in situ *pulse respirometric techniques. Parameters were obtained from respirograms by fitting ASM1 and ASM3 models, and from experiments performed by injecting pulses of different substrate concentrations (multiple concentration pulses respirometric method). The most adequate method was the multiple concentration pulses respirometric method, with several advantages such as a simpler experimental data interpretation, and results with better confidence. Affinity constant and maximum specific oxygen consumption rate were estimated with the multiple concentration pulses injection respirometric method to be 15.5 ± 2.4 mg COD-S L^{-1} and 0.12 ± 0.01 h^{-1}, respectively. Considering the assessment and comparison of the experimental and calculation methods presented, it is recommended that the estimation of kinetic and stoichiometric parameters in mixed aerobic cultures should preferentially be performed by using* in situ *respirometric techniques.*

This chapter is published as:

Oliveira CS, Ordaz A, Ferreira EC, Alves M, Thalasso F (**2011**). In situ *pulse respirometric methods for the estimation of kinetic and stoichiometric parameters in aerobic microbial communities*. Biochem. Eng. J. (doi:10.1016/j.bej.2011.08.001)

5.1. Introduction

Respirometry is the measurement of the biological oxygen consumption rate under well defined conditions (Spanjers *et al*, 1999). The interest of respirometry for parameter estimation, compared to techniques based on substrate concentration measurement, is that dissolved oxygen (DO) concentration can be measured easily and continuously with relative small input of experimental effort and obtaining high-quality data (Vanrolleghem and Verstraete, 1993). DO concentration changes in the order of ten parts-per-billion can be monitored online at high frequency.

Notwithstanding the potential advantages of respirometric methods, kinetic and stoichiometric parameters are still largely determined by substrate mass balances in batch or chemostat culture. From these, chemostat is still widely accepted as a suitable method for determining the substrate affinity constant (K_S) (Agarry *et al*., 2009; Lovanh *et al*, 2002; Duarte *et al*., 1994). It consists in measuring the residual limiting substrate concentration for different dilution rates. The growth limiting substrate is directly measured at concentrations close to K_S (Kovarova-Kovar and Egli, 1998), being precision and accuracy of substrate measurements pointed as the main limitation of the method (Koch, 1997). Additionally, reaching steady state takes considerable time, thus the method is especially time consuming as it requires the operation of the reactor under several steady states. Drawbacks of traditional methods may be overcome by respirometry (Ordaz *et al*., 2011; Oliveira *et al*., 2009).

Within many respirometric techniques, pulse respirometry, developed in the late 80s and mid 90s is probably one of the most used (Seoane *et al*., 2010; Riefler *et al*., 1998; Spanjers and Vanrolleghem, 1995; Cech *et al*., 1985). It consists in measuring DO concentration after the injection into the system of a defined substrate concentration pulse. The exogenous oxygen uptake rate (OUR_{exo}) curves reflect the kinetic of the aerobic biodegradation process and allow the estimation of kinetic and stoichiometric parameters. After the injection of substrate pulses, the kinetic parameters are usually estimated by direct model fitting to a respirometric curve (Oliveira *et al*., 2009; Goudar and Ellis, 2001; Spanjers and Vanrolleghem, 1995). Alternatively, Cech *et al*. (1985) proposed a method in which kinetic parameters are obtained from the observed respirometric response of the endogenous system to the injection of substrate pulses of increasing concentration.

The determination of the oxidation yield ($Y_{O2/S}$) and the growth yield ($Y_{X/S}$) by pulse respirometry is also commonly done by model fitting to a respirometric curve

(Vanrolleghem and Verstraete, 1993). However, parameter identifiability analysis showed that $Y_{X/S}$ cannot be estimated accurately and simultaneously with kinetic parameters by model fitting (Dochain *et al*., 1995). An alternative strategy for $Y_{X/S}$ determination is to consider the total exogenous oxygen consumed during the pulse injection (Sollfrank and Gujer, 1991).

Pulse respirometry is also of interest to determine inhibition constants (Insel *et al*., 2006; Kong *et al*., 1994), oxygen affinity constants (Guisasola *et al*., 2005), wastewater biodegradability (Lagarde *et al*., 2005; Sperandio *et al*., 2001), and to estimate maintenance coefficients (m) and endogenous respiration rates (b_H), which are both important for a proper description of microbial kinetics (Van Bodegom, 2007; Russel and Cook, 1995).

So far, literature on respirometry has given a special emphasis to parameters retrievability, identifiability, precision, and sensitivity, but it has comparatively been given less focus to the accuracy of the retrieved parameters through the comparison between parameters obtained by respirometry and other methods (Contreras *et al*., 2001). The aim of the present research paper is to find a suitable method for the estimation of kinetic and stoichiometric parameters in mixed cultures, using suspended activated sludge as model system. With this purpose two categories of estimation methods are assessed: (i) chemostat method, and (ii) *in situ* pulse respirometry. Additionally, two respirometric methods are compared: respirograms model fitting in the context of ASM1 and ASM3; and a method based on the injection of pulses of increasing substrate concentration.

5.2. Material and Methods

5.2.1. Experimental strategy

A lab-scale reactor was operated during 270 days under several dilution rates (D). This allowed the estimation of the main stoichiometric and kinetic parameters, namely $Y_{X/S}$ (biomass growth yield), $Y_{O2/S}$ (substrate oxidation yield), $q_{O2\ max}$ (maximum specific oxygen consumption rate), K_S, and maintenance coefficient (m) by respirometry and by traditional chemostat method. Additionally, the endogenous respiration rate (b_H) was only estimated by respirometry (Table 5.1).

Table 5.1. List of parameters estimated and methods used

Parameter	COD balance/Chemostat	Pulse respirometry
$Y_{X/S}$	✓	✓
$Y_{O2/S}$		✓
$q_{O2\ max}$	✓	✓
K_S	✓	✓
m	✓	✓
b_H		✓

5.2.2. Experimental Setup

A transparent acrylic reactor was used (0.14 m internal diameter, 0.56 m height, 8.6 L working volume). Air was continuously supplied through a porous plate (0.09 m diameter) located at the bottom of the reactor, with a constant air flow rate of 0.60 L min^{-1}. The air flow rate was controlled by a mass flow-controller (Aalborg, Model GFC 17, Denmark). The reactor was continuously fed with synthetic wastewater, containing (mg L^{-1}): gelatine peptone, 640; meat extract, 440; urea, 120; NaCl, 28; $CaCl_2 \cdot 2H_2O$, 16; $MgSO_4 \cdot 6H_2O$, 8; K_2HPO_4, 34; Na_2HPO_4, 134; NH_4Cl, 6.8; total chemical oxygen demand (COD), 1198 ± 11; soluble COD, 1087 ± 17; C/N ratio, 2.6 (g g^{-1}). Allylthiourea (ATU) was added to the synthetic wastewater solution (10 mg ATU L^{-1}) in order to inhibit nitrification. The synthetic wastewater was fed continuously with peristaltic pumps (Watson Marlow 101 U/R, 405 U/R1 or 401 U/D1, depending on the flow rate). Effluent was collected by overflow in a refrigerated tank (4 ºC) for posterior analysis. pH was maintained at 7.0 ± 0.5, by addition of 0.5 M NaOH or 0.2 M H_2SO_4 (Control System/Pump BL7917, Hanna Instruments, USA). The reactor was inoculated with 1 L of mixed liquor obtained from a conventional wastewater treatment plant (Cambados–Maia, Portugal). The reactor was maintained at ambient room temperature (19 – 23 ◦ C).

The reactor was characterised in terms of mixing time (t_{mix}) by lithium chloride pulse experiments (Ordaz *et al.*, 2008). t_{mix} was defined as the time required for the lithium concentration in the reactor, after the injection of a pulse, to reach 90 % of the final lithium concentration. t_{mix} was determined as follows: (i) the reactor feeding was stopped, (ii) a known concentration of lithium chloride was injected at the bottom of the reactor,

(iii) samples were taken from the top of the reactor, and (iv) after stable lithium concentration was observed, the reactor feeding was switched back on. The lithium concentration was measured by atomic absorption (Varian SPECTRAA 250 Plus, USA).

5.2.3. Reactor operation

After inoculation, the reactor was operated under fed-batch mode for 5 days. During this period, about 20 % of the mixed liquor was substituted every day. After this adaptation period, the reactor was operated continuously during 270 days under five dilution rates (D from 0.2 to 2.0 d^{-1}) and, consequently, five organic loading rates (from 0.2 to 2.3 g COD-S L^{-1} d^{-1}). Each D tested was maintained at least until steady state was reached, the steady state is defined as constant degradation rate and biomass concentration (variations within normal standard deviations).

5.2.4. Methods

Analytical Methods

Influent and effluent were characterised through triplicate measurements of the total and soluble COD. COD was determined using the closed reflux colorimetric method, according to standard methods (APHA, 1999). Substrate concentration (S) was considered to be the soluble COD fraction (COD-S), and biomass concentration (X) the insoluble COD fraction (COD-X), estimated as the difference between total COD and soluble COD. Soluble and insoluble COD fractions were separated by filtration (0.45 μm).

Pulse Respirometry and Data Interpretation

The DO concentration was measured online with a polarographic oxygen probe, located at the top of the reactor and connected to a DO-meter (Hannah Instrument HI2400, USA) and a computer for data acquisition. DO readings were corrected for temperature, salinity, and altitude through DO-meter automatic compensation adjustments. The oxygen probe was calibrated before each respirometric experiment. Saturation DO concentration (C^*) was experimentally measured under the experimental conditions of the reactor, using sterilised effluent coming out from the reactor. Oxygen mass transfer coefficient (k_La) was determined from the dynamic method, as it was described by Badino *et al*. (2000). The

response time of the electrode was taken into account during respirometric and k_La measurements.

In situ respirometric pulse experiments were done according to the following procedure: (i) the reactor was maintained until stable DO readings were obtained; (ii) the substrate feeding was stopped and the aeration maintained; (iii) the DO concentration slowly increased until reaching a new pseudo-stationary state, called baseline oxygen concentration (C_b) corresponding to endogenous respiration (Dircks *et al*., 1999); (iv) a pulse of synthetic wastewater, containing ATU (reactor concentration of 10 mg ATU L^{-1}), was injected in order to obtain a substrate concentration in the reactor (S_P) of approximately 20 mg COD-S L^{-1}; (v) the DO concentration was acquired until the system returned to C_b; (vi) additional pulses were eventually injected (10 – 40 mg COD-S L^{-1}); and (vii) the k_La was measured in triplicate before the feeding of the reactor was restored. The initial substrate to biomass ratio (S_0/X_0) applied with the pulses was between 0.03 and 0.2 g COD-S g COD-X^{-1}.

The respirometric data interpretation method was as previously reported (Ordaz *et al*., 2008; Ellis *et al*., 1996; Smets *et al*. 1994). Briefly, after the injection of a known substrate pulse concentration (S_P), the $Y_{O2/S}$ was given by the amount of oxygen consumed per unit COD of substrate oxidised (Equation 5.1). $Y_{X/S}$ expressed in COD units was estimated from $Y_{O2/S}$ (Equation 5.2).

$$Y_{O2/S}=\frac{\int_0^t OUR_{exo}\, dt}{S_P}=\frac{k_La\int_0^t(C_b - C)\, dt + (C_0 - C_f)}{S_P} \quad (5.1)$$

$$Y_{X/S} = 1 - Y_{O2/S}= 1 - \frac{k_La\int_0^t(C_b - C)\, dt + (C_0 - C_f)}{S_P} \quad (5.2)$$

The average $Y_{X/S}$ estimated at each D by respirometry were used to estimate the maintenance coefficient (m) according to the Pirt method (Pirt, 1965) (Equation 5.3). Models including a variable maintenance were also considered such as the Neijssel and Tempest model (Neijssel and Tempest, 1972) (Equation 5.4), and the 1982 Pirt model (Pirt, 1982) (Equation 5.5). In these models, since the system was considered at steady state and completely mixed, the specific growth rate (μ) was considered equal to D.

$$\frac{1}{Y_{X/S}} = \frac{1}{Y'_{X/S}} + m\frac{1}{\mu} \quad (5.3)$$

$$\frac{1}{Y_{X/S}} = \frac{1}{Y'_{X/S}} + m'\frac{1}{\mu} + c\,m' \quad (5.4)$$

$$\frac{1}{Y_{X/S}} = \frac{1}{Y'_{X/S}} + m\frac{1}{\mu} + m''\left(\frac{1-k\mu}{\mu}\right) \quad (5.5)$$

During pulse respirometry, C_b was typically inferior to C^*. This difference was accounted for endogenous respiration (Sin *et al*., 2005; Dircks *et al*., 1999). In this work, m estimated from Equations 5.3 – 5.5, was compared to the specific endogenous respiration rate (b_H) estimated from Equation 5.6.

$$b_H = \frac{k_L a\,(C^* - C_b)}{X} \quad (5.6)$$

$q_{O2\,max}$ and K_S were estimated by model fitting to respirometric data, as it was previously described (Ordaz *et al*., 2008). Briefly, after the injection of a substrate pulse, the DO concentration in the reactor was described by a balance between the exogenous respiratory activity and the oxygen provided by continuous aeration (Kong *et al*., 1996), being C the DO concentration in the liquid phase. Additionally, the response time of the process (t_r) was taken into account in a similar manner as described previously by Vanrolleghem *et al*. (2004).

$$\frac{dC}{dt} = [k_L a\,(C_b - C) - OUR_{exo}]\left(1 - e^{-t/t_r}\right) \quad (5.7)$$

In Equation 5.7, two models were used to describe OUR_{exo} and fitted to experimental DO data: the ASM1 model (Henze *et al*., 1987), and the ASM3 model (Gujer *et al*., 1999). Table 5.2 shows the matrix representation of the models used. The main difference between both models is that ASM3 model considers substrate storage.

Equation 5.7 was adjusted to the experimental data obtained from the pulse experiments with a fitting procedure based on Runge–Kutta method and a Marquardt optimisation method with 20 convergence steps (Model Maker, Cherwell Scientific Publishing, UK). $q_{O2\,max}$ was obtained by dividing the estimated OUR_{exo}max by the biomass concentration in the reactor (X).

Table 5.2. Simplified matrix of ASM1-like and ASM3 models for organic carbon removal, considering soluble biodegradable COD

Process	Component				Rate
	S	X_{Sto}	X	C	
Substrate consumption (ASM1)	$-\frac{1}{Y_{O2/S}}$			-1	$q_{O2\ max} X \frac{S}{K_S + S}$
Storage of S (ASM3)	-1	$Y_{X/Sto}$		$-(1 - Y_{Sto/S})$	$k_{Sto} X \frac{S}{K_S + S}$
Growth on X_{Sto} (ASM3)		$-\frac{1}{Y_{X/Sto}}$	1	$-\frac{(1 - Y_{X/Sto})}{Y_{X/Sto}}$	$\mu_{max} X \frac{X_{Sto}/X}{K_{Sto} + X_{Sto}/X}$
Endogenous respiration (ASM3)	-1		-1		$b_H X$
Respiration of X_{sto} (ASM3)		-1		-1	$b_{Sto} X_{Sto}$

Additionally to model fitting, $q_{O2\ max}$ and K_S were also estimated after the injection of pulses of increasing substrate concentration, as it was reported by Orupold *et al*. (2001). The observed $SOUR_{exo\ max}$ (specific $OUR_{exo\ max}$, obtained by dividing $OUR_{exo\ max}$ by X) was plotted against the substrate concentration pulse (S_P). The graph obtained showed a clear Monod-type shape (Equation 5.8), used to estimate $q_{O2\ max}$ and K_S.

$$SOUR_{exo\ max} = q_{O2\ max} \frac{S_P}{K_S + S_P} \quad (5.8)$$

Chemostat Method

$Y_{X/S}$ was estimated from the biomass produced (difference between total and soluble COD of the effluent) and the substrate consumed (difference between influent and effluent soluble COD). The average of $Y_{X/S}$ estimated at each D, were used to determine the maintenance coefficient (m) according to the Pirt method (Pirt, 1965) (Equation 5.3), as it was done with data obtained by respirometry. $q_{O2\ max}$ and K_S were estimated by fitting the Monod equation to the average experimental data ($SOUR_{exo}$ and S) determined at each dilution rate, under steady state. With that purpose, $SOUR_{exo}$ was estimated from the total COD removed.

Statistical Analysis

Models goodness of fit was estimated through the comparison of three parameters: (i) the correlation factor (r^2), (ii) the root mean squared error (RMSE), and (iii) the Kolmogorov–Smirnov test (Kirkman, 1996). Significance of difference between parameters was estimated through One-way ANOVA and Tukey's HSD post hoc test, using PASW Statistics 18 (SPSS Inc. Package).

Average values are presented with the corresponding standard error.

5.3. Results and Discussion

5.3.1. Reactor operation

The reactor was inoculated with activated sludge from a local wastewater plant, and operated under fed-batch mode. After 5 days, a clear biomass growth was observed (approximately from 400 to 500 mg COD-X L^{-1}), corroborated by an increase in substrate degradation activity. Time was reset and the reactor was then operated under continuous mode for 270 days. The reactor worked with a constant influent concentration of 1.06 ± 0.09 g COD-S L^{-1}. Five dilution rates were tested, from 0.19 to 1.95 d^{-1}. The first tested D (0.45 d^{-1}) was maintained for 170 days. The additional D (*i.e.*, 0.19, 0.28, 0.91, and 1.95 d^{-1}) were maintained for a time corresponding to six hydraulic retention times (HRT) at least. Figure 5.1 shows the reactor's behaviour during the continuous operation. The system adapted adequately to the variations of the organic loading rate, imposed by the variations of D, presenting a stable COD removal efficiency during the whole operation (90 – 100 % soluble COD removal).

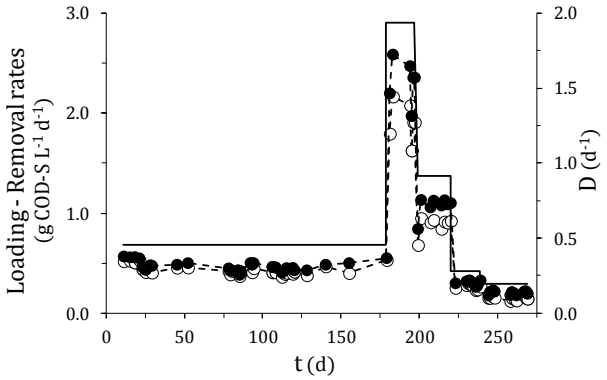

Figure 5.1. Behaviour of the reactor: dilution rate (*solid line*), loading rate (●), and removal rate (○).

Table 5.3 presents information on sludge retention time (SRT) and biomass concentration (X) achieved at each tested D. A quasi-linear (r^2 = 0.98) decrease of X was observed with the SRT increase. This can be explained by the increase of substrate limitations to biomass growth as dilution rate decreased, and SRT increased.

Table 5.3. Sludge retention time (SRT) and biomass concentration (X) achieved at each of the tested dilution rates (D)

D (d^{-1})	**SRT (d)**	**X (mg COD-X L^{-1})**
2.0	0.5	674.6 ± 203.0
0.9	1.1	595.4 ± 156.4
0.5	2.2	454.4 ± 191.2
0.3	3.6	377.7 ± 148.4
0.2	5.2	193.2 ± 57.2

The mixing time of the reactor (t_{mix}) was determined in two periods: at the beginning of operation, on day 10, when a t_{mix} of 19 ± 2 s was obtained; and at the end of operation, on day 250, when a t_{mix} of 22 ± 2 s was obtained. These low t_{mix} values, comparatively to HRT, show that the bubble column reactor was a well-mixed system.

The first pulse experiments were done on day 20. Figure 5.2 shows a superposition of two respirograms obtained after feeding suppression and injection of two successive pulses of 22 mg COD-S L^{-1}. Figure 5.2 shows that DO concentration decreased sharply immediately after pulse injection (time 0) and then, after 2 h, returned to the baseline value (C_b) of 8.2 mg L^{-1}. Both respirograms showed a similar shape with a square correlation coefficient

(r^2) between them of 0.99. At the end of the second pulse, after 6 h of respirometric experiments, the substrate feeding was turned back on, and the system returned to normal operation. No changes were observed in DO, biomass, nor substrate concentrations compared to the situation observed before the respirometric experiments (data not shown). These results confirm that *in situ* pulses were reproducible and that feeding suspension during approximately 6 h did not affect significantly the behaviour of the system.

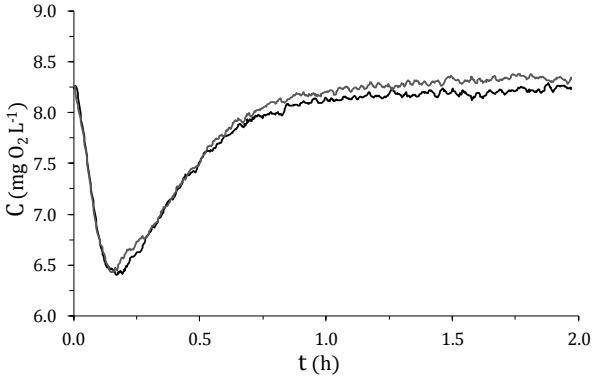

Figure 5.2. Superposition of two respirograms obtained after the injection of two consecutive pulses of 22 mg L^{-1}: first pulse (*black line*), and second pulse (*grey line*).

5.3.2. $Y_{X/S}$ and m

$Y_{X/S}$ was estimated by respirometry (Equation 5.2) from the area of the 51 respirograms obtained during the whole reactor operation, and also by COD mass balance. Figure 5.3 presents a comparison of the average $Y_{X/S}$ values for each dilution rate. The slope of the linear regression forced to cross the origin was 1.01, with a r^2 of 0.98, meaning that the values obtained with both methods were comparable. Very recently, Di Trapani *et al*. (2011) found, in a membrane bioreactor, a significant difference between the $Y_{X/S}$ values obtained by pulse respirometry and by COD mass balance. This discrepancy of values was suggested to be related with two terms: (i) the fact that respirometric pulses were done with a readily biodegradable substrate for characterisation of biomass acclimated to real wastewater, and (ii) the influence of biomass decay phenomenon, which is taken into account by the COD mass balance method, but not by the respirometric method due to the short time of experiments Biomass decay was probably an important factor in Di Trapani *et al*. (2011) work, as they used a membrane bioreactors with high sludge retention. In the present work no discrepancy was observed between $Y_{X/S}$ values obtained by pulse

respirometry and by COD mass balance, probably because the same complex substrate was used to feed the reactor and for respirometric pulses, and because the reactor used was completely mixed with no biomass retention in excess to hydraulic retention, thus where decay phenomenon was negligible. Regardless of the proximity of the $Y_{X/S}$ values obtained by pulse respirometry and by COD mass balance, the average standard deviation of the respirometric method (15 %) was lower than the average standard deviation of the COD balance method (27 %). The higher standard deviation of the COD method is likely due to the required biomass sampling procedures, which are not necessary with *in situ* respirometric methods. This constitutes one advantage of respirometry.

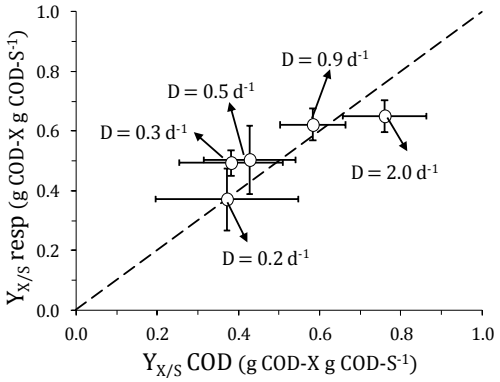

Figure 5.3. Correlation between the biomass growth yields estimated by respirometry ($Y_{X/S}$ resp) and by COD mass balance ($Y_{X/S}$ COD). The dotted line represents the linear regression forced to cross the origin (slope 1.01 ± 0.17; $r^2 = 0.98$).

From the $Y_{X/S}$ determined by respirometry, and by COD mass balance, m was determined graphically (Figure 5.4) according to the Pirt's method (Pirt, 1965) (Equation 5.3). Maintenance coefficients, m, estimated by the COD mass balance and by respirometry, were, respectively, 0.012 ± 0.012 and 0.010 ± 0.006 h^{-1}. Considering that the results were obtained over 270 days with a mixed culture that was certainly changing in composition over time (Novak *et al*., 1994), it is not surprising that with neither one of the methods a perfect linear correlation was obtained. Nevertheless, the linear correlation (r^2) of the respirometric method was significantly higher (0.90) than the correlation of the COD method (0.78), confirming that methods based on biomass sampling are affected by intrinsic errors due to the difficulty of sampling heterogeneous suspensions. The 1982 Pirt (Pirt, 1982), and the Neijssel and Tempest (Neijssel and Tempest, 1976) models were unsuccessfully applied ($r^2 < 0.70$) to the same experimental data (data not shown).

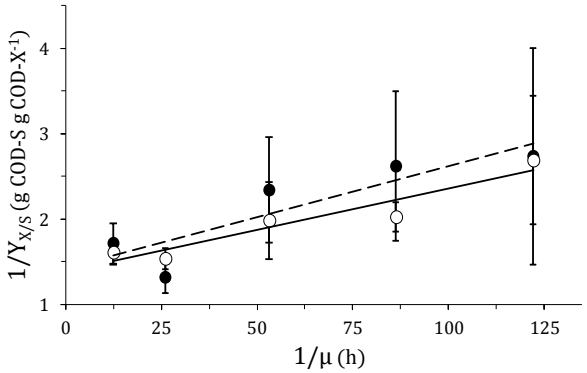

Figure 5.4. Pirt (1965) linearisation of the experimental growth yield estimated from COD mass balance (●, r^2 = 0.78, *dotted line*), and by respirometry (○, r^2 = 0.90, *solid line*).

As mentioned before, the difference between C_b and the C^* during respirometric experiments is typically accounted for endogenous respiration (Sin *et al.*, 2005; Dircks *et al.*, 1999). In order to compare maintenance (m) and endogenous respiration (b_H), the baseline DO concentration was measured before each of the 51 pulses made along the reactor operation. From these data, the estimation of b_H from Equation 5.6 was 0.025 ± 0.015 h^{-1}. This result shows that b_H was superior to m (0.010 ± 0.006 h^{-1}) estimated with respirometric data from Pirt's model (Pirt, 1965). The difference between b_H and m deserves a close attention. The difference between m and b_H can be explained by the fact that different non-growth processes are considered in each case (van Bodegom, 2007; van Loosdrecht and Henze, 1999). The endogenous respiration includes osmoregulation, cell mobility, defence mechanisms, proofreading, and internal turnover of macromolecular compounds. Maintenance (m) neglects some of these processes and is therefore expected to be lower than b_H, as it was observed in this work.

5.3.3. K_S and $q_{O2\ max}$

ASM1 and ASM3 models were adjusted to the respirograms obtained along the operation of the reactor. Figure 5.5 shows an example of data fitting using both models.

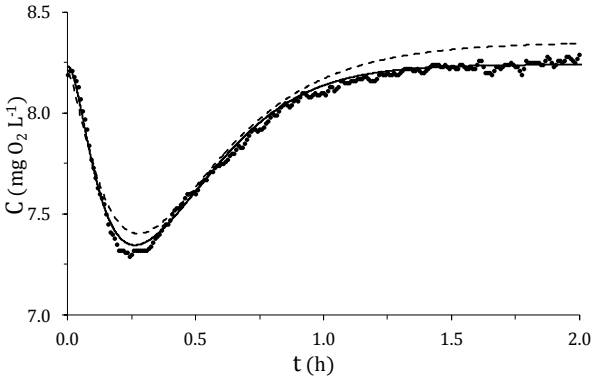

Figure 5.5. Example of a respirogram (•), model fitting using ASM1-like (r^2 =0.99, *solid line*) and ASM3 (r^2 = 0.95, *dotted line*).

Table 5.4 shows average values of the correlation factor, the RMSE and the Kolmogorov–Smirnov goodness of fit ($D_{(K-S)}$) after the analysis of 51 pulses made during the reactor operation. The correlation factor of ASM1 model was superior to that of ASM3. Both RMSE and $D_{(K-S)}$ were lower for the ASM1 than for the ASM3 model. These results confirm that ASM1 model adjusted better the experimental data, which is an indication that storage was not significant in this process. This is in accordance with literature, as storage mechanism is generally observed in sludge subjected to dynamic conditions. Krishna and van Loosdrecht (1999) stated, for instance, that, under continuous feeding, activated sludge systems have a low storage capacity. More recently, Ciggin *et al*. (2007) indicated that biomass acclimated to continuous feeding could not store the excess substrate even when a sudden change in the feeding was done. In the present work, the reactor was maintained under steady state, and the biomass never experienced dynamic conditions of substrate concentration, except when substrate pulses were done. However, a maximum of 2 pulses per day were done and each sequence of pulses was parted by 15 to 70 h. According to Vanrolleghem *et al*. (1998) it is expected that the biomass had no time to adapt its enzymatic system to storage. Prendl and Kroiss (1998) did not observe storage when the sludge age was below 5 days. In the present work, except in the last D tested (0.2 d^{-1}), the sludge age was below 5 days. At last, it has been reported that storage occurs when sludge is subjected to nutrient or oxygen limitation with excess of substrate. In this work, the pulses were made of complete medium, including nutrients, and DO was always above 2 mg L^{-1}. According to the results obtained and the literature reports, storage was discarded and ASM1 model was used further on.

Table 5.4. Average values of the correlation factor, the RMSE and the $D_{(K-S)}$ value for ASM1 and ASM3 fitting to respirograms

	ASM1	ASM3
r^2	0.97	0.91
RMSE	0.07	0.13
$D_{(K-S)}$	0.19	0.39

K_S and $q_{O2\ max}$ were estimated by ASM1 model fitting to the respirograms obtained during the reactor operation. Table 5.5 presents average results obtained from 51 pulses made over 270 days of experiment. K_S values estimated from model fitting were within the range generally observed in wastewater treatment plants (Metcalf and Eddy, 2003), and they were also similar to the K_S estimated by respirometry by Carucci *et al*. (2001) in real filtered wastewater (K_S = 12.3 ± 0.3 mg COD-S L^{-1}). The response time of the process was approximately 0.06 h (3.4 min), similar to those previously reported by Vanrolleghem *et al*. (2004). The One-way ANOVA test revealed that K_S was not significantly affected by D ($F_{(4,46)}$ = 0.253, p = 0.91). Regarding $q_{O2\ max}$, there was a significant difference between different D ($F_{(4,46)}$ = 4.617, p < 0.05). Tukey's HSD post hoc test showed that this difference was between the extremes, *i.e.*, between $q_{O2\ max}$ at D = 0.2 and 2.0 d^{-1} (Table 5.4).

Table 5.5. Average parameters obtained by ASM1 model fitting of 51 pulses injected at five dilution rates (D)

D (d^{-1})	Number of pulses	K_S (mg COD-S L^{-1})	$q_{O2\ max}$ (h^{-1})	t_r (h)
0.2	12	19.6 ± 2.7	0.11 ± 0.02	0.08 ± 0.03
0.3	9	18.7 ± 2.5	0.09 ± 0.01	0.07 ± 0.01
0.5	18	17.0 ± 2.6	0.07 ± 0.01	0.09 ± 0.01
0.9	6	15.8 ± 2.1	0.04 ± 0.00	0.00 ± 0.00
2.0	6	18.4 ± 2.7	0.08 ± 0.01	0.00 ± 0.00
Average		17.9 ± 2.5	0.08 ± 0.01	0.05 ± 0.01

K_S and $q_{O2\ max}$ were also estimated by respirometry from the injection of pulses of different concentrations. Pulses of 10.5, 21.0, and 42.3 mg COD-S L^{-1} were injected and between pulses the feeding was restored until stable DO readings were obtained to ensure repeatability of the experimental conditions. Figure 5.6a shows an example of the $SOUR_{exo}$

response after the injection of three different concentrations pulses. In each case, $SOUR_{exo\ max}$ depended on S_P. Figure 5.6b shows that $SOUR_{exo\ max}$ followed a Monod-type kinetic in relation to the substrate concentration ($r^2 = 1.00$). This allowed determining K_S and $q_{O2\ max}$ (Equation 5.8), 15.5 ± 2.4 mg COD-S L^{-1} and 0.12 ± 0.01 h^{-1}, respectively. By fitting ASM1 model simultaneously to the four respirograms used in the method of multiple concentration pulses injection (pulses of 10.5, 21.0, and 42.3 mg COD-S L^{-1}), the values obtained for K_S and $q_{O2\ max}$ were 19.9 ± 0.06 mg L^{-1} and 0.10 ± 0.02 h^{-1}, respectively, with a correlation factor of 0.92. By individual model fitting to the respirograms, model fitting to the 10.5 mg COD-S L^{-1} pulse failed; with the 21.0 mg COD-S L^{-1} pulse, the K_S and $q_{O2\ max}$ values estimated were 22.3 ± 0.13 mg COD-S L^{-1} and 0.12 ± 0.03 h^{-1}, respectively (r^2 = 0.96); and with the 42.3 mg COD-S L^{-1} pulse the values 33.7 ± 0.8 mg COD-S L^{-1} and 0.12 ± 0.02 h^{-1} were obtained for K_S and $q_{O2\ max}$, respectively ($r^2 = 0.93$). The discrepancy of values obtained by model fitting a single pulse confirms previous observations which state that a number of pulses higher than one further improve parameters practical identifiability (Seoane *et al*, 2010; Vanrolleghem and Verstraete, 1993). However, this compromises an increment in the computational effort, which has to be taken into account. The obtained values with the two respirometric data treatment methods were similar. Though the K_S associated error for model fitting was lower, the correlation factor of the model was worse than the one corresponding to the multiple concentration pulses respirometric method.

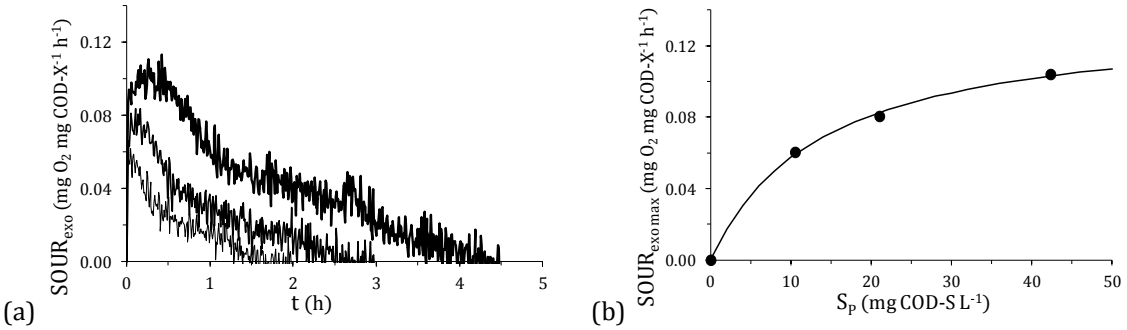

Figure 5.6. (a) Respirograms observed at three pulse concentrations (mg L^{-1}): 10.5 (*lighter line*), 21.0 (*medium line*), and 42.3 (*darker line*); and (b) best fitting Monod model to $SOUR_{exo}$max *vs.* S_P data ($r^2 = 1.00$).

For further comparison between both respirometric data treatment methods, results obtained by model fitting after the injection of a pulse of 21.8 mg COD-S L^{-1} were compared to those obtained after the injection of pulses of different concentrations. The results of these sensitivity analyses are presented in Figure 5.7, where the lines represent the dimensionless K_S and $q_{O2\ max}$ pairs for a specified r^2, as it is indicated. It is shown that

the r^2 of the model fitting method is less sensitive to changes in K_S and $q_{O2\,max}$ than the r^2 of the method based on pulses of different concentration. This indicates that the method based on the injection of multiple pulses of different concentrations is more precise than simple single pulse model fitting and it is confirmed as a suitable method to estimate $q_{O2\,max}$ and K_S. In order to improve the identifiability of parameters through ASM model fitting, more than one pulse is recommended. In the multiple concentration pulses method three pulses are needed, which means the experimental effort of both methods is equivalent. Nevertheless, the ASM model fitting requires a much higher computational effort in order to treat a large amount of data, while the multiple concentration pulses method uses a basic Monod-type model fitting.

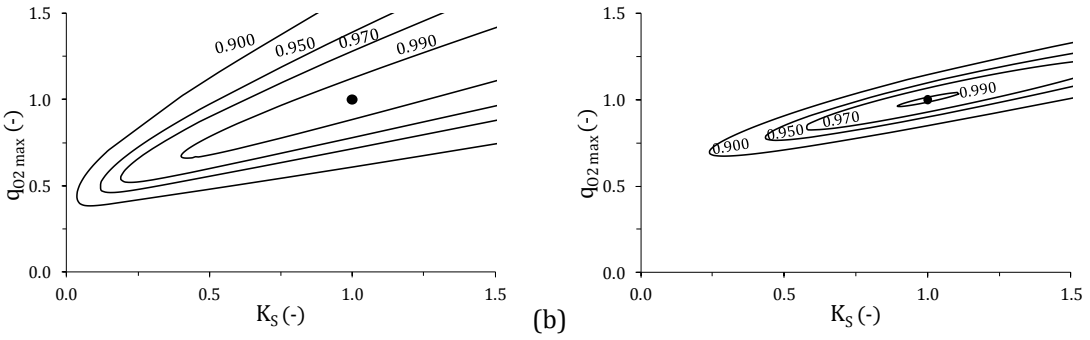

Figure 5.7. Contour-plot of the correlation factor as a function of the substrate affinity constant (K_S) and the maximum specific exogenous OUR ($q_{O2\,max}$), for the model fitting method (a), and for the multiple concentration pulses method (b).

K_S and $q_{O2\,max}$ were also determined from COD mass balance according to the chemostat method (Duarte *et al.*, 1994). Figure 5.8 shows the average specific substrate uptake rate expressed in oxygen demand versus the average substrate concentration at each dilution rate. The low r^2 obtained (0.61) did not allow the estimation of K_S nor $q_{O2\,max}$. The low sensitivity of substrate measurement methods and the difficulties of sampling heterogeneous biomass suspension are critical issues limiting the applicability of the chemostat method. Furthermore, the chemostat method applied in mixed cultures may be questioned in the sense that it involves changing the HRT, which is a selection pressure for microorganisms in continuous culture. Consequently, the selection of slower- or faster-growing microorganisms occurs (Novak *et al.*, 1994). The poor results obtained are in accordance with these drawbacks. Additionally, the time consuming nature of this method allows to conclude that no one single advantage can be pointed out to the chemostat method, in comparison with the simple *in situ* pulse respirometric techniques whatever the method used for mixed cultures parameters retrieval, although different methods of

calculation have different precision and sensitivity. Therefore, the estimation of kinetic and stoichiometric parameters in mixed aerobic cultures should be always performed by using *in situ* respirometric techniques.

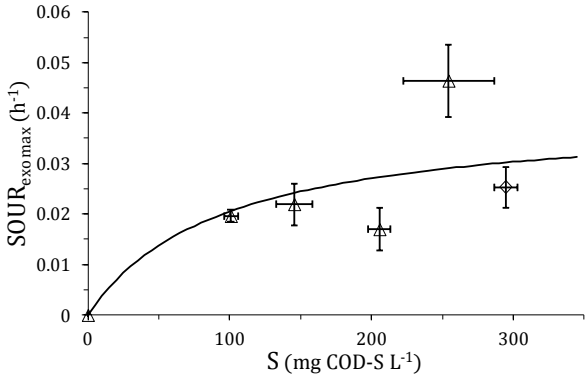

Figure 5.8. Average specific exogenous OUR ($SOUR_{exo}$) *versus* average S for each dilution rate steady state (•), and best fitting Monod model (r^2 = 0.610, *line*).

5.4. Conclusions

In situ pulse respirometry was applied to estimate stoichiometric and kinetic parameters in activated sludge systems, and a comparison with the chemostat method based on COD mass balances was done. $Y_{X/S}$, m, b_H, $q_{O2\ max}$ and K_S were better estimated by respirometry than by chemostat mass balance. A further comparison of two different respirometric methods, namely the injection of pulses of different concentration and model fitting to respirograms gave similar results. It is concluded that respirometry is a more satisfactory method than mass balance and that, within respirometric methods, the injection of multiple concentration pulses presents several advantages compared to model fitting to respirograms, mainly simpler experimental data interpretation and better results confidence.

5.5. References

Agarry SE, Audu TOK, Solomon BO (**2009**). *Substrate inhibition kinetics of phenol degradation by* Pseudomonas fluorescence *from steady state and wash-out data*. Int. J. Environ. Sci. Te. 6(3):443–450.

APHA (**1999**). *Standard methods for the examination of water and wastewater*. 20th edn. Washington, DC, American Publishers Health Association.

Badino A, Facciotti M, Schmidel W (**2000**). *Improving k_La determination in fungal fermentation, taking into account electrode response time*. J. Chem. Technol. Biot. 75(6):469–474.

Carucci A, Dionisi D, Majone M, Smurra P (**2001**). *Aerobic storage by activated sludge on real wastewater*. Water Res. 35(16):3833–3844.

Cech JS, Chudoba J, Grau P (**1985**). *Determination of kinetic constants of activated-sludge microorganisms*. Water Sci. Technol. 17(2-3):259-272.

Ciggin AS, Karahan O, Orhon D (**2007**). *Effect of feeding pattern on biochemical storage by activated sludge under anoxic conditions*. Water Res. 41(4):924–934.

Contreras E, Bertola N, Zaritzky N (**2001**). *The application of different techniques to determine activated sludge kinetic parameters in a food industry wastewater*. Water SA 27(2):169–176.

Dircks K, Pind P, Mosbaek H, Henze M (**1999**). *Yield determination by respirometry - The possible influence of storage under aerobic conditions in activated sludge*. Water SA 25(1):69–74.

Di Trapani D, Capodici M, Cosenza A, Di Bella G, Mannina G, Torregrossa M, Viviani G (**2011**). *Evaluation of biomass activity and wastewater characterization in a UCT-MBR pilot plant by means of respirometric techniques*. Desalination 269(1–3):190–197.

Dochain D, Vanrolleghem PA, Vandaele M (**1995**). *Structural identifiability of biokinetic models of activated-sludge respiration*. Water Res. 29(11): 2571–2578.

Duarte LC, Nobre AP, Gírio FM, Amaral-Collaço MT (**1994**). *Determination of the kinetic parameters in continuous cultivation by* Debaryomyces hansenii *grown on D-xylose*. Biotechnol. Tech. 8(12):859–864.

Ellis TG, Smets BF, Magbanua BS, Grady CPL (**1996**). *Changes in measured biodegradation kinetics during the long-term operation of completely mixed activated sludge (CMAS) bioreactors*. Water Sci. Technol. 34(5-6):35–42.

Goudar CT, Ellis TG (**2001**). *Explicit oxygen concentration expression for estimating extant biodegradation kinetics from respirometric experiments*. Biotechnol. Bioeng. 75(1):74–81.

Guisasola A, Jubany I, Baeza J, Carrera J, Lafuente J (**2005**). *Respirometric estimation of the oxygen affinity constants for biological ammonium and nitrite oxidation*. J. Chem. Technol. Biot. 80(4):388–396.

Gujer W, Henze M, Mino T, van Loosdrecht M (**1999**). *Activated sludge model no. 3*. Water Sci. Technol. 39(1):183–193.

Henze M, Grady CPL Jr, Gujer W, Marais GvR, Matsuo T (**1987**). *Activated Sludge Model No. 1. IAWPRC Scientific and Technical Report No. 1.* UK: IAWPRC.

Insel G, Karahan O, Ozdemir S, Pala L, Katipoglu T, Cokgor EU, Orhon D (**2006**). *Unified basis for the respirometric evaluation of inhibition for activated sludge*. J. Environ. Sci. Heal. A 41(9):1763–1780.

Kirkman TW (**1996**). *Statistics to Use*. http://www.physics.csbsju.edu/stats/.

Koch AL (**1997**). *Microbial physiology and ecology of slow growth*. Microbiol. Mol. Biol. R. 61(3):305–318.

Kong Z, Vanrolleghem P, Willems P, Verstraete W (**1996**). *Simultaneous determination of inhibition kinetics of carbon oxidation and nitrification with a respirometer*. Water Res. 30(4):825–836.

Kong Z, Vanrolleghem P, Verstraete W (**1994**). *Automated respiration inhibition kinetics analysis ARIKA with a respirographic biosensor*. Water Sci. Technol. 30(4):275–284.

Kovarova-Kovar K, Egli T (**1998**). *Growth kinetics of suspended microbial cells: from single-substrate-controlled growth to mixed-substrate kinetics*. Microbiol. Mol. Biol. R. 62(3):646–666.

Krishna C, van Loosdrecht MCM (**1999**). *Effect of temperature on storage polymers and settleability of activated sludge*. Water Res. 33(10):2374–2382.

Lagarde F, Tusseau-Vuillemin MH, Lessard P, Héduit A, Dutrop F, Mouchel JM (**2005**). *Variability estimation of urban wastewater biodegradable fractions by respirometry*. Water Res. 39(19):4768–4778.

Lovanh N, Hunt CS, Alvarez PJJ (**2002**). *Effect of ethanol on BTEX biodegradation kinetics: aerobic continuous culture experiments*. Water Res. 36(15):3739–3746.

Metcalf and Eddy Inc. (**2003**). *Wastewater Engineering: Treatment and Reuse*. Fourth Edition. Civil and Environmental Engineering Series, McGraw–Hill International Editions.

Neijssel OM, Tempest DW (**1976**). *Bioenergetic aspects of aerobic growth of* Klebsiella aerogenes *NCTC 418 in carbon-limited and carbon-sufficient culture*. Arch. Microbiol. 107:215–221.

Novak L, Larrea L, Wanner J (**1994**). *Estimation of maximum specific growth-rate of heterotrophic and autotrophic biomass – a combined technique of mathematical-modeling and batch cultivations*. Water Sci. Technol. 30(11):171–180.

Oliveira CS, Ordaz A, Alba J, Alves M, Ferreira EC, Thalasso F (**2009**). *Determination of kinetic and stoichiometric parameters of* Pseudomonas putida *F1 by chemostat and in situ pulse respirometry*. Chemical Product and Process Modeling 4(2):1–14. (*Chapter 4 of this Thesis*).

Ordaz A, Oliveira CS, Alba J, Carrión M, Thalasso F (**2011**). *Determination of apparent kinetic and stoichiometric parameters in a nitrifying fixed-bed reactor by* in situ *pulse respirometry*. Biochem. Eng. J. 55(2):123–130.

Ordaz A, Oliveira CS, Aguilar R, Carrión M, Ferreira EC, Alves M, Thalasso F (**2008**). *Kinetic and stoichiometric parameters estimation in a nitrifying bubble column through "in-situ" pulse respirometry*. Biotechnol. Bioeng. 100(1):94–102. (*Chapter 3 of this Thesis*).

Orupold K, Masirin A, Tenno T (**2001**). *Estimation of biodegradation parameters of phenolic compounds on activated sludge by respirometry*. Chemosphere 44(5):1273–1280.

Pirt SJ (**1982**). *Maintenance energy: a general model for energy-limited and energy-sufficient growth*. Arch. Microbiol. 133:300–302.

Pirt SJ (**1965**). *The maintenance energy of bacteria in growing cultures*. Proceedings of the Royal Society of London Series B 163:224–231.

Prendl L, Kroiss H (**1998**). *Bulking sludge prevention by an aerobic selector*. Water Sci. Technol. 38(8-9):19–27.

Riefler R, Ahlfeld D, Smets B (**1998**). *Respirometric assay for biofilm kinetics estimation: Parameter identifiability and retrievability*. Biotechnol. Bioeng. 57(1):35–45.

Russell JB, Cook GM (**1995**). *Energetics of bacterial-growth - Balance of anabolic and catabolic reactions*. Microbiol. Rev. 59(1):48–62.

Seoane J, Sin G, Lardon L, Gernaey KV, Smets BF (**2010**). *A new extant respirometric assay to estimate intrinsic growth parameters applied to study plasmid metabolic burden*. Biotechnol. Bioeng. 105(1):141–149.

Sin G, Guisasola A, Pauw DJWD, Baeza JA, Carrera J, Vanrolleghem PA (**2005**). *A new approach for modelling simultaneous storage and growth processes for activated sludge systems under aerobic conditions*. Biotechnol. Bioeng. 92(5):600–613.

Sollfrank U, Gujer W (**1991**). *Characterization of domestic wastewater for mathematical modelling of the activated sludge process*. Water Sci. Technol. 23(4-6):1057–1066.

Smets BF, Ellis TG, Brau S, Sanders RW, Grady CPL (**1994**). *Quantification of the kinetic differences between communities isolated from completely mixed activated-sludge systems operated with or without a selector using a novel respirometric method*. Water Sci. Technol. 30(11):255–261.

Spanjers H, Takacs I, Brouwer H (**1999**). *Direct parameter extraction from respirograms for wastewater and biomass characterization*. Water Sci. Technol. 39(4):137–145.

Spanjers H, Vanrolleghem P (**1995**). *Respirometry as a tool for rapid characterization of waste-water and activated-sludge*. Water Sci. Technol. 31(2):105–114.

Sperandio M, Urbain V, Ginestet P, Audic MJ, Paul E (**2001**). *Application of COD fractionation by a new combined technique: comparison of various wastewaters and sources of variability*. Water Sci. Technol. 43(1):181–190.

Van Bodegom P (**2007**). *Microbial maintenance: A critical review on its quantification*. Microb. Ecol. 53(4):513–523.

Van Loosdrecht MCM, Henze M (**1999**). *Maintenance, endogeneous respiration, lysis, decay and predation*. Water Sci. Technol. 39(1):107–117.

Vanrolleghem P, Sin G, Gernaey V (**2004**). *Transient response of aerobic and anoxic activated sludge activities to sudden substrate concentration changes*. Biotechnol. Bioeng. 86(4):277–290.

Vanrolleghem PA, Gernaey K, Coen F, Petersen B, de Clercq B, Ottoy JP (**1998**). *Limitations of short-term experiments designed for identification of activated sludge biodegradation models by fast dynamic phenomena*. In: Proceedings 7th IFAC Conference on Computer Applications in Biotechnology CAB7. Osaka, Japan, May 31–June 4.

Vanrolleghem PA, Vandaele M, Dochain D (**1995**). *Practical identifiability of a biokinetic model of activated-sludge respiration*. Water Res. 29(11):2561–2570.

Vanrolleghem PA, Verstraete W (**1993**). *Simultaneous biokinetic characterization of heterotrophic and nitrifying populations of activated-sludge with an online respirographic biosensor*. Water Sci. Technol. 28(11-12):377–387.

6. RESPIROMETRY APPLIED TO AEROBIC GRANULAR SLUDGE SYSTEMS

Abstract

The multiple concentration pulses respirometric method was applied to aerobic granular sludge.

On a first approach the pulse respirometric method was validated in aerobic granular sludge cultivated in a sequencing batch airlift reactor for the estimation of kinetic and stoichiometric parameters. The potential of the proposed method for monitoring aerobic granular sludge systems and for process control is considered.

On a second approach the pulse respirometric method was used for characterising two aerobic granular sludge systems operated under different shear force conditions, thus determining the impact of shear stress on aerobic granular sludge kinetics and stoichiometry.

6 A. Method Validation and Aerobic Granulation Assessment

Abstract

A respirometric method based on multiple concentration pulses was validated for the determination of extant kinetic and stoichiometric parameters in aerobic granular sludge systems. In a short time and using low cost equipment, the method allowed an exhaustive characterisation of the process in real-time through the determination of six central stoichiometric and kinetic parameters: (i) biomass growth yield, (ii) specific endogenous respiration rate, (iii) substrate affinity constant, (iv) maximum specific oxygen consumption rate, (v) maximum specific substrate consumption rate, and (vi) maximum specific growth rate. The developed method was used for the assessment of a complete aerobic granulation process carried out in a sequencing batch airlift reactor. Additionally, the determined parameters were those actually prevailing in the system under actual operating conditions, i.e. *apparent parameters, which is of major interest for control and process operation. At steady state the biomass growth yield was estimated to be 0.6 g COD-X g COD-S^{-1}, the specific endogenous respiration rate was 0.1 g O_2 g COD-X^{-1} d^{-1}, the affinity constant was approximately 20 mg COD-S L^{-1}, maximum specific oxygen consumption rate and maximum specific substrate consumption rate were 0.06 g O_2 g COD-X^{-1} h^{-1} and 0.17 g COD-S g COD-X^{-1} h^{-1}, respectively, and the maximum specific growth rate was roughly 2.5 d^{-1}.*

The potential of the proposed multiple concentration pulses respirometric method was shown for monitoring aerobic granular sludge systems, and controlling aeration in an efficient mode.

This chapter is in preparation for submission as:

Oliveira CS, Ordaz A, Ferreira EC, Thalasso F, Alves M (***in preparation***). Pulse respirometric method for the determination of extant kinetic and stoichiometric parameters in an aerobic granular sludge system.

6A.1. Introduction

Aerobic granular sludge is a relatively recent technology that has been gaining growing attention for biological wastewater treatment due to its small footprint (De Bruin *et al.*, 2004), high conversion capacity (Carvalho *et al.*, 2006), low sludge production (Di Iaconi *et al.*, 2007), operational flexibility (Di Iaconi *et al.*, 2008), and versatility in treating wastewater of various composition (De Kreuk *et al.*, 2005; De Kreuk and van Loosdrecht, 2006; Carucci *et al.*, 2008; Adav *et al.*, 2007; Jiang *et al.*, 2002; Inizan *et al.*, 2005). The fundamentals of aerobic granulation have been extensively investigated both in lab- and pilot-scale. Aerobic granular sludge has been shown to be a promising alternative to the conventional activated sludge process for wastewater treatment (Schwarzenbeck *et al.*, 2005; de Kreuk and van Loosdrecht, 2006; Zheng *et al.*, 2006; Ni *et al.*, 2009).

Many researchers have proposed models to describe aerobic granular sludge systems, including dynamic granulation process, physicochemical and biological conversion processes, and granule-based SBR performance, enlightening the interest of mathematical modelling both under scientific and engineering perspectives (Ni and Yu, 2010). However, the majority of the proposed models for aerobic granular sludge systems are complex and mainly comprehensive, *i.e.* intending to describe intricate processes at a microscopic-scale. Nonetheless, in order to evaluate the operational performance of a system, it is essential to investigate the global process kinetics and stoichiometry, related to biomass growth and substrate utilisation. Indeed, the determination of "user-friendly" parameters which readily give information about the actual condition of the system, allows simple monitoring and control of the process. However, to the best of our knowledge, there are only few reports in the literature on kinetics and stoichiometry of aerobic granulation process, and none of them assessed these parameters throughout a complete aerobic granulation process.

A simple pulse respirometric method for determination of biodegradation kinetic parameters in activated sludge systems was proposed by Cech *et al.* (1985). This method is based on the response of endogenous activated sludge samples to injections of different substrate concentration pulses in a closed respirometer. A Monod type relation exists between the initial substrate consumption rates and the substrate concentration of the pulses, allowing the estimation of the maximum specific substrate consumption rate (q_{max}) and the substrate affinity constant (K_S). Although this method has been used by other groups (Manser *et al.*, 2005; Lepik *et al.*, 2003; Orupold *et al.*, 1999 and 2001; Contreras *et al.*, 2001), it has ever been applied to aerobic granular sludge systems. In the present

work, a new procedure based on the basic principles of the mentioned method is proposed, and it is applied for the characterisation of an aerobic granular sludge systems.

The aim of the present work is (i) to validate a multiple concentration pulses respirometric method based on the Cech *et al*. (1985) method for the determination of extant kinetic and stoichiometric parameters of aerobic granular sludge systems, and (ii) to apply the developed method for the assessment of a complete aerobic granulation process.

6A.2. Material and Methods

6A.2.1. Experimental Setup

Aerobic granules were cultivated in a sequencing batch airlift reactor (SBAR). The SBAR was made of transparent acrylic, with a working volume of 5 L (Figure.6.1). Continuous aeration was supplied through a fine bubble aerator at the bottom of the reactor at an air flow rate of 5.0 L min^{-1}, controlled by a mass flow controller (GFC 17S Aalborg, USA).

The SBAR was operated at a cycle time of 4 h, consisting of four phases (1) influent filling – 3 min; (2) aeration – 229 to 232 min; (3) settling – 2 to 5 min; and (4) effluent discharge – 3 min. Influent and effluent were pumped with peristaltic pumps (Watson Marlow 405 U/R2, Sweden). The cycle operation was control by a programmable logic controller (PLC, α2 Series Controller, Mitsubishi).

The reactor was inoculated with concentrated activated sludge from a compact wastewater treatment plant (Tadim – Braga, Portugal). The activated sludge was previously sieved (0.3 mm) to remove suspended particles, and then introduced into the reactor. To remove most of the available substrate, the reactor was gently complemented with tap water and the biomass was left to settle down before supernatant was removed. The reactor was then maintained aerated with no feed addition for 24 h, before fresh substrate was added for another 24 h period. By the end of this period, the biomass was left to settle during 5 min and 50 % volume of the mixed liquor was withdrawn. Then, the normal sequencing batch mode, described above, was started.

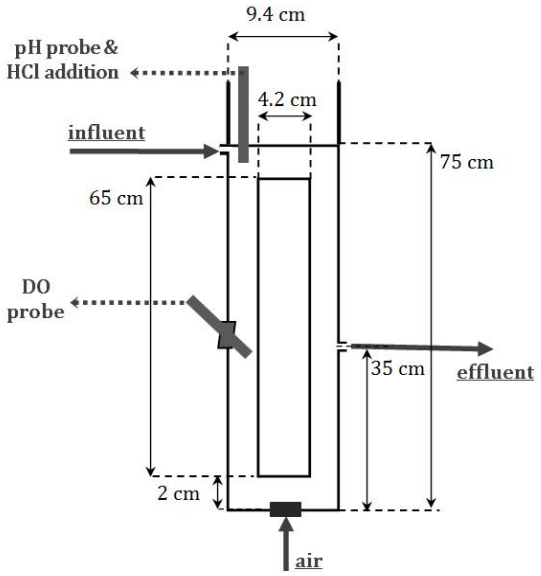

Figure.6.1. Schematic representation of the SBAR.

The reactor was fed with synthetic wastewater, containing (mg L^{-1}): $CH_3COONa{\cdot}3H_2O$, 2073; $(NH_4)_2SO_4$, 140; $MgSO_4{\cdot}7H_2O$, 25; KH_2PO_4, 44; $K_2HPO_4{\cdot}3H_2O$, 59; $CaCl_2{\cdot}2H_2O$, 30; $FeCl_3{\cdot}6H_2O$, 19; Na_2CO_3, 66; $NaHCO_3$, 105; and a trace mineral solution (Moy *et al.*, 2002), 1mL L^{-1}.

To promote granulation, the settling time was gradually decreased from 5 min, to 4 min, 3 min, and ultimately to 2 min each 3 days, hence on operation day 3, 6, and 9, respectively. During the whole operation, organic loading rate (OLR) was constant at 2.2 g COD-S L^{-1} d^{-1}, along with unvarying hydraulic residence time (HRT) of 8 h.

The reactor was maintained at ambient room temperature (17 – 22 ^{0}C), and pH was controlled to 7.0 ± 0.2 (pH 296 WTW, Germany) with the automatic addition of HCl 1 M with a peristaltic pump (Watson Marlow 401 U/DM3, Sweden). Dissolved oxygen (DO) concentration was measured with a polarographic oxygen probe located in the down-comer of the SBAR and connected to a dissolved oxygen meter (HI 2400, Hanna Instrument, Portugal) and a computer for data acquisition. The DO meter included automatic temperature and salt concentration correction. Once a week, the reactor's walls were cleaned in order to prevent attached biomass growth.

6A.2.2. Analytical methods

Influent and effluent were characterised in terms of chemical oxygen demand (COD), total suspended solids (TSS), and volatile suspended solids (VSS) concentrations. Biomass content was estimated as the VSS and the insoluble fraction of COD in the mixed liquor. During the experiment, in order to characterise the mixed liquor, samples were taken directly from the reactor during aeration phase. Granular biomass was separated from mixed liquor by wet-sieving (0.25 mm), smaller particles being considered as suspended biomass. The VSS and COD content of the two biomass fractions were determined separately: X^{Gran} refers to the biomass content of the granular biomass; and X^{Tot} is the total biomass content, *i.e.* suspended plus granular fraction.

COD was determined using cuvette test kits (Hach-Lange, Germany). Substrate concentration (S) was considered to be the soluble COD fraction, and biomass concentration (X) was considered as the insoluble COD, estimated as the difference between total COD and soluble COD. For soluble and insoluble COD determination, samples were separated by filtration (0.45 μm). Total and volatile suspended solids (TSS and VSS) and total solids (TS) were analysed according to standard methods (APHA, 1999).

Biomass settling ability was estimated through the sludge volume index (SVI) determined according to standard methods (APHA, 1999), after 5, 10, and 30 min of settling, corresponding to SVI_5, SVI_{10}, and SVI_{30}, respectively. Biomass aggregates were characterised in terms of equivalent diameter (D_{eq}) determined through quantitative image analysis, following the procedure presented by Oliveira *et al*. (*submitted* – Appendix I). Briefly, for image acquisition of macro-aggregates, slides with three 10 mm diameter etched rings were used. A volume of 0.1 mL of aggregates suspension was placed in each etched circle for visualisation and image acquisition with an Olympus SZ40 stereo microscope (Olympus, Tokyo, Japan) with 12 x magnification. The stereo microscope was coupled to a CCD AVC D5CE video camera (Sony, Tokyo) and a DT 3155 Data Translation frame grabber (Data Translation, Marlboro, MA), allowing images acquisition with 768 x 576 pixel size in 8 bits (256 grey levels) format by the Image Pro Plus software package (Media Cybernetics, Silver Spring, MD). Calibration from pixels to metric unit dimensions was performed by means of a micrometer slide, allowing the determination of the metric calibration factor (F_{cal}).

Image processing and analysis were achieved through a program previously developed in

MATLAB (The Mathworks, Inc., Natick, MA) for macro-aggregates (Amaral, 2003), which allowed the determination of the aggregates equivalent diameter (D_{eq}).

The kinetic model based on the linear phenomenological equation (LPE) developed by Yang *et al*. (2004) was applied to D_{eq} data (Equation 6A.1) for the estimation of the aggregates size-dependent growth constants (μ_{size}, $D_{eq\ ss}$, and t_{lag}).

$$\left(D_{eq} - D_{lag}\right) = \left(D_{eq\ ss} - D_{lag}\right)\left[1 - e^{-\mu_{size}\,(t\,-\,t_{lag})}\right] \qquad (6A.1)$$

where, t is the elapsed time (d), t_{lag} is the duration of the lag phase (d), μ_{size} is the specific growth rate of aggregates by size (d^{-1}), D_{lag} is the D_{eq} of aggregates at t_{lag} (mm), and $D_{eq\ ss}$ is D_{eq} of the aggregates at equilibrium (mm), *i.e.* when the system reaches a steady state.

Fitting the LPE (Equation 6A.1) to the D_{eq} of aggregates along time allowed estimating μ_{size}, $D_{eq\ ss}$, and t_{lag}.

6A.2.3. Multiple Concentration Pulses Method

Respirometric experiments were done in a 0.5 L transparent acrylic respirometer equipped with magnetic stirring. Air was supplied through a fine bubble aerator placed close to the bottom of the respirometer. Air flow rate was controlled by a mass flow controller (GFC 17S Aalborg, USA). DO concentration (C) was measured with a polarographic oxygen probe connected to a dissolved oxygen meter (HI 2400, Hanna Instrument, Portugal) and a computer for data acquisition. The DO meter included automatic temperature and salt concentration correction. The oxygen probe was calibrated before each respirometric experiment.

For respirometric experiments, a 0.5 L test sample of mixed liquor was collected from the SBAR through the effluent port in the last 30 min of the aeration phase, at a time when microorganisms were under endogenous respiration state. After collecting the test sample, the volume of the SBAR was corrected with tap water, so the hydrodynamic conditions were not affected. At the end of the respirometric experiment, the test sample was totally returned to the reactor in order to avoid biomass losses.

The pulse respirometric procedure was applied to the total biomass, and separately to the granular biomass. Granular biomass test samples were obtained by wet-sieving of 0.5 L mixed liquor (0.25 mm), and placing the granules in tap water until completing 0.5 L. Total biomass and granular biomass were characterised in terms of COD and VSS. The COD

concentration of the pulse solution was determined every day pulse experiments were done.

As previously mentioned, the proposed respirometric method was based on the Cech *et al.* (1985) method. The procedure of the multiple concentration pulses respirometric method was as follows: (i) the test sample was placed in the respirometer under constant aeration and subtle mixing, just enough to avoid granules from settling; (ii) the DO concentration reached a pseudo-stationary state, called baseline oxygen concentration (C_b), corresponding to endogenous respiration state (Spanjers *et al.*, 1996); (iii) a pulse of a concentrated synthetic wastewater solution (pulse solution) was injected to obtain the desired pulse concentration (S_P) in the respirometer; (iv) DO was acquired until returning to C_b; (v) steps *(iii)* and *(iv)* were repeated with different pulse concentration; and (vi) the oxygen volumetric mass transfer coefficient (k_La) was measured in triplicate according to the dynamic method described by Badino *et al.* (2000).

6A.2.4. Respirometric data interpretation

The respirometric data interpretation method was as previously reported (Oliveira *et al.*, 2011). Briefly, after the injection of a known substrate pulse concentration (S_P), the substrate oxidation yield ($Y_{O2/S}$) was given by the amount of oxygen consumed per unit COD of substrate oxidised (Equation 6A.2). The biomass growth yield ($Y_{X/S}$) expressed in COD units was estimated from $Y_{O2/S}$ (Equation 6A.3).

$$Y_{O2/S} = \frac{\int_0^t OUR_{exo}\,dt}{S_P} = \frac{k_La\int_0^t (C_b - C)dt}{S_P} \quad (6A.2)$$

$$Y_{X/S} = 1 - Y_{O2/S} = \frac{k_La\int_0^t (C_b - C)dt}{S_P} \quad (6A.3)$$

During pulse respirometric experiments, C_b was always inferior to C^*. This difference was accounted for endogenous respiration (Oliveira *et al.*, 2011) allowing the assessment of OUR_{end} (Equations 6A.4). The specific endogenous respiration rate (b_H) was determined through the OUR_{end} (Equation 6A.5).

$$\frac{dC}{dt} = k_La(C^* - C_b) - OUR_{end} = 0 \Rightarrow OUR_{end} = k_La(C^* - C_b) \quad (6A.4)$$

$$b_H = 24\frac{OUR_{end}}{X} \quad (6A.5)$$

where, b_H (g O_2 g COD-X^{-1} d^{-1}) is the specific endogenous respiration rate, and 24 is the

conversion factor from h to d.

A Monod-type relation exists between the maximum exogenous OUR ($OUR_{exo\ max}$) reached at each pulse and the S_P (Equation 6A.6).

$$OUR_{exo\ max} = q_{O2\ max}\ X\ \left(\frac{S_P}{K_S + S_P}\right) \quad (6A.6)$$

For each set of respirograms, the $OUR_{exo\ max}$ was plotted against S_p. Equation 6A.6 was fitted to the experimental S_P and $OUR_{exo\ max}$ data using the least square method implemented with the SOLVER tool of Excel for estimating the kinetic parameters maximum specific oxygen consumption rate ($q_{O2\ max}$) and substrate affinity constant (K_S).

Additionally the maximum specific substrate consumption rate (q_{max}) and the maximum specific growth rate (μ_{max}) were determined according to Equations 6A.7 and 6A.8, respectively.

$$q_{max} = \frac{q_{O2\ max}}{Y_{O2/S}} \quad (6A.7)$$

$$\mu_{max} = 24\frac{q_{O2\ max}\ Y_{X/S}}{Y_{O2/S}} \quad (6A.8)$$

All mean parameter values are presented along with the associated standard deviation. The comparisons of the mean parameter values obtained for the total and the granular biomass were made through one-way ANOVA tests (Statistics 18, SPSS Inc. Package).

6A.3. Results and Discussion

Granulation Process

Since the onset of the experiment, the SBAR showed a COD removal efficiency higher than 95 %. This COD removal efficiency was stable during the whole experiment (data not shown). In the first 5 days of operation there was a decrease on the biomass content of the reactor, depicted by the decrease in the TSS concentration from the initial 2000 mg L^{-1} to approximately 1300 mg L^{-1} (Figure 6.2). This was accounted for the wash out of the slower settling biomass present in the inoculum, caused by the short settling time applied. After this initial wash out, the retained faster-settling biomass increased rapidly, reaching stability around day 21.

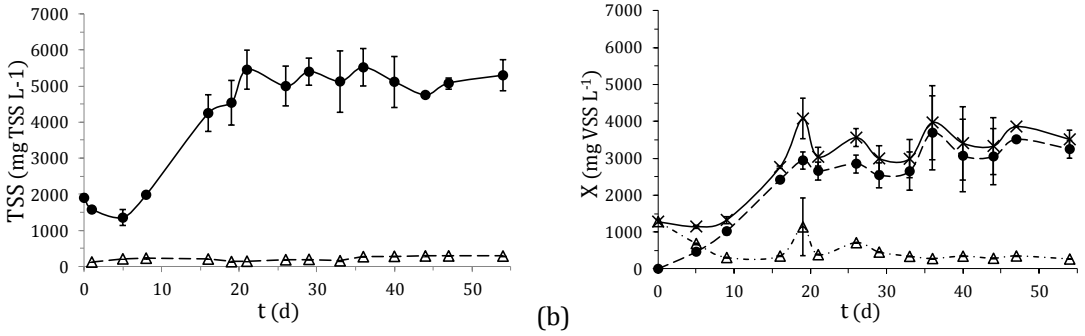

(a) (b)

Figure 6.2. Time course of (a) TSS in the mixed liquor (•) and effluent (Δ), and (b) total biomass (×), granular biomass (•), and suspended biomass (Δ) fractions in the reactor.

Biomass settling ability improved significantly during granulation. From day 16 onwards the biomass completely settled in 5 minutes, depicted by the SVI_5 being equal to SVI_{10} and SVI_{30}, approximately 50 mL g^{-1} (Figure 6.3).

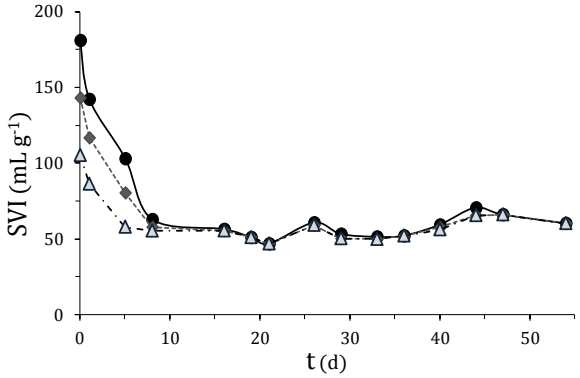

Figure 6.3. Time course of the SVI after: 5 min (•), 10 min (♦), and 30 min (▲) of settling time.

Aerobic granulation process could be clearly tracked by following the increase of aggregated equivalent diameter (Figure 6.4). Fitting the integrated LPE equation (Equation 6A.1) to the D_{eq} of macro-aggregates along time it was seen that stabilisation of aggregates size-growth was achieved from day 33 onward, with $D_{eq\ ss}$ 1.0 mm, μ_{size} 0.084 d^{-1}, and t_{lag} 2.6 d (Figure 6.4). The obtained μ_{size} value is in accordance with that found by Yang *et al*. (2004), 0.08 d^{-1}, for aerobic granules fed with acetate as sole carbon source and with an OLR of 1.5 g COD L^{-1} d^{-1}.

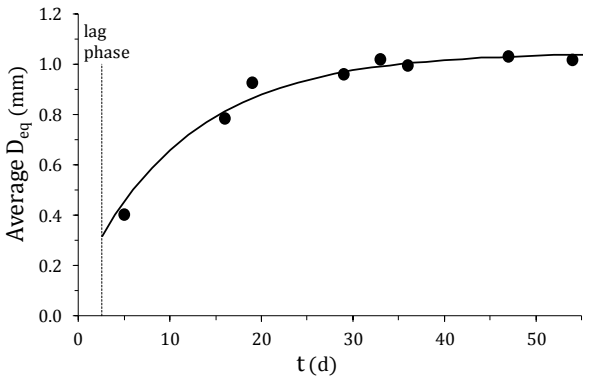

Figure 6.4. Time course of the average equivalent diameter of aggregates (•), and LPE fitting (*solid line, $r^2 = 0.98$*).

Pulse respirometry method

The multiple concentration pulses respirometric method was applied since the beginning of the SBAR operation. Figure 6.5 shows an example of DO profile obtained with the injection of four pulses of increasing concentration: 4.9, 9.7, 19.3, and 48.3 mg COD L^{-1}, observed on day 29. Figure 6.5a shows that between pulses C_b was constant and steadily below C*, suggesting that OUR_{end} was steady along the pulse experiment. This is an indication that the injection of successive pulse with short starvation periods had no effect on the overall process. Figure 6.5b shows OUR_{exo} observed during this experiment. It can be clearly observed that $OUR_{exo\ max}$ was dependent of the pulse concentration injected, Figure 6.5c shows that this dependence was related by a clear Monod-type shape, which allowed the estimation of $q_{O2\ max}$ and K_S.

Good correlations for both total biomass and granular biomass were attained with the multiple concentration pulses respirometric method ($r^2 > 0.99$), highlighting that this method is in fair agreement with the substrate biodegradation process. These results confirmed the applicability of the pulse respirometric method for the characterisation of granular biomass.

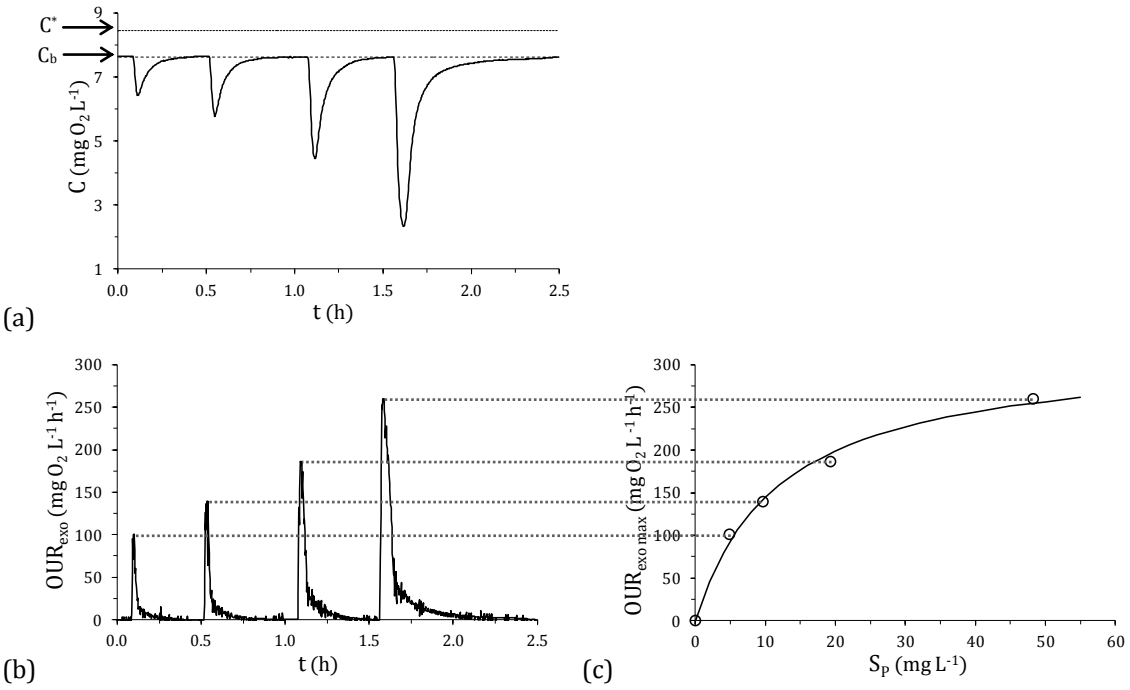

Figure 6.5. (a) DO concentration profile (*solid line*) obtained with the injection of four increasing substrate concentration pulses (S_P = 4.9, 9.7, 19.3, and 48.3 mg COD L^{-1}), and saturation DO concentration (C*, *dash-dotted line*) and DO baseline level (C_b, *dashed line*), (b) corresponding exogenous OUR profile, (c) and Monod type relation between maximum observed exogenous OUR and substrate concentration pulse (*solid line*).

Kinetic and stoichiometric characterisation of the granulation process

The pulse respirometric method was applied along the all SBAR operation, for granular and total biomass, in order to follow up the aerobic granulation process by assessing the biomass kinetics and stoichiometry (Figure 6.6). The obtained parameters are apparent ones, since they reflect the general behaviour of the bioprocess, not distinguishing particular processes such as substrate diffusion or substrate storage phenomena.

The biomass growth yield ($Y_{X/S}$) was stable, and the values for the total and granular biomass were similar during the whole operation time (Figure 6.6a). Specific endogenous respiration rate (b_H) may be an indicator of biomass activity (Figure 6.6b). In this sense an initial peak of bioactivity was observed in the granular biomass, (day 9), followed by a stabilisation around day 20; regarding total biomass bioactivity a progressive decrease was observed along the granulation process, stabilising after day 33. Maximum specific oxygen consumption rate (q_{max}) and affinity constant (K_S) were estimated from adjusting the Monod equation (Equation 6A.6) to the multiple concentration pulses respirometric data (Figure 6.6c). The q_{max} for total and granular biomass followed the same trend during

the whole operation (Figure 6.6c): there was an increased during the first 10 days, then a decreased throughout the granulation process, and finally a stabilisation after day 20. Concerning K_S a constant increase in both total and granular biomass values was observed during the first 20 days of operation, with K_S of granular biomass significantly higher than total biomass until day 33, when both K_S values merged. K_S corresponds to the substrate concentration at which cells grow at half its maximum growth rate. Substrate concentration reaching the cells "trapped" in the granules is lower than the bulk substrate concentration due to mass transport limitations in granules (Liu *et al*., 2005h), resulting in higher apparent K_s values. Consequently, changes in K_S serve as an indication for substrate-transport limitations around cells (Ni and Yu, 2010). This phenomenon explains why K_S values of granular biomass were higher than those of total biomass, where suspended biomass contributed for lowering the K_S.

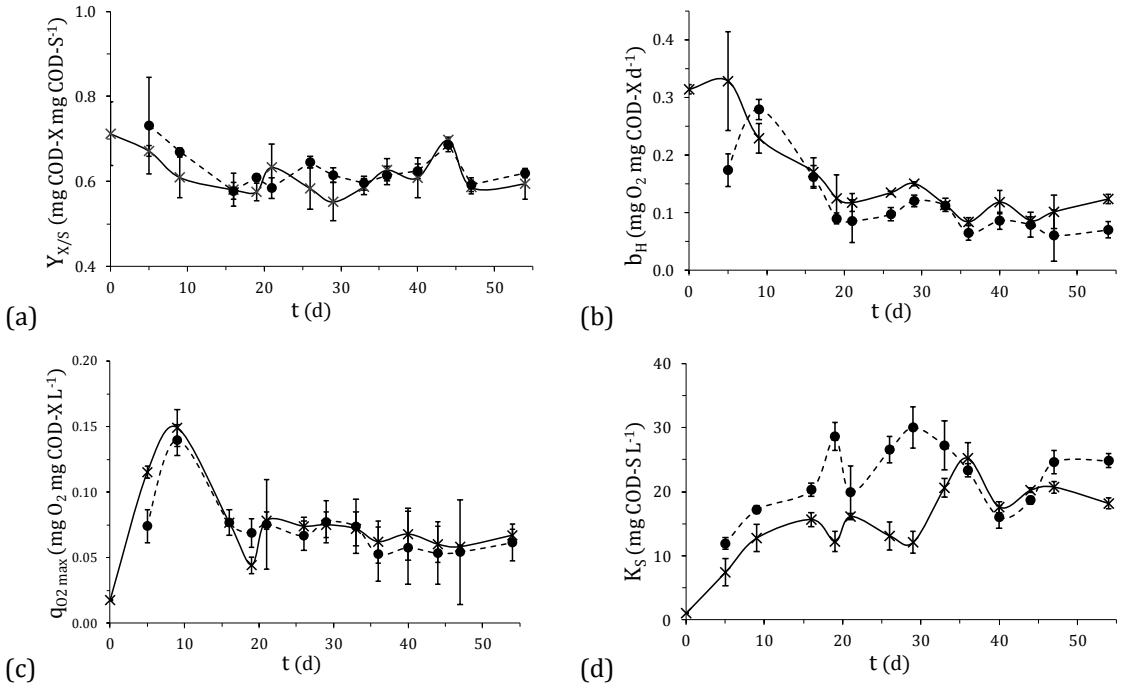

Figure 6.6. Time course of the total biomass (X) and granular biomass (●): biomass growth yield (a); specific endogenous respiration rate (b); maximum specific oxygen consumption rate (d); and substrate affinity constant (c), obtained with the multiple concentration pulses respirometric method.

Multiple concentration pulses respirometric method: comparison with literature values

For the validation of the multiple concentration pulses respirometric method in aerobic granular sludge, only results obtained while the system was stable are considered. From the previous presented results, it was concluded that the system reached stable state after day 33 (Figure 6.4). Table 6.1 presents the average values of the parameters obtained for the total biomass and the granular fraction (D_{eq} > 0.25 mm) when the system was at stable state, *i.e.* from day 33 onward. Kinetic and stoichiometric parameters values for both total biomass and granular biomass during the considered period showed no differences ($p > 0.05$), except for b_H. This similarity would be expected since at stable state granular biomass was the major biomass fraction in the reactor (Figure 6.2b), thus majority contributing for the biodegradation process. The difference found in b_H might be elucidated by the fact that in the present work biomass was considered to be the whole fraction of the insoluble COD. However, in practice the active biomass ought be only a fraction of the insoluble COD, since, for instance, extracellular polymeric substances (EPS), which compose a large portion of the aerobic granules (McSwain *et al*., 2005; Chen *et al*., 2007; Adav *et al*., 2008, 2009), also contribute for the measured insoluble COD. Therefore, the considered biomass content was overestimated, especially in granular biomass, contributing for the lower b_H values obtained.

Table 6.1. Average values, and respective standard deviations, of stoichiometric and kinetic parameters obtained for total and granular biomass during steady state; and comparison of total and granular biomass means by one-way ANOVA

Parameters	Total Biomass	Granular biomass	ANOVA	
			$F_{(1,5)}$	p-value
$Y_{X/S}$ (g COD-X g COD-S^{-1})	0.62 ± 0.01	0.63 ± 0.01	0.22	0.67
b_H (g O_2 g COD-X^{-1} d^{-1})	0.10 ± 0.01	0.07 ± 0.01	15.78	0.02
K_S (mg COD-S L^{-1})	20.4 ± 1.9	21.5 ± 2.2	0.46	0.54
$q_{O2\ max}$ (g O_2 g COD-X^{-1} h^{-1})	0.06 ± 0.01	0.06 ± 0.01	0.84	0.41
q_{max} (g COD-S g COD-X^{-1} h^{-1})	0.17 ± 0.02	0.15 ± 0.03	0.73	0.44
μ_{max} (d^{-1})	2.55 ± 0.29	2.28 ± 0.26	1.40	0.30

In previous papers on mathematical modelling of aerobic granular sludge systems, kinetic

and stoichiometric parameters values are often assumed from literature on activated sludge (Vazquéz-Padín *et al*., 2010; Ni *et al*., 2008). Table 2 presents parameters values found in literature both in activated sludge (AS) and aerobic granular sludge (AGS) systems.

Table 6.2. Overview of kinetic and stoichiometric parameter values found in literature

Parameters	Values	Sludge Type*	Sources
$Y_{X/S}$ (g COD-X g COD-S^{-1})	0.57	AS(a)	Sin *et al*. (2005)
K_S (mg COD-S L^{-1})	4.0	AS(b)	Henze *et al*. (2000)
	11.4	AGS(c)	Ni *et al*. (2008)
b_H (g O_2 g COD-X^{-1} d^{-1})	0.26	AS(b)	Henze *et al*. (2000)
	0.38	AGS(c)	Ni *et al*. (2008)
q_{max} (g COD-S g COD-X^{-1} h^{-1})	0.18	AS(a)	Sin *et al*. (2005)
μ_{max} (d^{-1})	2.60	AS(b)	Henze *et al*. (2000)
	1.68	AGS(c)	Ni *et al*. (2008)

* AS – Activated Sludge; and AGS – Aerobic Granular Sludge.
Substrate Type: (a) acetate; (b) readily degradable; (c) fatty-acids-rich wastewater

Overall, there was a good agreement between the obtained parameters values (Table 6.1) and those found in literature (Table 6.2). $Y_{X/S}$, q_{max}, and μ_{max} values are in the same range as those reported in literature. However, the b_H and K_S values obtained in this work differed from those found in literature, being b_H slightly lower and K_S significantly higher. The difference found in b_H may be due to the fact that in this work biomass was considered to be the whole fraction of the insoluble COD, as previously referred. Thus, the present b_H is the apparent value. The K_S value obtained was much higher than that reported for activated sludge. This may be ascribed to the existence of substrate-transport limitations in the granules, as previously mentioned (Ni and Yu, 2010). Nevertheless, the obtained K_S value was also higher than that reported by Ni *et al.* (2008) for aerobic granular sludge. This could mean that the granules in this work could be denser than those of Ni *et al*. (2008), thus substrate-transport limitation would be larger and K_S higher. This hypothesis is plausible regarding the different reactors configuration used in each work. In Ni *et al*. (2008) work a sequencing bubble column reactor was used; while in the present work we used a sequencing batch airlift reactor (SBAR). SBAR have shown to allow more dense granules than those obtained in bubble column reactors (Beun *et al*., 2000b). This has

been attributed to the highest shear forces existing in the bottom of an airlift reactor, where mixed liquor turn flow direction, while in bubble columns shear forces are homogeneously distributed throughout the column (Beun *et al*, 2000b). Another possible point supporting the hypothesis that the granules in this work could be denser than those in Ni *et al*. (2008) is the shorter settling time used. Shorter settling times, which lead to the selection of particles with higher minimal settling velocity, are known to favour the growth of denser granules (Li *et al*., 2006).

Nevertheless, overall the proposed method proved to well describe the substrate degradation process of aerobic granular sludge, producing reasonable values in the range of those reported in literature for similar systems.

Multiple concentration pulses respirometric method potential

The proposed multiple concentration pulses respirometric method shows great potential allowing fast characterisation of the aerobic granular system in terms of kinetic and stoichiometric behaviour. Among many possible applications, this technique may be useful for systems monitoring and control.

Up to date, few have been the simple unstructured kinetic models tested in aerobic granular sludge systems. Simple models are closest to be applicable in practice for monitoring and control of an existing operating system, proving "user-friendly" parameters which readily elucidate the actual condition of the system, thus being useful tools for end-users. For example, the knowledge of the oxygen consumption- rates is important for controlling the efficiency of the system. As biological wastewater treatment plants receive different influents along time, due to the different sources producing the wastewater and/or to the seasonal variation, traducing in variations on composition and concentration of the wastes, thus oxygen consumption may vary considerably during the operation of a treatment system due to the variety of influents collected. Oxygen supply to the system must compromise two factors: (i) supply sufficient oxygen for efficient aerobic treatment, as it has been shown that insufficient oxygen supply may lead to instability of aerobic granules (Gapes *et al*., 2004; de Kreuk and van Loosdrecht, 2004); and avoid excessive aeration which comprises unnecessary costs. Therefore, it is important to have a reliable estimate of the actual short-term oxygen demand of the system in order to appraise these two factors.

Aerobic granular sludge is mostly cultivated in sequencing batch reactors (SBR). In a SBR, wastewater is mixed with the activated sludge in a pulse-feed mode. Then, the sludge and input substrate "react" in a batch treatment mode (Ni and Yu, 2010). The pulse respirometric method proposed in this work mimics the feeding mode conditions which the microorganisms undergo at the parent SBR. As a result, the microorganisms physiological state is not changed, and thus the kinetic parameters determined are extant ones, *i.e.* represent the exact capability of the microbial culture in the system at the time of its collection from the parent reactor (Grady *et al.*, 1996). The extant kinetic parameters provide an insight into the immediate response of the system, for example facing a shock-loading, allowing to take measurements for maintaining an efficient operation. Since aspects such as, for example, substrate and oxygen diffusion through the granules and active biomass fraction were not taken into account in the unstructured model used, the obtained parameters are apparent ones, *i.e.* they reflect the actual biodegradation capability of the system as a whole under the strict conditions at which it is operated when biomass is sampled. Thus, the parameters obtained by the proposed method may be precious for monitoring the processes, and may be useful for controlling some operational aspects, such as aeration for example: the proposed method gives the oxygen demand of the system when fed with a determined influent, allowing the manipulation of aeration in accordance with this information in order to safe aeration costs.

Figure 6.7represents the DO response obtained in a reactor's cycle on day 42. It can be observed that the minimum DO concentration reached was around 5.0 mg O_2 L^{-1}, which is much higher than the reported K_{O2} values. The designed DO concentration in activated sludge systems is typically between 1 and 2 mg O_2 L^{-1}, in order to avoid excessive costs with aeration while providing enough oxygen to the system. Thus, it is concluded that the SBAR was being over-aerated, which in practical-economical terms represents an unnecessary spent in aeration.

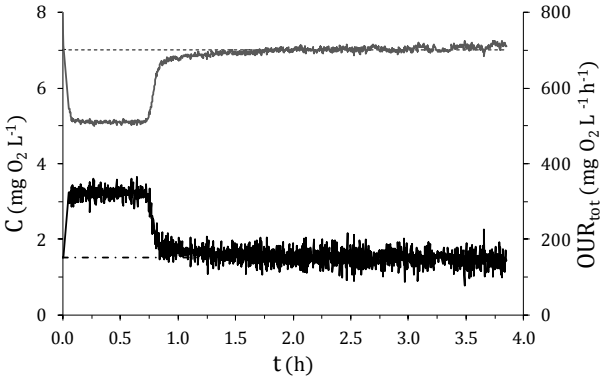

Figure 6.7. DO profile (*grey solid line*), and corresponding OUR profile (*black solid line*) obtained during a reactor's operational cycle at day 42. Baseline DO level (*dashed line*) and endogenous OUR (*dash-dotted line*) are also represented.

The information provided by the proposed respirometric method allows having an insight into the biological process, which may be used for controlling the process. A practical application example is subsequently presented for using the information obtained with the multiple concentration pulses respirometric method for controlling aeration.

Using the parameters K_S, $q_{O2\,max}$, and b_H, determined for the system (total biomass, Table 6.1), the maximum oxygen demand of the system (given by $OUR_{tot\ max} = OUR_{end} + OUR_{exo\ max}$) can be estimated. The $OUR_{tot\,max}$ was calculated to be 390.8 ± 66.3 mg O_2 L^{-1} h^{-1}. The observed $OUR_{tot\,max}$ was 321.2 mg O_2 L^{-1} h^{-1} (Figure 6.7), consequently, the predicted value was about 22 % above the observed one, which leaves a safety bond on the prediction since it prevents oxygen failure on the system.

According to Equation 2, considering the predicted $OUR_{tot\ max}$ value, and setting the minimum DO concentration (C_{min}) to 1.5 mg O_2 L^{-1}, the minimum admissible k_La value (k_La_{min}) was calculated to be 55.1 ± 9.2 h^{-1} (Equation 6A.9).

$$k_La_{min} = \frac{[OUR_{tot\,max} + (C^* - C_{min})]}{(C^* - C_{min})} \qquad (6A.9)$$

where, k_La_{min} (h^{-1}) is the minimum k_La value, and C_{min} (1.5 mg O_2 L^{-1}) is the set minimum DO concentration.

In the SBAR system used, a linear correlation between the air flow rate (F_g) and the k_La was observed (r^2 = 0.98, data not shown) thus allowing to determine the F_g to be applied in order to obtained a desired k_La value. To obtain the calculated k_La_{min}, the F_g applied to the system should be around 3.0 L min^{-1}. The system was working with a F_g of 5.0 L min^{-1} when the data of Figure 6 was collected, thus it was being excessively aerated taking into

account the oxygen demand of the biomass. Unfortunately, the proposed control procedure could not be tested in practice in the present system, since the air flow, besides being the oxygen provider for the system, also provided the necessary mixing. Modifications in the reactor would be required in order to use the proposed aeration control strategy, namely the mixing of the system would have to be separated from aeration, for example, by including an internal recycle of liquid in the system which would provide the mixing needs, while air flow would be used for oxygen supply only, allowing its manipulation without jeopardising the mixing regime.

The proposed multiple concentration pulses respirometric method was shown to be potentially useful for the particular case of controlling aeration considering the system momentary needs. Nevertheless, the applicability of the method is not exhausted on this point, as the knowledge of the extant characteristics of the biomass is much wider in monitoring and controlling perspectives.

6A.4. Conclusions

A respirometric method based on multiple concentration pulses was proposed for the determination of extant kinetic and stoichiometric parameters in aerobic granular sludge systems. The proposed model showed a good agreement with the aerobic biodegradation process occurring in the aerobic granular sludge system.

In approximately two hours and using low cost material, the method allowed an exhaustive characterisation of the process through the determination of six central stoichiometric and kinetic parameters during a complete granulation process: $Y_{X/S}$, b_H, K_S, $q_{O2\ max}$, q_{max}, and μ_{max}. Additionally, the determined parameters were apparent parameters, *i.e.* those actually prevailing in the system under actual operating conditions, which is of major interest for control and process operation. The potential of the proposed multiple concentration pulses respirometric method was shown for monitoring aerobic granular sludge systems, and controlling aeration in an efficient mode.

To the best of our knowledge, this is the first time the use of respirometry for the characterisation of granular biomass is reported, and this is also the first time that apparent kinetic and stoichiometric parameter are followed up during a complete granulation process.

Further studies, with the simultaneous analysis of apparent and actual kinetic and

stoichiometric parameters, would allow for a better understanding of diffusion-reaction processes in granules or other biofilm reactors.

6A.5. References

Adav SS, Chen MY, Lee DJ, Ren NQ (**2007**). *Degradation of phenol by aerobic granules and isolated yeast* Candida tropicalis. Biotechnol. Bioeng. 96(5):844–852.

Adav SS, Lee DJ, Tay JH (**2008**). *Extracellular polymeric substances and structural stability of aerobic granule*. Water Res. 42(6-7):1644–1650.

Adav SS, Lee DJ, Lai JY (**2009**) *Proteolytic activity in stored aerobic granular sludge and structural integrity*. Bioresource Technol. 100(1):68–73.

APHA (**1999**). *Standard methods for the examination of water and wastewater*. 20th Edn. Washington, DC, American Publishers Health Association.

Badino AC, Facciotti MCR, Schmidell W (**2000**) *Improving k(L)a determination in fungal fermentation, taking into account electrode response time*. J. Chem. Technol. Biot. 75(6):469–474.

Beun JJ, van Loosdrecht MCM, Heijnen JJ (**2000**). *Aerobic granulation*. Water Sci. Technol. 41(4–5):41-48.

Carvalho G, Meyer RL, Yuan Z, Keller J (**2006**). *Differential distribution of ammonia- and nitrite-oxidising bacteria in flocs and granules from a nitrifying/denitrifying sequencing batch reactor*. Enzyme Microb. Tech. 39(7):1392–1398.

Carucci A, Milia S, de Gioannis G, Piredda M (**2008**). *Acetate-fed aerobic granular sludge for the degradation of chlorinated phenols*. Water Sci. Technol. 58(2):309–315.

Cech JS, Chudoba J, Grau P (**1985**). *Determination of kinetic constants of activated-sludge microorganisms*. Water Sci. Technol. 17(2-3):259–272.

Chen MY, Lee DJ, Tay JH (**2007**). *Distribution of extracellular polymeric substances in aerobic granules*. Appl. Microbiol. Biot. 73(6):1463–1469.

Contreras E, Bertola N, Zaritzky N (**2001**). *The application of different techniques to determine activated sludge kinetic parameters in a food industry wastewater*. Water SA 27(2): 169–176.

Dawes EA, Ribbons DW (**1964**). *Some aspects of endogenous metabolism of bacteria*. Bacteriol. Rev. 28(2):126–149.

Di Iaconi C, Ramadori R, Lopez A, Passino R (**2007**). *Aerobic granular sludge systems: the new generation of wastewater treatment technologies*. Ind. Eng. Chem. Res. 46(21):6661–6665.

Di Iaconi C, de Sanctis M, Rossetti S, Ramadori R (**2008**). *Technological transfer to demonstrative scale of sequencing batch biofilter granular reactor (SBBGR) technology for municipal and industrial wastewater treatment*. Water Sci. Technol. 58(2):367–372.

De Kreuk MK, Heijnen JJ, van Loosdrecht MCM (**2005**). *Simultaneous COD, nitrogen, and phosphate removal by aerobic granular sludge*. Biotechnol. Bioeng. 90(6):761–769.

De Kreuk MK, van Loosdrecht MCM (**2006**). *Formation of aerobic granules with domestic sewage*. J. Environ. Eng.-ASCE 132(6):694–697.

Grady CPL, Smets BF, Barbeau DS (**1996**). *Variability in kinetic parameter estimates: A review of*

possible causes and a proposed terminology. Water Res. 30(3):742–748.

Gujer W, Henze M, Mino T, van Loosdrecht M (**1999**). *Activated Sludge Model No. 3*. Water Sci. Technol. 39(1):183–193.

Henze M, Gujer W, Mino T, van Loosdrecht M (**2000**). *Activated Sludge Models ASM1, ASM2, ASM2d and ASM3*. IWA Publishing, London.

Inizan M, Freval A, Cigana J, Meinhold J (**2005**). *Aerobic granulation in a sequencing batch reactor (SBR) for industrial wastewater treatment*. Water Sci. Technol. 52(10–11): 335–343.

Jiang HL, Tay JH, Tay STL (**2002**). *Aggregation of immobilized activated sludge cells into aerobically grown microbial granules for the aerobic biodegradation of phenol*. Lett. Appl. Microbiol. 35(5):439–445.

Lepik R, Orupold K, Viggor S, Tenno T (**2003**). *Study of biodegradability of methyl- and hydroxyphenols by activated sludge*. Oil Shale 20(2):99–112.

Li J, Chen Y, Li J, Zhang DH, Wang SG, Wang LJ, Jiang D, Sun FY, Zhang Q (**2006**). *Morphological and structural characteristics of aerobic granulation*. J. Chem. Technol. Biot. 81(5):823–830.

Liu YG, Liu Y, Tay JH (**2005**). *Relationship between size and mass transfer resistance in aerobic granules*. Lett. Appl. Microbiol. 40(5):312–315.

Manser R, Gujer W, Siegrist H (**2005**). *Membrane bioreactor versus conventional activated sludge system: population dynamics of nitrifiers*. Water Sci. Technol. 52(10–11):417–425.

McSwain B S, Irvine RL, Hausner M, Wilderer PA (**2005**). *Composition and distribution of extracellular polymeric substances in aerobic flocs and granular sludge*. Appl. Environ. Microb. 71(2):1051–1057.

Moy BYP, Tay JH, Toh SK, Tay TL (**2002**). *High organic loading influences the physical characteristics of aerobic sludge granules*. Lett. Appl. Microbiol. 34(6):407–412.

Ni BJ, Yu HQ, Sun YJ (**2008**). *Modeling simultaneous autotrophic and heterotrophic growth in aerobic granules*. Water Res. 42(6-7):1583–1594.

Ni BJ, Yu HQ (**2010**). *Mathematical modeling of aerobic granular sludge: A review*. Biotechnol. Adv. 28(6):895–909.

Oliveira CS, Ordaz A, Ferreira EC, Alves M, Thalasso F (**2011**). In situ *pulse respirometric methods for the estimation of kinetic and stoichiometric parameters in aerobic microbial communities*. Biochem. Eng. J. (*Chapter 5 of this Thesis*).

Oliveira CS, Thalasso F, Ferreira EC, Alves M. (***submitted***). *Early detection of fungal proliferation in aerobic granular sludge by quantitative image analysis*. (*Appendix I of this Thesis*).

Orupold K, Hellat K, Tenno T (**1999**). *Estimation of treatability of different industrial wastewaters by activated sludge oxygen uptake measurements*. Water Sci. Technol. 40(1):31–36.

Orupold K, Masirin A, Tenno T (**2001**). *Estimation of biodegradation parameters of phenolic compounds on activated sludge by respirometry*. Chemosphere 44(5):1273–1280.

Sin G, Guisasola A, de Pauw DJW, Baeza JA, Carrera J, Vanrolleghem PA (**2005**). A new approach for modelling simultaneous storage and growth processes for activated sludge systems under aerobic conditions. Biotechnol. Bioeng. 92(5):600–613.

Spanjers H, Vanrolleghem P, Olsson G, Dold P (**1996**). *Respirometry in control of the activated sludge process*. Water Sci. Technol. 34(3–4):117–126.

Vanrolleghem PA, Verstraete W (**1993**) *Simultaneous Biokinetic Characterization of Heterotrophic and Nitrifying Populations of Activated-Sludge with an Online Respirographic Biosensor*. Water

Sci. Technol. 28(11–12):377–387.

Vázquez-Padín JR, Mosquera-Corral A, Campos, JL, Mendez R, Carrera J, Pérez J (**2010**). *Modelling aerobic granular SBR at variable COD/N ratios including accurate description of total solids concentration*. Biochem. Eng. J. 49(2):173–184.

Xavier JB, de Kreuk MK, Picioreanu C, van Loosdrecht MCM (**2007**). *Multi-scale individual-based model of microbial and bioconversion dynamics in aerobic granular sludge*. Environ. Sci. Technol. 41(18):6410–6417.

Yang SF, Liu QS, Tay JH, Liu Y (**2004**). *Growth kinetics of aerobic granules developed in sequencing batch reactors*. Lett. Appl. Microbiol. 38(2):106–112.

6 B. Respirometry for the Assessment of Aerobic Granulation under different Operational Conditions

Abstract

Aerobic granulation was carried out in sequencing batch airlift reactors under two different hydrodynamic shear stress intensities, manipulated as aeration rate (5.0 and 6.6 L min^{-1}), and the process was followed by assessing stoichiometric and kinetic parameters progression through pulse respirometry, and morphological changes through quantitative image analysis. Higher hydrodynamic shear stress induced a faster granulation process with a shorter lag phase, and supported a higher biomass concentration with higher percentage of granules. Additionally, at higher shear stress the obtained biomass was compacter and denser, and granules were rounder. Both systems presented similar COD removal efficiency, but the system worked at higher shear stress produced a better quality effluent regarding solids content. The biomass growth yield was constant during the granulation process under the two shear stress intensities, and it was higher for the sludge cultivated under higher shear stress [0.6 (0.02) versus *0.5 (0.02) g COD-X g COD-S^{-1} at lower shear stress]. The substrate affinity constant increased notoriously along granulation process, as substrate transport limitation on granules would be reinforced. A direct relation between the substrate affinity constant and the granules size (equivalent diameter) was found to exist. The biomass subjected to the higher shear stress presented a much higher substrate affinity constant [16.4 (2.6) and 9.1 (0.2) mg COD-S L^{-1}, at higher and lower shear stress, respectively], and also a higher maximum specific substrate consumption rate [5.4 (0.9) and 2.5 (0.5) g COD-S g COD-X d^{-1}, at higher and lower shear stress, respectively] at the end of the granulation process. It is concluded that aerobic granulation carried out under higher hydrodynamic shear stress, as aeration rate, may be advantageous as it allows a faster granulation process, and the obtainment of higher biomass concentration, with denser, compacter, and rounder granules.*

This chapter is in preparation for submission as:

Oliveira CS, Ordaz A, Ferreira EC, Thalasso F, Alves M (***in preparation***). Kinetic and stoichiometric assessment of aerobic granulation process carried out under different shear stress intensities.

6B.1. Introduction

Granulation is considered a special case of biofilm growth, in which self-immobilisation occurs without a carrier (Beun *et al*., 2000; Wilderer and McSwain, 2004; McSwain *et al*., 2005). During aerobic granulation process, loose sludge flocs convert to compact aggregates, and further to mature granules (Tay *et al*., 2001b). For granulation process to occur, an inducing force must act on microorganisms bringing them together and making them aggregate. Shear stress is a recognised key factor influencing aerobic granulation, and it is thought to be involved in the initial cell-to-cell attachment phenomena (Liu and Tay, 2002; De Kreuk and van Loosdrecht, 2006).

Aerobic granulation is preferably carried out in pneumatic bioreactors, *i.e.* aerated bioreactors with no mechanical stirring. In these reactors, shear force is caused by gas and liquid flows and by particles collisions. In column type reactors, shear stress is imposed mainly by superficial gas velocity, directly determined by the aeration rate. Shear forces produced by superficial air velocity above 1.2 cm s^{-1}, have been shown to be required for enhancing aerobic granulation, whereas at lower superficial air velocity, stable aerobic granules do not form (Beun *et al.,*1999; Tay *et al.,* 2001c; Tay *et al.,*2004). Additionally to generating shear forces, aeration is also involved in promoting oxygen mass transfer, which may also affect the granulation process. McSwain and Irvine, (2008) showed that dissolved oxygen concentration is a controlling parameter of granulation, that may even more significantly affect granule formation than shear force.

If moderate shear forces promote granulation, in contrast excessive shear promotes granules erosion and rupture, with a direct impact on granules morphology and characteristics. Thus, a compromise between growth and erosion imposed by a higher aeration rate must be found (Beun *et al*., 1999; Chen *et al*., 2008; Liu *et al*., 2004). The influence of operational factors on granules morphology and parameters such as density, settling ability, hydrophobicity, and extracellular polysaccharides content has been well addressed (Beun *et al*., 2000; Tay *et al*., 2001c; Tay *et al*., 2001a; Beun *et al*., 2002; Jang *et al*., 2003; Liu *et al*., 2003a). Paradoxically, relatively little attention has been given to the impact of shear forces on biomass stoichiometry and kinetics. To the best of our knowledge, kinetic and stoichiometric parameters have never been assessed during a granulation process conducted under different operating conditions.

Recently, a pulse respirometric method has been suggested for determining apparent stoichiometric and kinetic parameters in suspended activated sludge systems (Oliveira *et*

al., 2011). Oliveira *et al*. (*in preparation [a]*) further applied a similar method for the characterisation of aerobic granular sludge. These previous studies showed that pulse respirometry is a suitable tool for granular biomass characterisation. The purpose of the present work is to determine the impact of shear forces on biomass morphology, stoichiometry and kinetics of aerobic granular sludge. With that purpose, granulation is followed in two sequential batch reactors operated under two different superficial gas velocities by assessing (i) morphological parameters through quantitative image analysis, and (ii) stoichiometric and kinetic parameters through pulse respirometry.

6B.2. Material and Methods

6B.2.1. Experimental Setup

Aerobic granules were cultivated in two sequencing batch airlift reactors (SBARs). Each SBAR was made of transparent acrylic, with a working volume of 5 L. The internal diameter of the down-comer was 9.4 cm and the filling height was 75 cm. The riser was 65 cm height with an internal diameter of 4.2 cm and was positioned at a distance of 2 cm from the bottom of the reactor. Effluent was withdrawn at a 35 cm height from the bottom of the reactor, equivalent to a volume exchange ratio of 50 %. Both reactors were inoculated and operated under the same conditions except aeration rates, in order to maintain different shear forces conditions: the air flow rate was 5.0 L min^{-1} in reactor 1 (R1), and 6.6 L min^{-1} in reactor 2 (R2), corresponding to a riser superficial air velocity of 6.0 and 7.9 cm s^{-1}, respectively. Air was supplied through a fine bubble aerator at the bottom of the reactor, and airflow was controlled by a mass flow controller (GFC 17S Aalborg, USA).

Both SBAR were operated according to the following sequence: (i) 3 min influent filling, (ii) 229 to 232 min aeration, depending on the settling time, (iii) 2 to 5 min settling, and (iv) 3 min effluent discharge; for a total cycle duration of 240 min. Settling time was gradually decreased from 5 min, to 4 min, 3 min, and ultimately to 2 min, on operation days 3, 6, and 9, respectively. Influent and effluent were pumped with peristaltic pumps (Watson Marlow 405 U/R2, Sweden). The cycle operation was controlled by a programmable logic controller (PLC, α2 Series Controller, Mitsubishi).

Both reactors were fed with a synthetic wastewater, containing (mg L^{-1}): $CH_3COONa.3H_2O$,

2073; $(NH_4)_2SO_4$, 140; $MgSO_4.7H_2O$, 25; KH_2PO_4, 44; $K_2HPO_4.3H_2O$, 59; $CaCl_2.2H_2O$, 30; $FeCl_3.6H_2O$, 19; Na_2CO_3, 66; $NaHCO_3$, 105; and a trace mineral solution (Moy *et al.*, 2002), 1mL L^{-1}.

The reactors were inoculated with concentrated activated sludge from an aerobic wastewater treatment plant (Oliveira – Barcelos, Portugal). The activated sludge was priorly sieved (0.3 mm) to remove suspended particles (mainly sand) and then introduced into the reactors. To remove most of the available substrate, reactors were complemented gently with tap water and the biomass was left to settle down before supernatant was removed. Reactors were then maintained aerated with no feed addition for 24 h, before fresh substrate was added for another 24 h period. By the end of this period, the biomass was left to settle during 5 min and 50 % volume of the mixed liquor was withdrawn. Then, the normal sequencing batch mode, described above, was started. During the whole operation in both reactors, organic loading rate (OLR) and hydraulic retention time (HRT) were maintained constant, 2.70 g COD L^{-1} d^{-1} and 8 h, respectively.

The reactors were maintained at ambient temperature (17 – 22 ^{0}C), and pH was controlled to 7.0 ± 0.2 (pH 296 WTW, Germany) with the automatic addition of HCl 1 M (Watson Marlow 401 U/DM3, Sweden). Once a week, the reactors' walls were cleaned in order to prevent attached biomass growth.

6B.2.2. Analytical methods

Influent and effluent were characterised in terms of chemical oxygen demand (COD), total suspended solids (TSS) and volatile suspended solids (VSS) concentrations, according to standard methods (APHA, 1999). Substrate concentration (S) was considered to be the soluble COD fraction (COD-S). Biomass concentration (X) was estimated as VSS and insoluble COD (COD-X). Soluble and insoluble COD fractions were separated by filtration (0.45 μm).

In order to characterise the mixed liquor, samples were taken directly from the reactor during aeration phase. Granular biomass was separated from mixed liquor by wet-sieving (0.25 mm), smaller particles being considered as suspended biomass. The VSS of the two biomass fractions were determined separately: X^{Gran} refers to the granular biomass content, and X^{Tot} is the total, *i.e.* suspended plus granular biomass content. Biomass settling ability was estimated through the sludge volume index (SVI) according to Standard Methods (APHA 1999), after 5 and 30 min of settling time, corresponding to SVI_5

and SVI_{30}, respectively. Biomass density, defined as the concentration of biomass in the aggregates, was determined as g TSS L biomass^{-1} using dextran blue, according to the method described by Beun *et al*. (2002).

Biomass aggregates were characterised through quantitative image analysis, following the procedure presented by Oliveira *et al*. (*in preparation – Appendix I*). Briefly, for image acquisition of granules, slides with three 10 mm etched rings were used. A volume of 0.1 mL of aggregates suspension was placed in each etched circle for visualisation and image acquisition on an Olympus SZ40 stereo microscope (Olympus, Tokyo, Japan) with 12 x magnification. The stereo microscope was coupled to a CCD AVD D5CE Sony grey video camera (Sony, Tokyo, Japan), which along with a DT 3155 Data Translation frame grabber (Data Translation Marlboro, Massachusetts) allowed images acquisition in 768 x 576 pixel and 8 bit (256 grey levels) format through the Image Pro Plus (Media Cybernetics, Silver Spring, MD) software. Calibration from pixels to the metric unit dimensions was performed by means of a micrometer slide, allowing the determination of the metric calibration factor (F_{cal}).

Image processing and analysis were achieved through a programme previously developed in MATLAB (The Mathworks, Inc., Natick, MA) for macro-aggregates characterisation (Amaral and Ferreira, 2005). The parameters determined by the program used in this study were the aggregates equivalent diameter (D_{eq}) and the aggregates roundness (1 = circle).

To describe granulation, a model based on the linear phenomenological equation (LPE) developed by Yang *et al*. (2004c) was applied to the D_{eq} data (Equation 6B.1) for the estimation of the aggregates size-dependent growth constants (μ_{size}, $D_{eq\,ss}$, and t_{lag}).

$$\left(D_{eq} - D_{lag}\right) = \left(D_{eq\,ss} - D_{lag}\right)\left[1 - e^{-\mu_{size}\,(t - t_{lag})}\right] \qquad (6B.1)$$

where, t is the time (d); t_{lag} (d) is the duration of the aggregates size-dependent growth lag phase; μ_{size} (d^{-1}) is the specific aggregates size-dependent growth rate; D_{lag} (mm) is the D_{eq} of aggregates at t_{lag}; and $D_{eq\,ss}$ (mm) is D_{eq} of the aggregates at equilibrium, *i.e.* when the system reaches a steady state.

6B.2.3. Pulse respirometric method

Apparent kinetic and stoichiometric parameters were determined by respirometry. The respirometric method used in this work was based on the injection of multiple concentration pulses, as previously described by Oliveira *et al*. (*in preparation [a]*). The procedure is briefly explained.

Pulse respirometric experiments were made in a 0.5 L transparent acrylic respirometer equipped with magnetic stirring. Air was supplied through a fine bubble aerator placed close to the bottom of the respirometer, and air flow rate was controlled by a mass flow controller (GFC 17S Aalborg, USA). Dissolved oxygen (DO) concentration was measured with a polarographic oxygen probe connected to a DO meter (HI 2400, Hanna Instrument, Portugal) and a computer for data acquisition. The DO probe was calibrated before each respirometric experiment. DO readings were automatically corrected for temperature and salt concentration. When respirometric determinations were made, a 0.5 L test sample of mixed liquor was collected from the SBAR in the last 30 min of the aeration phase. After collecting the test sample, the volume of the SBAR was corrected with tap water, so the hydrodynamic conditions were not affected. At the end of the respirometric experiment, the test sample was totally returned to the reactor in order to avoid biomass losses.

Pulse respirometric experiments were done according to the following procedure: (i) the test sample was placed in the respirometer under constant aeration and gentle mixing (just enough to avoid granules from settling) until stable DO readings were obtained; (ii) the DO concentration (C) reached a pseudo-stationary state, called baseline oxygen concentration (C_b), corresponding to endogenous respiration state (Spanjers *et al.*, 1996); (iii) a pulse of synthetic wastewater was injected to obtain the desired substrate pulse concentration (S_P) in the respirometer; (iv) C was acquired until returning to C_b; (v) steps *(iii)* and *(iv)* were repeated with the injection of different volumes of pulse solution, in order to obtain different substrate concentrations in the respirometer; and finally, (vi) the oxygen mass transfer coefficient (k_La) was measured in triplicate according to the dynamic method described by Badino *et al.* (2000). The COD concentration of the pulse solution was determined every time pulse experiments were done.

6B.2.4. Data Analysis

The respirometric data interpretation method was as previously reported (Oliveira *et al.*, *in preparation [a]*). Briefly, DO concentration in the respirometer can be described by a balance between the exogenous oxygen uptake rate (OUR_{exo}) and the oxygen provided by continuous aeration (Equation 6B.2).

$$\left|\frac{dC}{dt}\right| = k_L a(C_b - C) - OUR_{exo} \quad (6B.2)$$

Because substrate and oxygen are directly linked by a stoichiometric relation, exogenous oxygen consumption profiles yield the same information as substrate consumption profiles (Equation 6B.3), allowing the determination of substrate degradation kinetics.

$$OUR_{exo} = -Y_{O2/S}\frac{dS}{dt} \quad (6B.3)$$

where, S (mg COD-S L^{-1}) is the substrate concentration and $Y_{O2/S}$ (g O_2 g COD-S^{-1}) is the substrate oxidation yield.

$Y_{O2/S}$ is defined as the amount of oxygen consumed (OC) per COD unit of substrate oxidised (Equation 6B.4). $Y_{O2/S}$ was determined as the slope of the linear correlation applied to the OC *versus* S_P data obtained with the multiple concentration pulses respirometric experiments. In terms of COD balance, a portion of the consumed substrate is converted to biomass ($Y_{X/S}$ – biomass growth yield) while the remaining fraction is oxidised to provide the energy required by the process ($Y_{O2/S}$). Thus, $Y_{X/S}$, expressed in COD units, was estimated from $Y_{O2/S}$ (Equation 6B.5).

$$Y_{O2/S} = \frac{OC}{S_P} = \frac{\int_{t_0}^{t_P} OUR_{exo}\,dt}{S_P} = \frac{k_L a \int_{t_0}^{t_P}(C_b - C)dt + (C_0 - C_f)}{S_P} \quad (6B.4)$$

$$Y_{X/S} = 1 - Y_{O2/S} \quad (6B.5)$$

where, OC (mg O_2 L^{-1}) is the amount of oxygen consumed during a pulse; S_P (mg COD L^{-1}) is the pulse substrate concentration; t_0 and t_P (h) are the time at which a pulse is injected and the time the same pulse ends, respectively; and C_0 and C_f (mg O_2 L^{-1}) are the DO concentration at the time the pulse is injected and at the time the same pulse ends, respectively. Usually,, usually C_0 and C_f have the same value, C_b.

For each substrate pulse, the specific substrate consumption rate (q) was determined according to Equation 6.

$$q = 24 \frac{S_P}{X (t_0 - t_P)} \quad (6B.6)$$

where, q (g COD-S g COD-X^{-1} d^{-1}) is the specific substrate consumption rate, X (mg COD-X L^{-1}) is the biomass concentration, and 24 is the conversion factor from h to d.

Assuming a Monod type kinetic, the substrate aerobic biodegradation at a constant biomass concentration can be described by Equation 6B.7 (Oliveira *et al.*, *in preparation [a]*).

$$\frac{dS}{dt} = -q_{max} X \left(\frac{S}{K_S + S}\right) \quad (6B.7)$$

where, q_{max} (g COD-S g COD-X^{-1} h^{-1}) is the maximum specific substrate consumption rate and K_S (mg COD-S L^{-1}) is the substrate affinity constant.

In view of Equations 3 and 6, the maximum exogenous oxygen uptake rate ($OUR_{exo\ max}$) obtained for each pulse can be related to the pulse concentration by a Monod-type model (Equation 6B.8).

$$OUR_{exo\ max} = q_{max} Y_{O2/S} X \left(\frac{S_P}{K_S + S_P}\right) \quad (6B.8)$$

K_S and q_{max}, were determined after the injection of pulses of different substrate concentrations. For each set of respirograms (4 pulses concentrations), the $OUR_{exo\ max}$ was plotted against S_p. Equation 9 was fitted to the experimental S_P and $OUR_{exo\ max}$ data using the least square method implemented with the SOLVER tool of Excel for estimating the kinetic parameters q_{max} and K_S.

All mean parameter values are presented along with the associated standard deviation. The comparisons of the mean parameter values obtained for R1 and R2 were made through one-way ANOVA tests (Statistics 18, SPSS Inc. Package).

6B.3. Results and Discussion

Reactors Operation

Granulation process was followed during 22 days in R1 and 24 days in R2. Since the onset of the experiment, a COD removal efficiency above 90 % was observed in both reactors (Table 6.3). The average effluent COD obtained in R1 and R2 was 60.4 ± 11.8 and 35.2 ±

18.9 mg COD-S L^{-1}, respectively, which are not significantly different ($F_{(1,5)}$ = 3.8, p = 0.12).

Table 6.3. Parameters regarding COD removal efficiency, sludge settling ability, biomass density, aggregates size-dependent growth, roundness of the aggregates, and fraction of granules, in R1 and R2

Parameter	R1	R2	ANOVA	
			F(1,5)	p
COD removal (%)[(a)]	93 ± 2	97 ± 3	0.6	0.07
SVI_5 (mL g^{-1})[(b)]	95 ± 18	63 ± 10	7.2	0.05
t(SVI_{30} = SVI_5) [(d)]	11	8	-	-
biomass density (g L^{-1})[(c)]	21.0 ± 0.3	33.6 ± 2.4	81.7	0.00
Size-dependent growth constants				
t_{lag} (d)	7.6	5.2	-	-
$D_{eq\ lag}$ (mm)	0.48	0.47	-	-
$D_{eq\ ss}$ (mm)	1.22 ± 0.02	1.23 ± 0.05	0.1	0.78
μ_{size} (d^{-1})	0.23 ± 0.02	0.14 ± 0.03	20.5	0.01
(X^{Gran} / X^{Tot})[(c)] (VSS %)	81 ± 8	93 ± 4	5.8	0.07
Roundness > 0.8[(c)] (nr aggregates %)	31 ± 12	64 ± 8	16.2	0.01

[(a)] average values of the whole operation
[(b)] average values after t(SVI_{30} = SVI_5)
[(c)] average values after t_{lag}

In both reactors, an initial decrease of biomass was observed (Figure 6.8), that could be ascribed to the initial washout of the slower settling suspended biomass present in the inocula, and to the possible detachment of biomass from flocs due to the erosion effect of shear stress. Minimum biomass concentrations of 1135 ± 91 and 1080 ± 226 mg TSS L^{-1} were attained in R1 and R2, respectively. Additionally, the time period of biomass loss was longer in R2 (5 d) than in R1 (3 d), likely due to the higher shear stress imposed in R2, which may have caused severe erosion on aggregates.

After the initial biomass wash out, biomass concentration in both reactors increased, reaching 2670 ± 240 and 5815 ± 1053 mg VSS L^{-1} in R1 and R2, respectively. Hence, higher aeration rate and the consequent hydrodynamic shear stress, supported higher biomass concentration. During the formation of granules, hydrodynamic shear caused by aeration is the main detachment force, but once granules are formed, interactions between granules also contribute for detachment. Consequently, the shear stress in R2 was higher

than in R1, not only due to the higher aeration rate applied but also due to its higher biomass content, which results in more particle-particle collisions, thus in an increase in the shear stress on the granules (Gjaltema *et al*., 1997). Additionally, it was observed that granular sludge was the major sludge fraction in both reactors, with a weight fraction of 82 and 93 %, in R1 and R2, respectively, by the end of the experiment (Table 6.3).

After the initial period of biomass wash out, the solids content in the effluent was in average 250 ± 6 and 174 ± 5 mg TSS L^{-1} in R1 and R2, respectively. Therefore, the reactor with higher hydrodynamic shear stress due to higher aeration rate, R2, produced a better quality effluent regarding solids content.

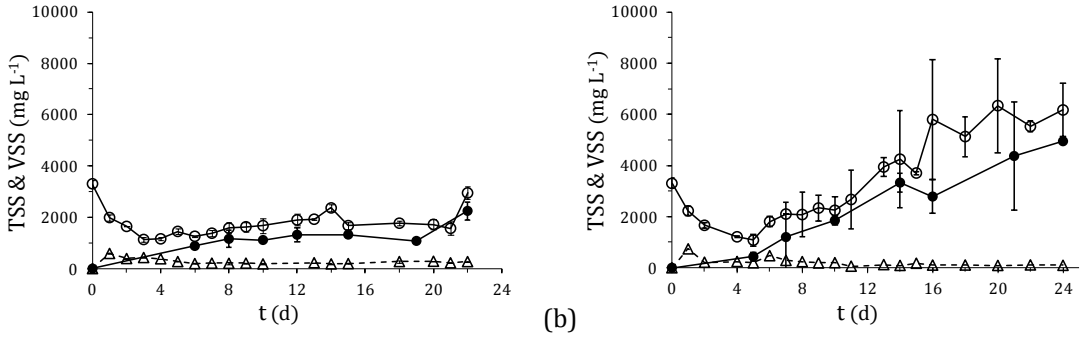

Figure 6.8. Time course of the mixed liquor TSS (○), VSS (●), and the effluent TSS (Δ) in R1 (a), and in R2 (b).

Granulation Process

Morphological changes during the granulation process were clearly distinguished (Figure 6.9).

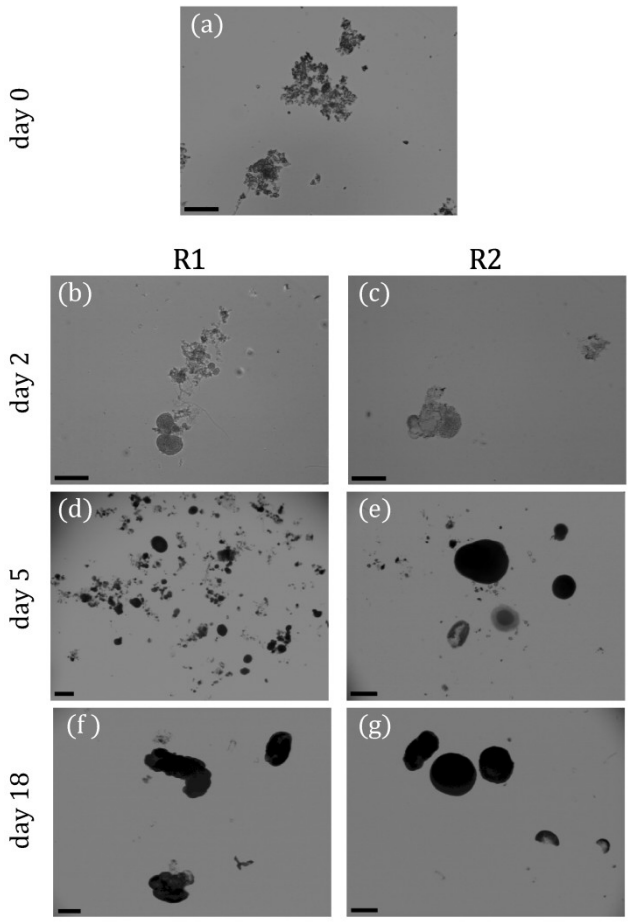

Figure 6.9. Morphology of the seed sludge (a), micro-aggregates on day 2 in R1 (b) and R2 (c), granules on day 5 in R1 (d) and R2 (e), and compact granules on day 18 in R1 (f) and R2 (g). Scale bar 0.1 mm (a–c), and 1 mm (d–g).

The increase in aggregates equivalent diameter was successfully modelled by the integrated LPE equation (Equation 6B.1), as shown in Figure 6.10, allowing the determination of the aggregates size-dependent growth constants (Table 6.3). A longer lag phase (t_{lag}) was observed in R1 (7.6 d) than in R2 (5.2 d), but after the initial lag phase, no significant differences were observed between D_{lag} and $D_{eq\ ss}$ in both reactors (Table 1; $p > 0.05$). The lag phase corresponds to the time it takes the suspended biomass to convert into compact aggregates. Thus, these results indicate that granulation was faster with higher hydrodynamic shear stress; nevertheless no difference was observed between granules size formed in both reactors. On the other hand, the specific size-growth rate (μ_{size}) was higher ($p < 0.05$) in R1 than in R2, 0.23 ±0.02 and 0.14 ± 0.03 d^{-1}, respectively (Table 6.3). Granules may be considered a special case of biofilm growth, in which self-immobilisation occurs with no need for a carrier (Beun *et al.*, 2000; Wilderer and McSwain, 2004; McSwain *et al.*, 2005). A general accepted growth mechanism suggests

biofilms to outgrow preferentially in protuberances extending from the biofilm surface which are exposed to detachment by shear force (Van Loosdrecht *et al*., 1995). Therefore, granules exposed to higher shear forces are expected to grow slower in size, since shear forces will result in less growth of protuberances. This may explain why the specific size-growth rate was lower in R2. This model of biofilm growth can also explain the fact that a higher biomass density was observed in R2 (Table 6.3). The protuberances layer surrounding the granules surface has a lower density than the inner core, due to the voids between protuberances (Van Loosdrecht *et al*., 1995). In R1, where the shear stress was lower, the protuberances layer would be larger due to less detachment, explaining why the global biomass density was lower in this reactor.

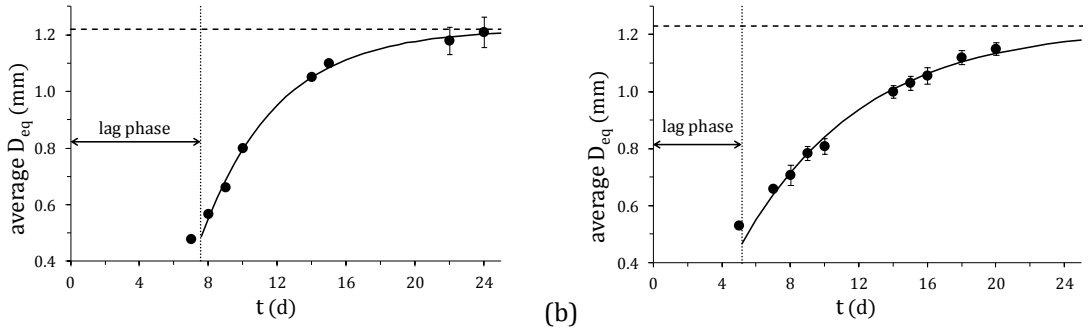

Figure 6.10. Time course of the average equivalent diameter of aggregates (•) and LPE fitting (*solid line, $r^2 > 0.99$*), in R1 (a) and in R2 (b).

During the granulation process, a considerable modification of sludge settling characteristics was observed. SVI_5 of the seed sludge was 162 ± 27 mL g^{-1}, but during granulation it rapidly decreased (data not shown). The observed decrease of SVI_5 was faster in R2 than in R1. Indeed, the elapsed time, from the onset of the experiment, to reach a complete settling time inferior to 5 min (when $SVI_{30} = SVI_5$) was 10 days in R1 and 7 days in R2 (Table 6.3). After this moment, SVI_5 did not change significantly until the end of granulation process, being in average 95 ± 18 and 63 ± 10 mL g^{-1} in R1 and R2, respectively (Table 6.3). SVI gives a measurement of the sludge compactness, thus the higher shear stress in R2 produced a more compact sludge ($p \approx 0.05$). These results were corroborated by the average granule density, which was much higher ($p < 0.05$) in R2 than in R1, 35.7 ± 2.6 and 21.6 ± 2.0 g L^{-1}, respectively (Table 6.3). Clear morphological differences were also observed between granules formed in R1 and R2. In R2, rounder granules were formed ($p < 0.05$), with 64 % of the granules having a roundness above 0.8, in contrast with 31 % in R1 (Table 6.3). This was also clearly observed by direct visualisation of the granules (Figure 6.9f and 10g). Hence, the higher hydrodynamic shear

stress produced rounder granules. Similar results were obtained in a bubble column by Liu *et al*. (2003a), as they observed a direct proportionality between granules roundness and superficial air velocity.

The results obtained from comparing the two different hydrodynamic shear stresses are in accordance with the literature: higher hydrodynamic shear forces favour higher biomass concentrations in the reactor and better effluent quality in terms of solids content, the formation of more compact, denser and better settling granules (Tay *et al.,*2001c; Liu and Tay, 2002; Di Iaconi *et al.,*2006; Ramadori *et al.,*2006; Chen *et al.,*2007; Chen *et al*., 2008).

Stoichiometry and Kinetics

The stoichiometric and apparent kinetic values were monitored throughout the granulation process using pulse respirometry. R2 had a higher biomass growth yield than R1 (Table 6.4; $F_{(1,5)}$ = 8.54, p = 0.04). This may be due to granulation occurring in the balance between two opposite forces: the biomass growth and biomass detachment (Liu *et al*., 2003b; Liu and Tay, 2006; Chen *et al*., 2007). Being detachment forces higher, enhanced by the higher hydrodynamic shear stress, more energy is "canalised" for growth in order to counterbalance. Thus in R2 the biomass, subjected to higher detachment forces, presented a higher growth yield, *i.e.* more substrate was used for cell growth.

Table 6.4. Biomass growth yield average values in R1 and R2

	R1	**R2**
$Y_{X/S}$ (g COD-X g COD-S^{-1})	0.5 ± 0.02	0.6 ± 0.02

The kinetic parameters were obtained with the multiple concentration pulses respirometric method. Figure 4 shows an example of model (Equation 6.B.7) fitting to the $OUR_{exo\ max}$ *versus* S_p experimental data obtained with the injection of five pulses of different substrate concentrations. Similar results were obtain along the entire reactors operation (average r^2 = 1.00 ± 0.00).

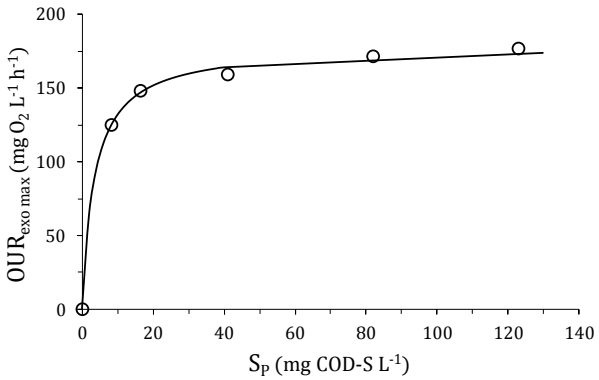

Figure 6.11. Example of a Monod type model fitting (*solid line, r^2 = 1.00*) to the maximum observed exogenous OUR and substrate concentration pulse experimental data (○) obtained with the injection of five increasing substrate concentration pulses (S_P = 8.2, 16.4, 41.0, 82.0, and 123.0 mg COD L^{-1}).

Metabolic activity was evaluated via the specific substrate consumption rate (q; Figure 6.12a). In both reactors an initial increase of q occurred. In R1, this increase was observed in the first 2 days, while in R2 it was observed during the first 5 days. This showed that at the first stage of granulation process, during acclimatisation phase, the biomass was more active in both reactors. After the initial increase, q decreased and stabilised: in R1 from day 6 onward, and in R2 from day 10 onward. In R2 the biomass showed higher activity than in R1 during the granulation process, but from day 10 onward, q values in R1 and in R2 were alike ($F_{(1,5)}$ = 0.95, p = 0.38), 0.47 ± 0.01 and 0.44 ± 0.06 g COD-S g COD-X^{-1} d^{-1}, respectively. Sludge retention time, as a measurement of sludge age, is generally recognised as an indicator of microbial activity (Li *et al*., 2006). In fact it could be observed that microbial activity varied inversely to SRT (Figure 6.12a and 6.13b). In R1, the SRT was very constant along the granulation process, and so was microbial activity as substrate metabolism. In R2, on the other hand, a large variation on the SRT was observed along the granulation process, which was accompanied by a variation on metabolic activity: on the beginning of the process, when SRT was relatively low, the metabolic activity was high (first 8 days of operation); then, as biomass was longer retained in the reactor and SRT progressively increased, the metabolic activity decreased.

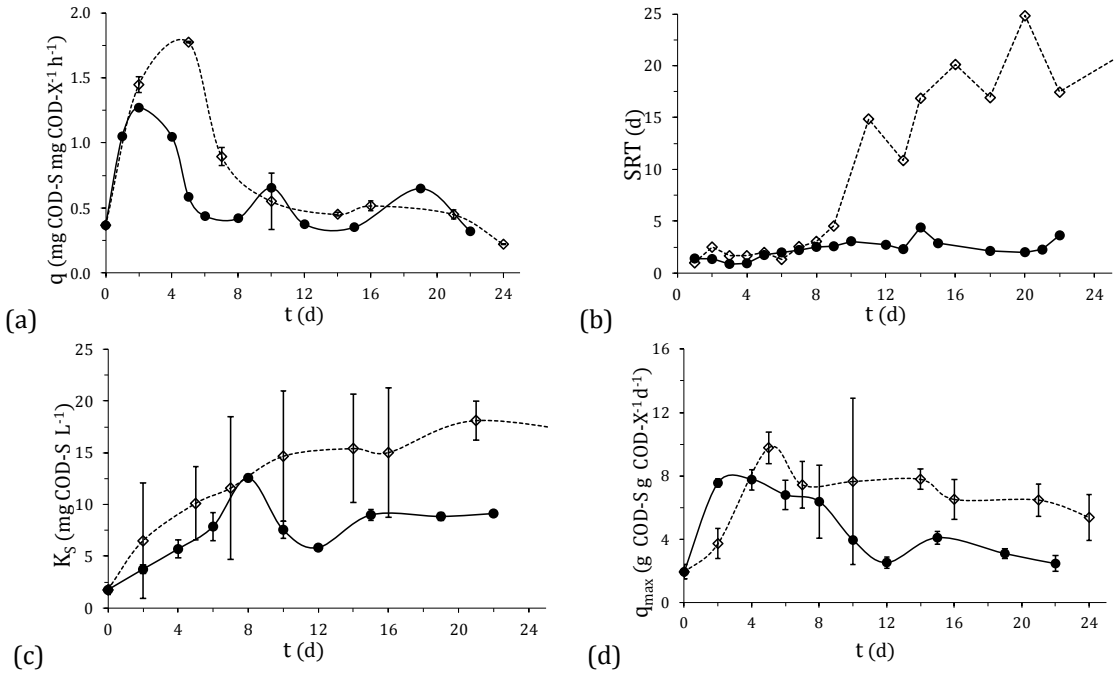

Figure 6.12. Time course, in R1 (●) and R2 (◇), of the:
specific substrate consumption rate (a); sludge retention time (b);
substrate affinity constant (c); and maximum specific substrate consumption rate (d).

The true kinetic parameters are intrinsic to a microbial community. Both reactors were operated on the same mode, fed with the same substrate, and with equal substrate loading rates, thus no major community changes would be expected between the two reactors. Consequently, through the differences in apparent kinetic parameters it is possible to infer some phenomena occurring in the reactors.

The apparent substrate affinity constant (K_S) was obtained through the multiple concentration pulses respirometric method (Figure 6.12c). Changes in the apparent affinity constant of granular sludge give an indication for substrate transport limitation in granules (Ni and Yu, 2010). An increase in apparent K_S values points towards an increase in resistance for substrate transport, since it indicates that the substrate reaching the cells "trapped" in the granules is lower than the substrate detected in the bulk liquid. That is why the apparent K_S values for granular biomass are generally higher than those of suspended biomass (Oliveira *et al.*, *in preparation – Chapter 6.A.*). In R1 the K_S values did not vary much all through the granulation process. This seems to indicate that the K_S of granular biomass did not differ much from that of suspended biomass, and it was found that the K_S of granular biomass did not increase with the increase diameter of the granules ($r^2 < 0.10$, data not shown). This may mean that active biomass was located at the surface of the granules in a thin layer where substrate suffered low transport resistance reaching

the cells, or that granules were somehow porous structures in which substrate did not found much transport resistance since biomass density did not change much through granulation process (data not shown). On the other hand, in R2 K_S increased considerably during granulation (Figure 6.12c). It thus appears that substrate transport limitations were occurring in the granules in R2, and that these limitations increased along granulation process as granules grew in size and density (data not shown). The apparent K_S, by the end of the granulation process, was much higher in R2 than in R1, 16.4 ± 2.6 and 9.1 ± 0.2 mg COD-S L^{-1}, respectively, which was in conformity with granules being denser in R2 than in R1 (Table 6.3; $p < 0.05$). Additionally, a direct correlation was found between granules equivalent diameter and K_S for R2 ($r^2 > 0.90$; Figure 6.13).

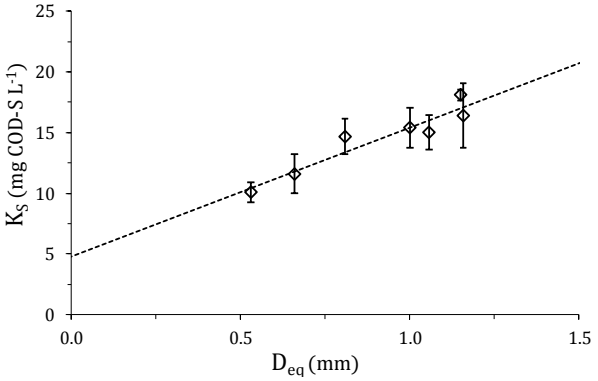

Figure 6.13. Relation between aggregates equivalent diameter and K_S in R2 (◇), and linear correlation (*solid line, $r^2 > 0.90$*).

The apparent maximum specific substrate consumption rate (q_{max}) was estimated through the multiple concentration pulses respirometric method (Figure 6.12d). q_{max} showed the same trend in both reactors: it increased in a first stage, until day 4 in R1 and day 5 in R2; subsequently decreasing progressively during the granulation process. The apparent q_{max} depends on how biomass is considered. In the present work, biomass was considered the insoluble COD, therefore including besides active biomass also other substances such as extracellular polymeric substances (EPS). In this sense, the more EPS present in the granules, the lower the apparent q_{max}. This may explain the observed trend in apparent q_{max} observed: in a first stage of granulation, when granules are smaller and composed preponderantly of active biomass, the apparent q_{max} approximates the intrinsic q_{max}; as granulation progresses, EPS are incorporated in the granules giving them strength and stability against shear stress (Tay *et al.*, 2001a & c), the active biomass fraction in insoluble COD diminishes, *i.e.* the considered biomass is overestimated, and the apparent q_{max} values decrease. The decrease of q_{max} along granulation processes reflects the

stabilisation of granules through the production of EPS. During the granulation process, q_{max} was higher in R2 than in R1. This could mean the active layer, *i.e.* the outer layer of the granules, where the active biomass is located (Chiu *et al*., 2007), was deeper in R2 than in R1. This would be expected since DO concentration in R2 was higher in R2 due to the higher aeration rate, thus the penetration depth of oxygen could allow sustaining microbial activity at higher depths (Wilén *et al*., 2004). Previous studies have pointed to independence of the mature granules EPS content towards hydrodynamic shear stress (Di Iaconi *et al*., 2006). The observed difference between the final q_{max} values in R1 and R2, 2.5 ± 0.5 and 5.4 ± 0.9 g COD-S g COD-X^{-1} d^{-1}, respectively, may mean that mature granules were not obtained during the considered period of operation.

6B.4. Conclusions

Aerobic granules were cultivated in two reactors with aeration rates of 5.0 (R1) and 6.6 L min^{-1} (R2). The higher shear stress in R2, resulted in a faster granulation process (lag phase of 5 d *versus* 8 d with lower aeration rate), higher biomass concentration (5815.0 *versus* 2670.0 mg VSS L^{-1}) with a higher percentage of granules in the reactor (93 % *versus* 82 %), production of a better quality effluent in terms of solids (173.5 *versus* 249.9 mg TSS L^{-1}), compacter sludge (SVI_5 of 63 *versus* 95 mL g^{-1}), higher biomass density (33.6 *versus* 21.0 g L^{-1}), and rounder granules.

The apparent stoichiometry and kinetic parameters were monitored throughout granulation process by pulse respirometry. The sludge cultivated at higher shear stress had higher biomass growth yields (0.6 *versus* 0.5 g COD-X g COD-S^{-1}) and higher apparent affinity constant values (16.4 *versus* 9.1 mg COD-S L^{-1}), which could indicate higher substrate transport limitations in the denser granules. A clear relation between the affinity constant and the granules equivalent diameter was found in the granules formed at higher shear stress. The metabolic activity, given by the specific substrate consumption rate, followed a similar trend during the granulation process, and reached the same value (approximately 0.45 g COD-S g COD-X^{-1} d^{-1}) under the two studied shear stresses. The maximum specific substrate consumption rate at the end of the granulation process was also higher in the reactor operated at higher shear stress (5.4 *versus* 2.5 g COD-S g COD-X^{-1} d^{-1}).

It can be concluded that the cultivation of aerobic granules at a higher aeration rate, though comprising higher costs, might be beneficial since it may allow a faster granulation,

obtaining compacter and denser granules, which, even though presenting higher resistance to substrate transport to the cells, may allow better quality effluent in terms of solids. Additionally, under higher aeration rate a higher biomass content may be achieved in the system, which may be advantageous as gaining robustness against organic shock loads.

6B.5.References

Amaral, A.L. Ferreira, E.C. (**2005**). *Activated Sludge Monitoring of a Wastewater Treatment Plant using Image Analysis and Partial Least Squares Regression*. Anal. Chim. Acta 544(1–2):246–253.

APHA (**1999**). *Standard methods for the examination of water and wastewater*. 20th Edn. Washington, DC, American Publishers Health Association.

Badino AC, Facciotti MCR, Schmidell W (**2000**). *Improving k(L)a determination in fungal fermentation, taking into account electrode response time*. J. Chem. Technol. Biot. 75(6):469–474.

Beun J J, Hendriks A, van Loosdrecht MCM, Morgenroth E, Wilderer PA, Heijnen JJ (**1999**). *Aerobic granulation in a sequencing batch reactor*. Water Res. 33(10):2283–2290.

Beun JJ, van Loosdrecht MCM, Heijnen JJ (**2000**). *Aerobic granulation*. Water Sci. Technol. 41(4–5):41–48.

Beun JJ, van Loosdrecht MCM, Heijnen JJ (**2002**). *Aerobic granulation in a sequencing batch airlift reactor*. Water Res. 36(3):702–712

Chen Y, Jiang W, Liang DT, Tay JH (**2007a**). *Structure and stability of aerobic granules cultivated under different shear force in sequencing batch reactors*. Appl. Microbiol. Biot. 76(5):1199–1208.

Chen Y, Jiang W, Liang DT, Tay JH (**2008**). *Aerobic granulation under the combined hydraulic and loading selection pressures*. Bioresource Technol. 99(16):7444–7449.

Chiu ZC, Chen MY, Lee DJ, Wang CH, Lai JY (**2007**). *Oxygen diffusion and consumption in active aerobic granules of heterogeneous structure*. Appl. Microbiol. Biot. 75(3):685–691.

De Kreuk MK, van Loosdrecht MCM (**2006**). *Formation of aerobic granules with domestic sewage*. J. Environ. Eng.-ASCE 132(6):694–697.

Di Iaconi C, Ramadori R, Lopez A, Passino R (**2006**). *Influence of hydrodynamic shear forces on properties of granular biomass in a sequencing batch biofilter reactor*. Biochem. Eng. J. 30(2):152–157.

Gjaltema A, Vinke JL, van Loosdrecht MCM, Heijnen JJ (**1997**). *Abrasion of suspended biofilm pellets in airlift reactors: Importance of shape, structure, and particle concentrations*. Biotechnol. Bioeng. 53(1):88–99.

Jang A, Yoon YH, Kim IS, Kim KS, Bishop PL (**2003**). *Characterization and evaluation of aerobic granules in sequencing batch reactor*. J. Biotechnol. 105(1–2):71–82.

Li ZH, Kuba T, Kusuda T (**2006**). *Selective force and mature phase affect the stability of aerobic granule: An experimental study by applying different removal methods of sludge*. Enzyme

Microb. Tech. 39(5):976–981.

Liu Y, Yang SF, Tay JH (**2004**). *Improved stability of aerobic granules by selecting slow-growing nitrifying bacteria*. J. Biotechnol. 108(2):161–169.

Liu Y, Yang SF, Liu QS, Tay JH (**2003a**). *The Role of Cell Hydrophobicity in the Formation of Aerobic Granules*. Curr. Microbiol. 46(4):270–274.

Liu Y, Lin YM, Yang SF, Tay JH (**2003b**). *A balanced model for biofilms developed at different growth and detachment forces*. Process Biochem. 38(12):1761–1765.

Liu YQ, Tay JH (**2006**). *Variable aeration in sequencing batch reactor with aerobic granular sludge*. J. Biotechnol. 124(2):338–346.

Liu Y, Tay JH (**2002**). *The essential role of hydrodynamic shear force in the formation of biofilm and granular sludge*. Water Res. 36(7):1653–1665.

McSwain BS, Irvine RL (**2008**). *Dissolved oxygen as a key parameter to aerobic granule formation*. Water Sci. Technol. 58(4):781–787.

McSwain BS, Irvine RL, Hausner M, Wilderer PA (**2005**). *Composition and distribution of extracellular polymeric substances in aerobic flocs and granular sludge*. Appl. Environ. Microb. 71(2):1051–1057.

Moy BYP, Tay JH, Toh SK, Tay TL (**2002**). *High organic loading influences the physical characteristics of aerobic sludge granules*. Lett. Appl. Microbiol. 34(6):407–412.

Ni BJ, Yu HQ (**2010**). *Mathematical modeling of aerobic granular sludge: A review*. Biotechnol. Adv. 28(6):895-909.

Oliveira CS, Ordaz A, Ferreira EC, Alves M, Thalasso F (**2011**). In situ *pulse respirometric methods for the estimation of kinetic and stoichiometric parameters in aerobic microbial communities*. Biochem. Eng. J. (*Chapter 5 of this Thesis*).

Oliveira CS, Ordaz A, Ferreira EC, Thalasso F, Alves M (***in preparation – Chapter 6.A.***). Pulse respirometric method for determination of extant kinetic and stoichiometric parameters in an aerobic granular sludge system.

Oliveira CS, Thalasso F, Ferreira EC, Alves M (*in* ***preparation – Appendix I***). *Early detection of fungal proliferation in aerobic granular sludge by quantitative image analysis*.

Ramadori R, Di Iaconi C, Lopez A, Passino R (**2006**). *Wastewater treatment by periodic biofilter characterized by aerobic granular biomass*. J. Environ. Sci. Heal. A 41(9):1781–1792.

Tay JH, Liu QS, Liu Y (**2001a**). *The role of cellular polysaccharides in the formation and stability of aerobic granules*. Lett. Appl. Microbiol. 33(3):222–226.

Tay JH, Liu QS, Liu Y. (**2001b**). *Microscopic observation of aerobic granulation in sequential aerobic sludge blanket reactor*. J. Appl. Microbiol. 91(1):168–175.

Tay JH, Liu QS, Liu Y (**2001c**). *The effects of shear force on the formation, structure and metabolism of aerobic granules*. Appl. Microbiol. Biot. 57(1-2):227–233.

Tay JH, Liu QS, Liu Y (**2004**). *The effect of upflow air velocity on the structure of aerobic granules cultivated in a sequencing batch reactor*. Water Sci. Technol. 49(11-12):35–40.

Van Loosdrecht MCM, Eikelboom D, Gjaltema A, Mulder A, Tijhuis L, Heijnen JJ (**1995**). *Biofilm structures*. Water Sci. Technol. 32(8):35–43.

Wilén BM, Gapes D, Keller J (**2004**). *Determination of external and internal mass transfer limitation in nitrifying microbial aggregates*. Biotechnol. Bioeng.86(4):445–457.

Wilderer PA, McSwain BS (**2004**). *The SBR and its biofilm application potentials*. Water Sci. Technol. 50(10):1–10.

7. Conclusions and Future Perspectives

Abstract

This chapter presents a summary of the study developed in this thesis. The general conclusions withdrawn at each stage of work, and the global conclusion from this work are also presented.

Furthermore, some suggestions for future research in the field of respirometric techniques applied to microbial processes are also given.

7.1. Conclusions

This thesis aimed to test and develop respirometric techniques for the characterisation of aerobic microbial processes.

Respirometric techniques were applied to four types of microbial communities: a nitrifying system (*Chapter 3*), a pure culture system (*Chapter 4*), a suspended activated sludge system (*Chapter 5*), and aerobic granular sludge systems (*Chapters 6A and 6B*).

The general conclusions withdrawn at each step of the research are compiled below.

Nitrifying System

- *In situ* pulse respirometry was applied to a suspended biomass nitrifying system. Stoichiometric parameters were retrieved directly from pulse respirograms, and kinetic parameters were obtained through model adjustment to the pulse respirograms using ASM1. Three important parameters could be retrieved: the oxidation yield, the growth yield, and the substrate affinity constant. Additionally, through the injection of pulses of increasing concentration, the maximum oxygen uptake rate could be determined.

- Model adjustment was successfully applied to a portion of the respirogram, but not to the complete respirogram. It was hypothesised that a more complex model taking into account biological and electrode response time as well as a two step biological model should give better correlation.

- Two methods for the determination of the oxygen volumetric mass transfer coefficient were tested (the Pratt method and the dynamic method), and it was concluded that the dynamic method gave better results, for it has been chosen as the determination method in all the subsequent work.

Pure culture System

- *In situ* pulse respirometry was applied to a pure culture system of *Pseudomonas putida* F1. Stoichiometric parameters were retrieved directly from the pulse respirograms, and kinetic parameters were obtained through model adjustment using ASM1 and ASM3. Based on the previous results, the models included terms which took into account the biological and electrode response time, thus the

entire respirogram could be successfully used for model fitting. As expected, the model which best fitted the experimental data was ASM3. ASM3 takes into account storage phenomena, which is a recognised metabolic capability of *Pseudomonas putida*.

- *In* situ pulse respirometry was compared with the traditional chemostat method for estimation of kinetic and stoichiometric parameters: the respirometric method was validated, implying relatively lower experimental effort. Thus, *in situ* pulse respirometry was found to be a suitable method for the kinetic and stoichiometric characterisation of axemic cultures of *Pseudomonas putida* F1.

Suspended Activated Sludge

- *In situ* pulse respirometry was applied to a suspended activated sludge system. The pulse respirometric method was compared with the traditional chemostat method for the estimation of stoichiometric and kinetic parameters, and it was shown that the chemostat method produced parameters with larger standard deviation. It was argued that this would be due to the difficulty of sampling heterogeneous suspensions, thus underlying the potential advantage of *in situ* respirometry, as no biomass sampling is needed.

- Two respirometric data treatment methods for the estimation of kinetic and stoichiometric parameters were compared: the model adjustment to the respirogram using ASM1 and ASM3, and the multiple concentration pulses injection method. ASM1 fitted the pulse respirogram better than ASM3, since no storage phenomena were occurring. ASM1 model fitting and the multiple concentration pulses gave similar results both for the substrate affinity constant and the maximum specific oxygen consumption rate. Nevertheless, the model fitting method was shown to be less precise when a single pulse was used. It was concluded that for achieving a similar precision as the multiple concentration pulses method, the model fitting method would require a large computational effort. It was concluded that *in situ* pulse respirometry gives more confident and precise results when compared to traditional method based on substrate concentration for the kinetic and stoichiometric characterisation of a suspended activated sludge system. Within respirometric techniques, it was shown that the multiple concentration pulses method is the most adequate for stoichiometric and kinetic characterisation of mixed cultures, with several advantages such as

shorter time requirements, due to simpler experimental data interpretation, and producing better confidence results.

Aerobic granular sludge

- The multiple concentration pulses respirometric method was applied in an aerobic granular sludge for the characterisation of the culture kinetics and stoichiometry. The respirometric method was validated through comparison with literature values, for the estimation of six central parameters: substrate oxidation yield, biomass growth yield, specific endogenous respiration rate, maximum specific oxygen consumption rate, substrate affinity constant, and maximum specific growth rate.

- Aerobic granulation process was successfully followed up by assessing kinetic and stoichiometric parameters along time.

- The determined parameters were extant (traducing the real metabolic state of the biomass) and apparent parameters, thus traducing those actually prevailing in the system under the real operating conditions. This allowed showing the potential of the proposed method for monitoring aerobic granular sludge systems, and controlling it in an efficient mode. A control strategy example was given in which the obtained results are shown to be useful for aeration control.

- Additionally, the multiple concentration pulses respirometric method was used to assess the kinetic and stoichiometry aerobic granulation in two systems operated under different shear stress intensities. The multiple concentration pulses respirometric method allowed to show that the sludge cultivated at higher shear stress had higher biomass growth yields and higher apparent affinity constant values, which could indicate higher substrate transport limitations in the granules. A clear relation between the affinity constant and the granules equivalent diameter was found in the granules formed at higher shear stress. The metabolic activity, given by the specific substrate consumption rate, followed a similar trend during the granulation process, and reached the same value under the two studied shear stresses. The maximum specific substrate consumption rate at the end of the granulation process was higher in the reactor operated at higher shear stress.

Overall

The global conclusion withdrawn from the work presented in this thesis is that respirometry, especially pulse respirometry, is a valid and promising technique for kinetic and stoichiometric characterisation of aerobic microbial processes, whether these are pure or mixed cultures, and suspended or aggregated cultures. Though the major outbreak of respirometry has occurred a couple of decades ago, in the mid 80s and 90s, there are still new approaches to study and new possibilities to explore in this area.

A respirometric method was developed, the multiple concentration pulses method, which allows an exhaustive characterisation of aerobic microbial processes in approximately two hours, using low cost material and requiring low computational power.

7.2. Future Perspectives

The outcome of this thesis, particularly the multiple concentration pulses respirometric method, may present good future prospect in the area of real systems monitoring and control. Some future perspectives are listed below.

- To test the practical control strategy suggested in Chapter 6A in a real system 1st in a lab- or pilot-scale, and after tuning the control method test its application in a real system. Different kinds of disturbances, e.g. organic loading disturbances, toxic and/or inhibitory compounds concentration and time of exposure.

- To apply and adjust the method to more complex systems, namely to combined systems, where nitrification may be assessed through ammonium pulses.

- Further studies, with the simultaneous analysis of apparent and actual kinetic and stoichiometric parameters, would allow for a better understanding of diffusion-reaction processes in granules or other biofilm reactors.

- To develop an automatic control system based on the multiple concentration pulses respirometric method, which allows controlling the process according to the influent characteristics.

- To develop a control algorithm based on respirometric response of endogenous biomass to influent wastewater pulses, which controls the aeration intensity in the aeration tank, and in the case of SBRs additionally adjusts the time of the

cycle regarding influent characteristics.

- To develop an online respirometer, in which (1) biomass is collected automatically from reactor to the respirometer, (2) multiple concentration pulses are made automatically, and DO response recorded, (3) an algorithm (i) transforms DO signal in OUR signal, (ii) determines the stoichiometric parameters, (iii) detects OUR_{max} for each pulse, (iv) adjusts Monod curve to data, and (v) estimates the apparent kinetic parameters (K_S and $q_{O2\ max}$). In SBR systems, the time at which the microbial consortia enter famine regime may be identified; thus allowing to control the famine time in accordance with the influent characteristics, which is important for several processes such as aerobic granular sludge stability, and storage compounds production

8. APPENDIX I – QUANTITATIVE IMAGE ANALYSIS APPLIED TO AEROBIC GRANULAR SLUDGE

Abstract

Aerobic granular sludge was produced and cultivated in a sequencing batch airlift reactor (SBAR) fed with acetate-based synthetic wastewater. Granulation was assessed by quantitative image analysis. Micro-aggregates (D_{eq} < 0.25 mm), macro-aggregates (D_{eq} > 0.25 mm) and free thin filaments (likely bacterial) were quantified and three phases were distinguished in the granulation process: acclimatisation (days 0 to 9), granulation (days 9 to 24), and fungal proliferation (days 24 to 42). The acclimatisation phase was dominated by the washout of slow settling biomass, and by the brief abundance of bacterial filaments, which latter built the backbone of future granules. In the granulation phase, granules were formed as stable and compact structures. After day 24, the aggregates within a defined size range between 0.025 and 0.25 mm, became elongated due to the growth of thick filamentous structures (likely fungal filaments) that were not detected as filaments by the "filaments program". Fungal growth was accounted for in the micro-aggregates program and the initial phase of fungal growth occurred for the aggregates within the size range between 0.025 and 0.25 mm which turned suddenly elongated but rapidly became bigger and surrounded by a compact structure of nonbacterial filaments. A precise and sensitive detection of the early stage of fungal contamination was possible through the length (L) to width (W) ratio of aggregates with equivalent diameter between 0.025 and 0.25 mm. Between days 22 and 26 an increase of 29 % in this parameter anticipated the detection of fungal growth, that was macroscopically visible only on the day 28. In that day, the aggregates were completely surrounded by fungal filaments and regained the apparent roundness that had before the contamination. Thus, the morphological parameter L/W ratio showed to be an early warning indicator of fungal contamination, allowing foregoing control of operational conditions to avoid problems in the efficiency and stability of the system.

8.1. Introduction

Aerobic wastewater treatment processes based on granular sludge have gained growing attention due to its small footprint (De Bruin *et al*., 2004), high conversion capacity (Carvalho *et al*., 2006), low sludge production (Di Iaconi *et al*., 2007), operational flexibility (Di Iaconi *et al*., 2008), and versatility in treating wastewater of various composition (De Kreuk *et al*., 2005; De Kreuk and van Loosdrecht, 2006; Carucci *et al*., 2008, Adav *et al*. 2007, Jiang *et al*., 2002; Inizan *et al*., 2005). Nevertheless a wide application of aerobic granular sludge systems has been limited by the relatively low long-term stability of aerobic granules (Chen *et al*., 2007b), mainly due to the proliferation of filamentous microorganisms, in particular filamentous fungi (Li *et al*., 2010; Weber *et al.*, 2007). Filamentous dominant growth leads to instability of the aerobic granules, decreases the removal efficiency (Morgenroth *et al*., 1997), the settling ability, and, subsequently, biomass washout can occur (Liu and Liu, 2006).

Fungi are not usually observed in significant quantities in aerobic treatment systems. Nevertheless, given the right set of growth conditions, fungi can proliferate with detrimental consequences on treatment and effluent quality. One recognised consequence of fungal proliferation is the nefarious effect in the medium rheology: a viscous, plastic medium is obtained which offers high resistance to stirring and aeration (Prescott et at., 2004). The growth of fungi should therefore be early detected and controlled. Consequently, practical methodologies for monitoring and control of granules stability at physiological, microbial, and structural levels are needed. Granules structure and morphology, assessed by morphological parameters, density and characteristic dimensions are related to the microbial composition, affecting the respective physiological activity (Chen *et al*., 2007a). Most of the events occurring during aggregates history, e.g. granulation and fragmentation, are accompanied by a change in aggregates morphology and measuring these changes allows detecting and altering operational conditions such as threatening or existing operation problems at an early stage (Heine *et al*., 2002).

Quantitative image analysis techniques along with physiological information have been applied to monitor and detect operational problems in advance to reactor performance failure in anaerobic granular sludge systems (Costa *et al*., 2009; Abreu *et al*., 2007). These techniques have also been applied to quantify the formation and the deterioration of anaerobic granular sludge (Araya-Kroff *et al*., 2004, Amaral *et al*., 2004).

No troubleshoot diagnosis strategies have been proposed so far to detect structural

instability of aerobic granular sludge. This work demonstrates the sensitivity of quantitative image analysis in the process of aerobic granules formation and its usefulness to early detect and anticipate in two days an episode of fast filamentous fungal proliferation in those granules.

8.2. Material and Methods

8.2.1. Experimental Setup

An acrylic airlift reactor, with a working volume of 5 L and a filling height of 75 cm, was used. The internal diameter of the down-comer was 9.4 cm. The riser was 65 cm height with an internal diameter of 4.2 cm and was positioned at a distance of 2 cm from the bottom of the reactor. Air was supplied through a fine bubble aerator at the bottom of the reactor at an aeration flow rate of 5.0 L min-1. Effluent was withdrawn at a 35 cm height from the bottom of the reactor, equivalent to a volume exchange ratio of 50 %.

The airlift reactor was operated in sequencing batch mode (sequencing batch airlift reactor, SBAR) with a cycle time of 4 h. Each cycle consisted of four phases: influent filling (3 min); aeration (231 min); settling (2 min, which allowed to retain in the reactor only the particles that settled faster than 11 m h-1); and effluent discharge (3 min). The cycle operation was control by a PLC (programmable logic controller).

The reactor was fed with synthetic wastewater, composed by (mg L-1): $CH_3COONa{\cdot}3H_2O$, 2073; $(NH_4)_2SO_4$, 140; $MgSO_4{\cdot}7H_2O$, 25; KH_2PO_4, 44; $K_2HPO_4{\cdot}3H_2O$, 59; $CaCl_2{\cdot}2H_2O$, 30; $FeCl_3{\cdot}6H2O$, 19; Na_2CO_3, 66; $NaHCO_3$, 105; and a trace mineral solution (Moy *et al*., 2002), 1mL L^{-1}.

The reactor was inoculated with concentrated activated sludge from a compact wastewater treatment plant (Oliveira–Barcelos, Portugal). The activated sludge was previously sieved (0.3 mm), washed with tap water, and maintained aerated and with no feed addition for 24 h, then it was acclimatised to the synthetic wastewater in batch mode for 24 h. By the end of this period, the biomass was left to settle during 5 min and 50 % of the mixed liquor was withdrawn. The biomass retained in the reactor was considered as the inoculum seed and normal sequencing batch mode was started. The settling time was gradually decreased from 5 min, to 4 min, to 3 min, and ultimately to 2 min each 3 days, so

on operation day 3, 6, and 9, respectively.

During the whole operation, organic loading rate was constant along with unvarying hydraulic residence time. The reactor was maintained at ambient room temperature (17–22 ^{0}C), and pH was controlled to 7 ± 0.2 (pH 296 WTW, Germany) with the automatic addition of HCl 1 M (Watson Marlow 401 U/DM3, Sweden). Once a week, the walls of the reactor were cleaned in order to prevent biomass attached growth.

8.2.2. Analytical methods

Chemical oxygen demand (COD) was determined using cuvette test kits (Hach- Lange, Germany). Total and volatile suspended solids (TSS and VSS) and total solids (TS) were analysed according Standard Methods (APHA, 1999).

Influent and effluent were characterised by COD, TSS, and VSS concentrations. Biomass content was estimated as the VSS in the mixed liquor. The mixed liquor was sieved (0.25 mm) in order to separate the granular biomass, aggregates larger than 0.25 mm, and the smaller aggregates. The VSS of the two biomass fractions was determined separately. Biomass settling ability was estimated through the sludge volume index (SVI) according to Standard Methods, after 5, 10, and 30 min of settling, corresponding to SVI_5, SVI_{10}, and SVI_{30}, respectively.

Biomass density (the concentration of biomass in the aggregates) was determined as g TSS L biomass-1 using dextran blue, according to the method described by Beun *et al*. (2002).

8.2.3. Image acquisition, processing, and analysis

Image acquisition was done in accordance with Costa *et al*. (2009). Three different objects were identified: micro-aggregates with equivalent diameter smaller than 0.25 mm, macro-aggregates with equivalent diameter larger than 0.25 mm, and filaments. Briefly, for image acquisition of micro-aggregates and filaments, 20 µL of sample were placed on a slide and covered with a 20 x 20 mm cover slip for visualisation and image acquisition. Approximately 200 images were acquired in bright field, and another 200 images were acquired in phase contrast, for micro-aggregates and filaments image acquisition, respectively. Both bright field and phase contrast images were acquired on a Nikon Diaphot 300 microscope (Nikon Corporation, Tokyo, Japan) with a 100 x magnification. For image acquisition of macro-aggregates, slides with three 10 mm etched rings were

used. A volume of 0.1 mL of aggregates suspension was placed at each etched circle for visualization and image acquisition on an Olympus SZ40 stereo microscope (Olympus, Tokyo, Japan) with 12 x magnification. Both the microscope and the stereo microscope were coupled to a CCD AVD D5CE Sony grey video camera (Sony, Tokyo, Japan), which along with a DT 3155 Data Translation frame grabber (Data Translation Marlboro, Massachusetts) allowed images acquisition in 768 x 576 pixel and 8 bit (256 grey levels) format through the Image Pro Plus (Media Cybernetics, Silver Spring, MD) software. Calibration from pixels to the metric unit dimensions was performed by means of a micrometer slide, allowing the determination of F_{cal}, the metric calibration factor.

Image processing and analysis were achieved through three programs previously developed in MATLAB (The Mathworks, Inc., Natick, MA) for filaments, micro-, and macro-aggregates (Amaral, 2003).

Image analysis parameters

Parameters were determined both directly from the image analysis programs and in association with biomass physical properties, namely the TSS.

The parameters determined by the filaments program used in this study were the filaments number (N_{fil}) and filament length (L_{fil}). Filaments considered are not only the dispersed free filaments, but also include protruding filaments, those that are attached to an aggregate and still have one free extremity (Figure 8.1). Prior to the filament length determination, the filaments image was thinned to a 1 pixel width and pruned to eliminate fake branches connected to the filaments. Thus, all the branches of the filaments inferior to 8 pixels were removed (Amaral, 2003).

The L_{fil} is given by Equation 8.1.

$$L_{fil} = N \times 1.1222 \times F_{cal} \quad (8.1)$$

where, N is the number of pixels of the skeletonised filament. The factor of 1.1222 was used to homogenise the different angles of the filaments (Walsby and Avery, 1996). The total filaments length (TL_{fil}) is given by the cumulative length of all the filaments. Ultimately, the filaments content and the specific total filament length (TL_{spec}) were calculated by dividing N_{fil} and TL_{fil}, respectively, by the volume of sample analysed.

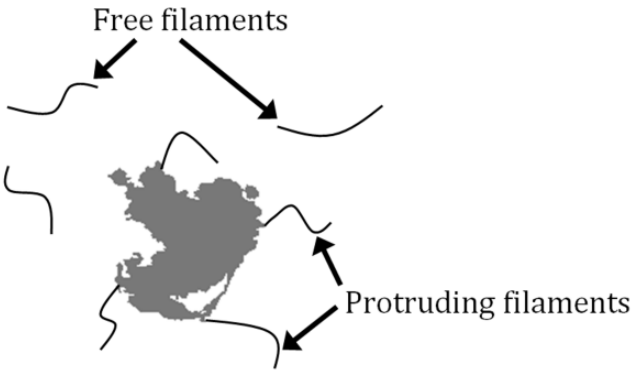

Figure 8.1. Schematic representation of free and protruding filaments.

The parameters determined by the micro- and macro-aggregates program used in this study were the aggregates number (N_{agg}), area (A), equivalent diameter (D_{eq}), length (L) and width (W) of the aggregate.

Area is calculated as the projected aggregate surface and is given by the number of pixels belonging to the aggregate converted to metric units. The total area (TA) is given by the cumulative area of all aggregates, including those cut off by the image boundaries (Amaral, 2003). The aggregates content and the specific total area (TA_{spec}) were calculated by dividing N_{agg} and TA, respectively, by the volume of sample.

The aggregates individual equivalent diameter (Figure 8.2a) is given by the diameter of a circle with the same area surface as the aggregate. Accordingly, D_{eq} is calculated based on the aggregate's area according to Equation 8.2.

$$D_{eq} = 2\sqrt{\frac{A}{\pi}} \tag{8.2}$$

Length and width of the aggregates were determined based on the Feret diameter, which corresponds to the maximum distance between two parallel tangents touching opposite borders of an object (Glasbey and Horgan, 1995). Hence, length was given as the maximum Feret diameter of the aggregate, and width as the minimum Feret diameter of the aggregate (Figure 8.2b). A new parameter was included to estimate the elongation level of the aggregates, the length/width ratio (L/W).

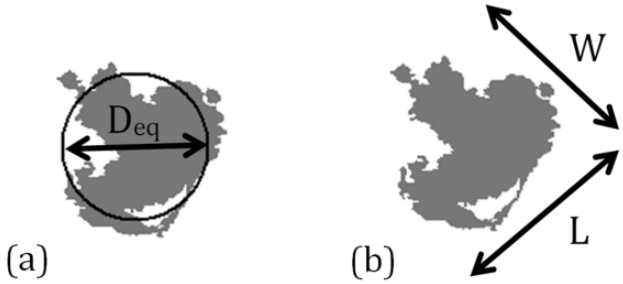

Figure 8.2. Schematic representation of the projected image of an aggregate (*grey*) and the morphological parameters (a) equivalent diameter (D_{eq}), (b) length (L) and width (W).

Furthermore, the aggregates were subsequently divided into four size classes. Two classes regarded micro-aggregates (Mesquita *et al*., 2009b): smaller aggregates (D_{eq} below 0.025 mm); and intermediary aggregates (D_{eq} between 0.025 and 0.25 mm). The other two classes regarded macro-aggregates, or granules: intermediary granules (D_{eq} between 0.25 and 1 mm); and larger granules (D_{eq} above 1 mm).

Morphological parameters representing the dynamic evolution of filaments and aggregates inside the reactor was calculated as the ratio between total filaments length per TSS (TL_{fil}/TSS).

8.3. Results and Discussion

The SBAR, fed with a constant organic loading rate of 2.7 g COD L^{-1} d^{-1} and a hydraulic retention time of 8 h, achieved a COD removal efficiency higher than 95 % since the first day of operation (data not shown).

Granulation was followed by image analysis. The morphological changes of the sludge aggregates were evident, from seed sludge flocs (Figure 8.3a), to first round aggregates on day 2 (Figure 8.3b), followed by the first granules on day 5 (Figure 8.3c) which then became compact, with a stable and clear outer surface on day 12 (Figure 8.3d); afterwards fungal filaments appeared on the granules surface on day 28 (Figure 8.3e and 8.3f).

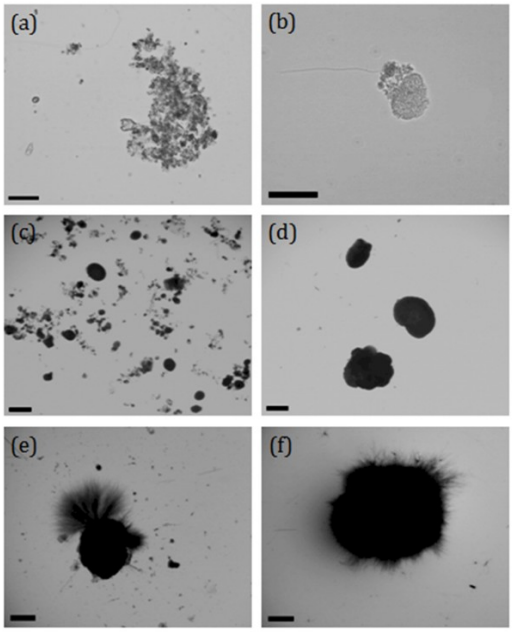

Figure 8.3. Morphology of the seed sludge (a), micro-aggregates on day 2 (b), granules on day 5 (c), compact granules on day 12 (d), granule with protruding fungal filaments on day 28 (e), and fungal granule on day 42 (f). Scale bar 0.1 mm (a) and (b), and 1 mm (c)–(f).

Three phases could be identified during operation of the reactor on the basis of solids content (Figure 8.4a), settling ability (Figure 8.4b), aggregates size distribution (Figure 8.4c), and filaments dominance (Figure 8.4d): a first phase which lasted until the day 8 (acclimatisation phase), followed by a second phase lasting for day 8 until day 24 (granulation phase); and finally a third phase from day 24 onward.

In the acclimation phase, the faster settling biomass was retained, while the slower settling biomass was washed out from the reactor. This was clearly seen in the suspended solids profile during the first 4 days of operation, when the VSS in the reactor decreased from approximately 2000 mg L^{-1} until approximately 1000 mg L^{-1} (Figure 8.4a). In terms of biomass fraction in the reactor during the acclimatization phase, as soon as granular sludge (D_{eq} > 0.25 mm) appeared, it became the dominant fraction of the total biomass (Figure 8.4a and Table 8.1).

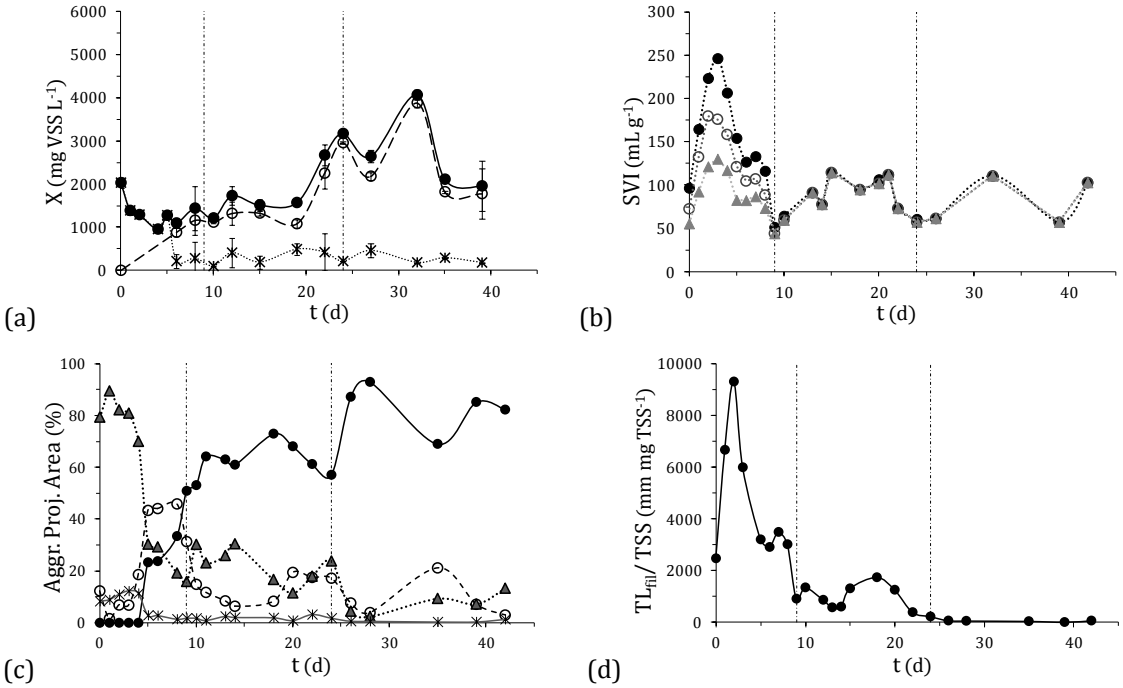

Figure 8.4. Time course of: (a) total biomass (●), granular biomass (○), and suspended biomass (∗) fractions in the reactor; (b) SVI after: 5 min (●), 10 min (○), and 30 min (▲) of settling time; (c) percentage of aggregates area for the different size classes of equivalent diameter: $D_{eq} \leq 0.025$ mm (∗), $0.025 < D_{eq}$ (mm) < 0.25 (▲), $0.25 \leq D_{eq}$ (mm) ≤ 1 (○), and $D_{eq} > 1$ mm (●); and (d) dynamics between total filaments length and TSS. *Dash-dotted vertical lines separate the three operational phases: acclimatisation, granulation, and fungal proliferation.*

During the first 3 days of operation, the settling ability of the biomass decreased, observed by an increase of SVI, reaching a peak at day 3. SVI then decreased significantly until day 9 (Figure 8.4c). Regarding aggregates size distribution, until day 3 there was a dominance of aggregates with D_{eq} inferior to 0.25 mm; then from day 4 to day 7 aggregates sizing from 0.25 to 1 mm D_{eq} were the most abundant; finally from day 9 onward granules with Deq larger than 1 mm were dominant (Figure 8.4c). During the acclimatisation phase, the biomass density was very unstable, and the difference between the density of aggregates retained in the reactor and those being washed out with the effluent was not clear (Table 8.1).

Table 8.1. Average values of biomass density in the mixed liquor and in the effluent, and percentage of granular sludge obtained during the three phases of operation

	Phase I		Phase II		Phase III	
	mixed liquor	effluent	mixed liquor	effluent	mixed liquor	effluent
biomass density ($g\ L^{-1}$)	14.3 ± 0.2	14.4 ± 1.0	22.4 ± 0.4	7.0 ± 0.3	22.2 ± 0.4	6.6 ± 0.3
(X_{gran} /X_{tot}) (VSS %)	63 ± 46	–	82 ± 9	–	90 ± 5	–

Filamentous structures were detected during the whole acclimatisation phase. A proliferation of filamentous bacteria was detected on day 3, followed by a sharp decrease of the free filaments (Figure 8.4d). This phenomenon is in accordance with the granulation process mechanism previously proposed by Beun *et al*. (1999) and more recently by Etterer (2001) in which filaments play a preponderant role in the initiation of granulation, building up pellets which settle well and are therefore retained in the reactor. These filamentous pellets function as an immobilisation support where bacteria can grow out to form colonies. Latter, the filamentous pellets break out and the bacterial colonies are released to form granules, while filaments are discharged from the reactor due to their low settling ability. Thus, after the release of the filaments the settling ability improved significantly (Figure 8.4b). A clear linear correlation was observed in this phase between the SVI_5 and the abundance of thin filaments per amount of TSS (Figure 8.5). A strong relation between these two parameters had already been shown for suspended activated sludge systems (Amaral and Ferreira, 2005; Mesquita *et al*., 2009a), however it had never been shown so far for aerobic granular sludge.

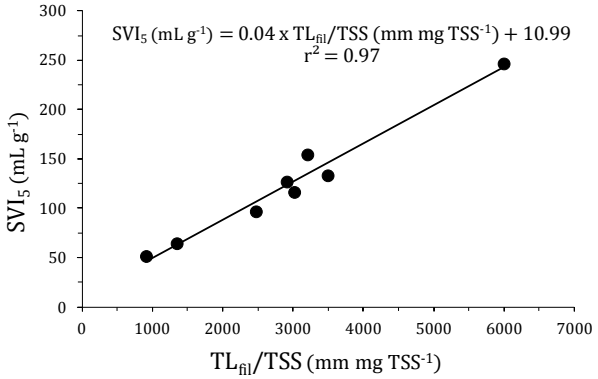

Figure 8.5. Correlation between the filaments in the aggregates and sludge settling ability.

At the end of Phase I, small round bacterial aggregates were formed (Figure 8.3b), and grew to form granules (Figure 8.3c), which became the dominant biomass form. This moment marked the beginning of the second phase of operation, the granulation phase, which was characterised by a stabilisation of the system. In the granulation phase (from day 9 until day 22) granular biomass was the main biomass fraction in the reactor (Figure 8.4a and Table 8.1). Settling ability was also stable, the biomass completely settled in 5 min, depicted by the SVI_5 being equal to SVI_{10} and SVI_{30}, approximately 100 mL g^{-1} (Figure 8.4b). Aggregates with D_{eq} larger than 1 mm dominated the reactor (Figure 8.4c), and filaments showed a tendency to decrease (Figure 8.4d). During the granulation phase, it was notable that denser aggregates were retained in the reactor, while less dense aggregates were being washed out in the effluent (Table 8.1). During the granulation phase, fast settling granules grew and became stable (Figure 8.4d).

On the last phase of operation, a destabilisation of the system occurred. This destabilisation was later determined to have been caused by fungi. Around day 22 the suspended solids drastically increased both in the mixed liquor, from approximately 1500 to 3500 mg VSS L^{-1} (Figure 8.4a), and in the effluent, from 250 to 350 mg TSS L^{-1} (data not shown). The biomass fractions in the reactor did not change much from day 24 onward (Figure 8.4a). Settling ability did not change significantly after day 24 (Figure 4b), neither did the density of the biomass in the reactor (Table 8.1). In terms of aggregate size distribution also no significant change occurred, the aggregates with D_{eq} larger than 1 mm continued to be dominant with a slight increase in this dominance (Figure 8.4d). No filaments were detected by the Filaments program in the mixed liquor (Figure 8.4d), neither in the effluent (data not shown).

Although no filaments were detected by the Filaments program from day 24 onward, the presence of filamentous structures was detected from direct microscopic visualisation in micro-aggregates aggregates on day 24 (Figure 8.6a and 8.6b), and it was obvious macroscopically from day 28 onward (Figure 8.3e and 8.3f). These filamentous structures were identified as fungal filaments. No molecular analysis was necessary to confirm that the thicker filamentous structures were filamentous fungi.

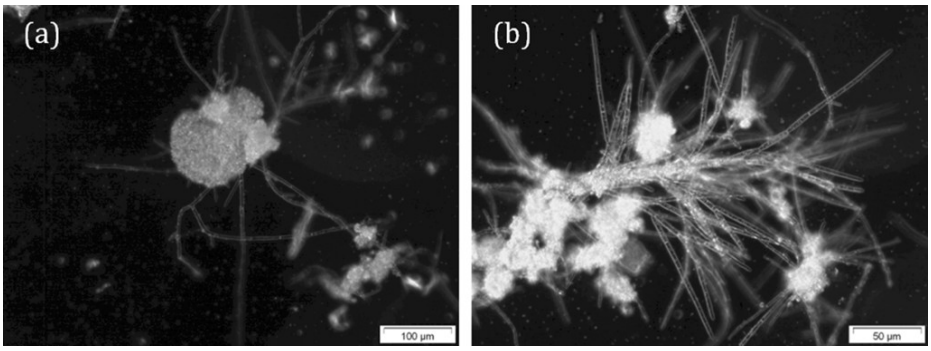

Figure 8.6. Phase contrast image of fungi at the surface of a granule 100x (a) and 200x (b).

The fungal filaments are significantly different from the initial bacterial filaments (Figure 8.7a, and 8.7c). This difference is notorious as bacterial filaments are much thinner than fungal filaments. The difference is also notoriously observed in phase contrast images, where bacterial filaments appear as darker structures in contrast with aggregates which are seen as brighter, whereas fungal filaments are seen as bright structures as the aggregates (Figure 8.7a). This was the reason for the Filaments program to be unable to discriminate between fungal filaments and aggregates as it does for bacterial filaments, (Figure 8.7b). Also in bright field images, the fungal filaments have the approximate appearance in terms of grey tonality as aggregates (Figure 8.7c), thus the micro-aggregates program identifies them as part of the aggregates (Figure 8.7d). Since the first fungi appeared as protruding filaments on the surface of the micro-aggregates, the program identifies them as elongated structures, *i.e.* with a high length/width (L/W) ratio (Figure 8.7d).

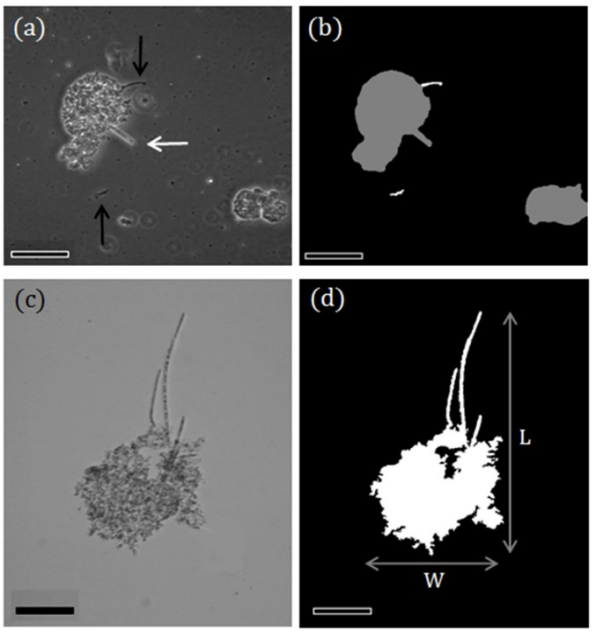

Figure 8.7. Original phase contrast image (a) with bacterial filaments (*grey arrows*) and fungal filament (*white arrow*), and corresponding binary image (b) of an aggregate on day 24, obtained with the Filaments program. Original bright field image (c) and corresponding binary aggregate image (d) of an aggregate on day 24, obtained with the Flocs program, with representation of length (L) and width (W). Scale bar 0.1 mm.

Following the L/W ratio of aggregates in the different range sizes along time (Figure 8a) it was clear that on day 24, when fungal filaments were detected in the reactor, only the L/W ratio of the aggregates with Deq smaller than 0.25 mm was affected, namely the smaller aggregates (Deq < 0.025 mm), but specially the intermediary aggregates (0.025 < Deq (mm) < 0.25; from day 22 to day 26 a 29 % increase in the L/W ratio was observed, and from day 22 to day 28 a 73 % increase (Figure 8.8a). As expected, the L/W ratio of macro-aggregates was not affected, since the fungal filaments are microscopic, thus are not detected by the stereomicroscope. The fungal filaments could only be observed macroscopically when they reached a high concentration and length. By that time, around day 28 (Figure 8.3e), the L/W ratio of macro-aggregates was not significantly affected either (Figure 8.8a), because by then, the protruding filaments were dispersed throughout the aggregates surface, surrounding it and thus the L and W of the macro-aggregates were balanced. For terms of comparison the data obtained in a system operated under the same operational parameters but which was not affected by fungal filaments (Oliveira *et al.*, *in preparation*) is presented (Figure 8.8b). It is clear, by Figure 8.8b, that when granules were not contaminated by fungi the L/W ratio was constant along the entire operation time.

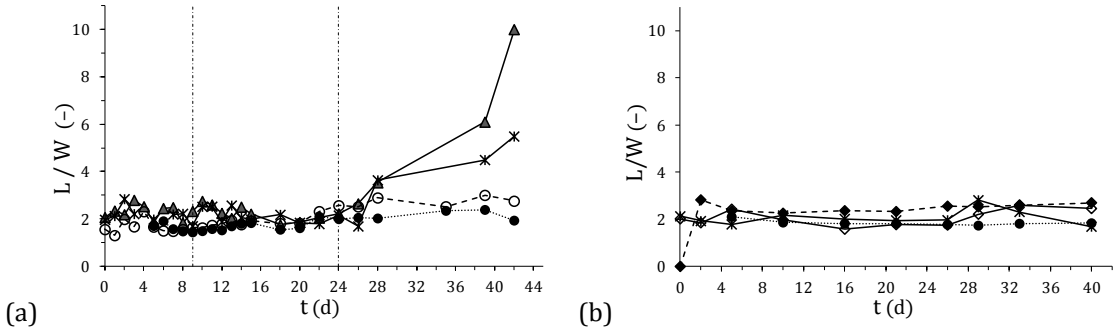

Figure 8.8. Time course of the morphological parameter L/W ratio in the present system, where fungal contamination occurred (a), and for terms of comparison in a system where fungal contamination did not occur (b), for the different size classes of equivalent diameter: $D_{eq} \leq 0.025$ mm (∗), $0.025 < D_{eq}$ (mm) < 0.25 (▲), $0.25 \leq D_{eq}$ (mm) ≤ 1 (○), and $D_{eq} > 1$ mm (●).

The number of fungal filaments on the mixed liquor (determined by manual counting from both bright field and phase contrast images) and the L/W ratio of smaller and intermediary aggregates were linked through a linear relation (Figure 8.9). This relation was stronger for the aggregates sizing in D_{eq} between 0.025 and 0.25 mm ($r^2 = 0.97$) than for the aggregates with D_{eq} smaller than 0.025 mm ($r^2 = 0.79$). Additionally the slope of the linear relation was also higher (0.001) for the aggregates with D_{eq} between 0.025 and 0.25 mm, than that of the aggregates with D_{eq} smaller than 0.025 mm (0.0005), thus the L/W ratio of the intermediary aggregates ($0.025 < D_{eq}$ (mm) < 0.25) was much more sensitive to the early detection of fungal growth, which suggests that this parameter may be a precise early warning of aerobic granules fungal contamination. The reason why the L/W ratio of $D_{eq} < 0.025$ mm aggregates was not so affected by the appearance of fungal filaments can be explain by the fact that when the fungal filaments appear on the surface of the smaller aggregates, this caused the increment of the aggregates size, thus the aggregates turned to intermediary aggregates. This is depicted by the dynamics of the aggregates percentage number: from day 22, when no fungal filaments were yet detected, until day 24, when fungal filaments were first microscopically detected, the percentage number of aggregates with D_{eq} smaller than 0.025 mm decreased 24 %, and the percentage number of aggregates with D_{eq} between 0.025 and 0.25 mm increased 125 % (data not shown).

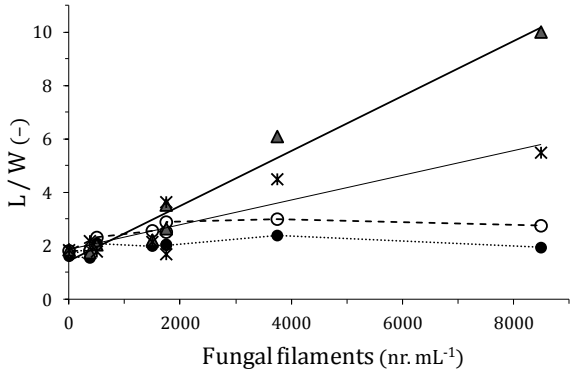

Figure 8.9. Correlation between number of fungal filaments and the L/W ratio for the different size classes of equivalent diameter: $D_{eq} \leq 0.025$ mm (∗), $0.025 < D_{eq}$ (mm) < 0.25 (▲), $0.25 \leq D_{eq}$ (mm) ≤ 1 (○), and $D_{eq} > 1$ mm (●).

The proliferation of fungal filaments in aerobic granules is a commonly reported phenomena causing troubleshoot in aerobic granular sludge. Fungal granules are larger and weaker than bacterial granules (Xiao *et al*., 2008), and biomass content and removal efficiency have been reported to decrease when granules become fungal (Morgenroth *et al*., 1997). In the present work there was no biomass loss due to the fungal proliferation, or significant decrease in COD removal. (data not shown). Nevertheless, image analysis allowed the detection of the fungal proliferation at an early stage, by the sharp increase of the L/W ratio of particles with equivalent diameter between 0.025 and 0.25 mm, 4 days before it was macroscopically observed (Figure 8.8a). This suggests that L/W ratio may be used as an early warning tool to anticipate fungal proliferation, allowing to apply strategies to avoid it, for example by adding anti-fungal agents (De Kreuk *et al*., 2010), or by increasing the organic loading rate (Li *et al*., 2010) whether increasing the substrate concentration fed to the system through the manipulation of the volume of influent fed, or by decreasing the cycle time.

8.4. Conclusions

Early detection of fungal growth in aerobic granular sludge was demonstrated using image analysis tools that quantify the morphology of micro-aggregates, macro-aggregates and filaments. Three phases were distinguished in the granulation process: acclimatisation, granulation, and structural instability caused by filamentous fungi proliferation. Acclimatisation phase was marked by slow settling biomass washout, and presence of free or protruding bacterial filaments, quantified by image analysis, which built the backbone

of upcoming granules. In this phase, a linear relation between the content of bacterial filaments in the aggregates and the Sludge Volume Index was established, which indicates that through the knowledge of the bacterial filaments content of aggregates it is possible to estimate the settling ability of aerobic granules.

During granulation phase stable compact granules were formed, and the system was stabilised. The phenomenon of aerobic granules fungal proliferation was clearly detected at an early stage through the length (L) to width (W) ratio of aggregates with equivalent diameter between 0.025 and 0.25 mm. Between days 22 and 26, an increase of 29 % in this parameter, anticipated the detection of fungal growth that was macroscopically visible only on the day 28. Thus, this morphological parameter L/W ratio was identified as an early warning indicator of fungal contamination, allowing foregoing control of operational conditions to avoid problems in the efficiency and stability of the system.

8.5. References

Abreu AA, Costa JC, Araya-Kroff P, Ferreira EC, Alves MM (**2007**). *Quantitative image analysis as a diagnostic tool for identifying structural changes during a revival process of anaerobic granular sludge*. Water Res. 41(7): 1473–1480.

Adav SS, Chen MY, Lee DJ, Ren NQ (**2007**). *Degradation of phenol by aerobic granules and isolated yeast Candida tropicalis*. Biotechn. Bioeng. 96(5):844–852.

Amaral AL (**2003**). *Image analysis in biotechnological processes: Applications to wastewater treatment*. Ph.D. thesis, University of Minho, Braga, Portugal.

Amaral AL, Ferreira EC (**2005**). *Activated sludge monitoring of a wastewater treatment plant using image analysis and partial least squares regression*. Anal. Chim. Acta 544(1–2):246–253.

APHA (**1999**). *Standard methods for the examination of water and wastewater*. 20th Edn. Washington, DC: American Publishers Health Association.

Beun JJ, Hendriks A, van Loosdrecht MCM, Morgenroth E, Wilderer PA, Heijnen JJ (**1999**). *Aerobic granulation in a sequencing batch reactor*. Water Res. 33(10): 2283-2290.

Beun JJ, van Loosdrecht MCM, Heijnen JJ (**2002**). *Aerobic granulation in a sequencing batch airlift reactor*. Water Res. 36(3):702–712.

Carucci A, Milia S, De Gioannis G, Piredda M (**2008**). *Acetate-fed aerobic granular sludge for the degradation of chlorinated phenols*. Water Sci. Technol. 58(2):309–315.

Carvalho G, Meyer RL, Yuan Z, Keller J (**2006**). *Differential distribution of ammonia- and nitrite-oxidising bacteria in flocs and granules from a nitrifying/denitrifying sequencing batch reactor*. Enzyme Microb. Tech. 39(7):1392–1398.

Chen MY, Lee DJ, Tay JH (**2007a**). *Distribution of extracellular polymeric substances in aerobic granules*. App. Microbiol. Biot. 73(6) :1463–1469.

Chen Y, Jiang W, Liang DT, Tay JH (**2007b**). *Structure and stability of aerobic granules cultivated*

under different shear force in sequencing batch reactors. App. Microbiol. Biot. 76(5): 1199–1208.

Costa JC, Moita I, Ferreira EC, Alves MM (**2009**). *Morphology and physiology of anaerobic granular sludge exposed to an organic solvent*. J. Hazard. Mater. 167(1-3):393–398.

De Bruin LMM, de Kreuk MK, van der Roest HFR, Uijterlinde C, van Loosdrecht MCM (**2004**). *Aerobic granular sludge technology: an alternative to activated sludge?* Water Sci. Technol. 49(11–12):1–7.

De Kreuk MK, van Loosdrecht MCM (**2006**). *Formation of aerobic granules with domestic sewage*. J. Environ Eng.-ASCE 132(6):694–697.

De Kreuk MK, Kishida N, Tsuneda S, van Loosdrecht MCM (**2010**). *Behavior of polymeric substrates in an aerobic granular sludge system*. Water Res. 44(20):5929–5938.

Di Iaconi C, Ramadori R, Lopez A, Passino R (**2007**). *Aerobic granular sludge systems: the new generation of wastewater treatment technologies*. Ind. Eng. Chem. Res. 46:6661–6665.

Di Iaconi C, de Sanctis M, Rossetti S, Ramadori R (**2008**). *Technological transfer to demonstrative scale of sequencing batch biofilter granular reactor (SBBGR) technology for municipal and industrial wastewater treatment*. Water Sci. Technol. 58(2):367–372.

Etterer T, Wilderer PA (**2001**). *Generation and properties of aerobic granular sludge*. Water Sci. Technol. 43(3):19–26.

Glasbey CA, Horgan GW (**1995**). *Image analysis for the biological science*. John Wiley and Sons, Chichester.

Heine W, Sekoulov I, Burkhardt H, Bergen L, Behrendt J (**2002**). *Early warning-system for operation-failures in biological stages of WWTPs by on-line image analysis*. Water Sci. Technol. 46(4-5):117–124.

Inizan M, Freval A, Cigana J, Meinhold J (**2005**). *Aerobic granulation in a sequencing batch reactor (SBR) for industrial wastewater treatment*. Water Sci. Technol. 52(10–11): 335–343.

Li AJ, Zhang T, Li XY (**2010**). *Fate of aerobic bacterial granules with fungal contamination under different organic loading conditions*. Chemosphere 78(5):500–509.

Liu Y, Liu QS (**2006**). *Causes and control of filamentous growth in aerobic granular sludge sequencing batch reactors*. Biotechnol. Adv. 24(1):115–127.

Oliveira CS, Ordaz A, Ferreira EC, Thalasso F, Alves M (***in preparation***). *Pulse respirometric method for the determination of extant kinetic and stoichiometric parameters in an aerobic granular sludge system* (*Chapter 6A of this Thesis*).

Mesquita DP, Dias O, Dias AMA, Amaral AL, Ferreira EC (**2009a**). *Correlation between sludge settling ability and image analysis information using partial least squares*. Anal. Chim. Acta 642(1–2):94–101.

Mesquita DP, Dias O, Amaral AL, Ferreira EC (**2009b**). *Monitoring of activated sludge settling ability through image analysis: validation on full-scale wastewater treatment plants*. Bioproc. Biosyst. Eng. 32(3):361–367.

Morgenroth E, Sherden T, van Loosdrecht MCM, Heijnen JJ, Wilderer PA (**1997**). *Aerobic granular sludge in a sequencing batch reactor*. Water Res. 31(12): 3191–3194.

Moy BYP, Tay JH, Toh SK, Tay TL (**2002**). *High organic loading influences the physical characteristics of aerobic sludge granules*. Lett. Appl. Microbiol. 34(6):407–412.

Prescott LM, Harley JP, Klein DA (**2002**). *Microbiology*. 5th Edition. New York: McGraw-Hill. pp:1001.

Walsby AE, Avery A (**1996**). *Measurement of filamentous Cyanobacteria by image analysis*. J. Microbiol. Meth. 26(1–2):11–20.

Xiao F, Yang SF, Li XY (**2008**). *Physical and hydrodynamic properties of aerobic granules produced in sequencing batch reactors*. Sep. Purif. Technol. 63(3):634–641.